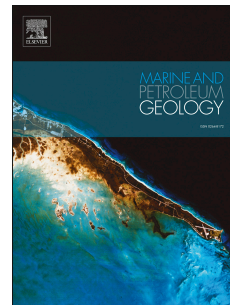


Journal Pre-proof

A conceptual model for glaciogenic reservoirs: From landsystems to reservoir architecture

Bartosz Kurjanski, Brice R. Rea, Matteo Spagnolo, David G. Cornwell, John Howell, Stuart Archer



PII: S0264-8172(19)30659-2

DOI: <https://doi.org/10.1016/j.marpetgeo.2019.104205>

Reference: JMPG 104205

To appear in: *Marine and Petroleum Geology*

Received Date: 31 August 2019

Revised Date: 19 December 2019

Accepted Date: 22 December 2019

Please cite this article as: Kurjanski, B., Rea, B.R., Spagnolo, M., Cornwell, D.G., Howell, J., Archer, S., A conceptual model for glaciogenic reservoirs: From landsystems to reservoir architecture, *Marine and Petroleum Geology* (2020), doi: <https://doi.org/10.1016/j.marpetgeo.2019.104205>.

This is a PDF file of an article that has undergone enhancements after acceptance, such as the addition of a cover page and metadata, and formatting for readability, but it is not yet the definitive version of record. This version will undergo additional copyediting, typesetting and review before it is published in its final form, but we are providing this version to give early visibility of the article. Please note that, during the production process, errors may be discovered which could affect the content, and all legal disclaimers that apply to the journal pertain.

© 2019 Published by Elsevier Ltd.

Bartosz Kurjanski: Conceptualization, Methodology, Investigation, Writing – Original Draft, Writing - Review & Editing Visualization

Brice R. Rea: Conceptualization, Methodology, Writing - Review & Editing, Supervision

Matteo Spagnolo: Conceptualization, Methodology, Writing - Review & Editing, Supervision

David G. Cornwell: Methodology Writing - Review & Editing, Supervision

John Howell: Conceptualization, Methodology, Supervision, Writing - Review & Editing

Stuart G. Archer: Conceptualization, methodology Writing - Review & Editing

Journal Pre-proof

1 A conceptual model for glaciogenic 2 reservoirs: from landsystems to reservoir architecture

3 Bartosz Kurjanski¹, Brice R. Rea¹, Matteo Spagnolo¹, David G. Cornwell¹, John Howell¹, Stuart Archer²

4 ¹School of Geosciences, University of Aberdeen, Aberdeen, AB24 3FX, UK

5 ²RPS, Goldvale House, 27-41 Church Street West, Woking, Surrey GU21 6DH, United Kingdom

6 7 Abstract

8 Glaciogenic sediments are present in many hydrocarbon-producing basins across the globe but their
9 complex nature makes it difficult to characterise the reservoir-quality sedimentary units. Despite
10 this, Ordovician glacial deposits in North Africa, and Carboniferous-Permian glaciogenic sequences in
11 the Middle East, have been proven to host significant, economical, hydrocarbon accumulations.
12 Additionally, discoveries have been made in the shallow (<1000 m below seabed), glacial,
13 Pleistocene sedimentary succession of the North Sea (e.g. Peon and Aviat). This paper provides a
14 predictive exploration framework in the form of a conceptual model of glaciogenic sediment-
15 landform distributions. The model is based on the extensive onshore glacial sedimentary record
16 integrated with available offshore data. It synthesises the published knowledge, drawing heavily on
17 glacial landsystem models, glacial geomorphology and sedimentology of glaciogenic deposits to
18 provide a novel conceptual model allowing for the efficient description and interpretation of glacial
19 sediments and landforms in the subsurface. Subsequently, land-terminating and water-terminating
20 ice sheet depositional systems are described and discussed, with respect to ice advance and retreat
21 cycles. This detailed description focuses on the macro-scale stratigraphic organisation of glacial
22 sediments with relation to the ice margin, aiding the prediction of glaciogenic sediment
23 distributions, and their likely geometry, architecture and connectivity as reservoirs.

24 1 Introduction

25 Glacial sediments and landforms have long been studied but, to date, a comprehensive overview of
26 their properties and characteristics from a hydrocarbon reservoir perspective has been lacking.
27 Sediments of glaciogenic origin have been targeted during hydrocarbon exploration and, in some
28 cases, have demonstrated good reservoir properties (e.g. South Oman Salt Basin, Ghadames-Illizi
29 Basin, North Africa, Murzuq Basin in Libya) (e.g. Forbes et al., 2010; Huuse et al., 2012; Klett, 2000).
30 Shallow gas accumulations in the Pleistocene succession of the North Sea, previously viewed as
31 drilling hazards, are now being considered an attractive target for relatively low cost/low risk fuel for
32 infrastructure (Aviat gas field) and, when large enough, for full scale production (Peon discovery)

33 (Huuse et al., 2012; Ottesen et al., 2012; Rose et al., 2016). Improvements in geophysical methods
34 and analytical techniques over the last two decades resulted in multiple publications describing
35 glaciogenic sequences. Especially worth mentioning are Special Publications and Memoirs from The
36 Geological Society, London including: “Glaciogenic reservoirs and hydrocarbon systems” (Huuse et
37 al., 2012); “Glaciated margins: the sedimentary and geophysical archive” (Le Heron et al., 2019);
38 “Glacier influenced sedimentation on high-latitude continental margins” (Dowdeswell and O’Cofaigh,
39 2002); “Engineering Geology and Geomorphology of Glaciated and Periglaciated Terrains:
40 Engineering Group Working Party Report” (Griffiths and Martin, 2017); “Atlas of Submarine Glacial
41 Landforms” (Dowdeswell et al., 2016a). From these, and other, publications it is clear that the
42 distribution and nature of glaciogenic sediments is more complex, and less predictable, than more
43 traditional clastic sequences. As a result, glaciogenic packages are less well understood and often
44 underexplored for their reservoir potential than sediments associated with more “typical”
45 depositional environments. Although glaciogenic sediments can be complex, there are some general
46 rules and/or characteristics that can be of use in petroleum exploration.

47 This paper bridges the gap between the academic and the applied perspective, by providing a
48 framework for investigating the distribution and characteristics of ice sheet sediments and
49 landforms, with a specific focus on their identification in the subsurface and subsequent assessment
50 of their hydrocarbon reservoir potential. While this paper presents some general glaciology as
51 background in the first few sections, it assumes a degree of *a priori* knowledge regarding glacial
52 processes, landforms and sediments and is not focused on detailed descriptions thereof. For such
53 information readers are referred to specialist publications mentioned throughout the text or
54 textbooks (e.g. Glaciers and Glaciation by Benn and Evans (2010)). Here, a conceptual model of
55 glaciogenic deposition relevant to the subsurface and hydrocarbon exploration potential is
56 developed.

57 2 Glaciations and glacial Processes

58 Ice sheets are masses of ice larger than 50,000 km² (Benn and Evans, 2010). During a single
59 glaciation an ice sheet will typically experience multiple phases of advance and retreat, leaving a
60 highly complex sedimentary record and assemblage of landforms, often referred to as a glacial
61 mosaic (Bennett and Glasser, 2009; Evans et al., 2006). Here, we introduce some key concepts
62 related to glaciation to provide the necessary background to understand ice sheet sediment and
63 landform distribution.

64 2.1 Timescales of glaciation

65 The rock record shows that during the last 2.5 billion years, Earth has undergone multiple shifts in
66 climate between periods of relatively high ice cover (icehouse) and periods where glaciers were
67 either missing or present in small isolated pockets (greenhouse) (e.g. Craig et al., 2009; Eyles, 2008,
68 1993; Le Heron et al., 2009; Strand, 2012). From a geological point of view, the Earth, at present, is
69 in an icehouse which began around 37 Ma ago, during the Late Cenozoic, with the first glaciation of
70 Antarctica (Anderson et al., 2011). Within this icehouse, ice sheets have advanced and retreated
71 many times, but never disappeared completely at a global scale (Eyles, 2008). The Pleistocene (2.58
72 Ma to 11.5 ka), part of the Late Cenozoic, is the best understood and temporarily-resolved icehouse
73 period (e.g. Ehlers et al., 2011; Farmer and Cook, 2013). During this time, ice sheets periodically
74 expanded and retreated, following a cyclical orbital climatic forcing that is well-recorded in benthic
75 foraminifera oxygen isotope ratios ($\delta^{18}\text{O}$) (Figure 1), recovered from marine sediments (Lisiecki and
76 Raymo 2005). Lower $\delta^{18}\text{O}$ is linked to warmer periods and interglacials (i.e. marine isotope stage odd
77 numbers), while higher $\delta^{18}\text{O}$ indicates colder periods and glacials (i.e. even-numbered marine
78 isotope stage) (Figure 1). Glacial – interglacial changes are attributed mainly to cyclical Milankovitch
79 orbital forcing (100 ka eccentricity cycles, 41 ka obliquity cycles and 21 ka precession cycles) (Eyles,
80 1993). Pleistocene glaciations are further subdivided into relatively colder (stadials) and warmer
81 (interstadials) periods, where ice sheets advance and retreat. They are forced by internal dynamics
82 within the coupled Earth climate systems (Bradley, 2015; Lisiecki and Raymo, 2005; Spratt and
83 Lisiecki, 2016).

84 2.2 Ice motion, glacial erosion, transport and deposition

85
86 Ice moves from the ice sheet interior (ice divide) outwards, towards the ice margin via three possible
87 mechanisms: internal deformation, basal sliding and subglacial deformation of the underlying bed
88 (sediments) (Benn and Evans, 2010). The prevailing mechanism depends on the thermal regime at
89 the ice-bed interface, the type of bed and presence or absence of meltwater (Benn and Evans,
90 2010).

91 The thermal regime of an idealised circular ice sheet, at a given time, can be described in a tripartite
92 subdivision (Boulton, 1996; Jamieson et al., 2008). Cold based (frozen to the bed) and slow moving,
93 via internal deformation, in the ice sheet centre proximal to the ice divide. A transition zone
94 (polythermal zone), where fast-flowing corridors of ice, known as ice streams, are initiated. Towards
95 the margin the thermal regime is warm-based (ice is at the pressure melting point) with lubricating
96 water at the ice-bed interface. This tripartite zonation is transgressive during ice advances, and
97 regressive during ice retreat, and the rate of change is dependent on the climate forcing

98 mechanisms and internal ice dynamics (Benn and Evans, 2010). When ice accumulation outpaces
99 ablation, ice masses expand and advance. When the opposite is true, the ice margin steps back as ice
100 masses shrink and retreat.

101 Basal sliding and/or subglacial deformation causes areas of bedrock and pre-existing sediments to be
102 eroded. Rock fragments and/or sediments are then incorporated into the basal ice and/or advected
103 in a layer coupled to the ice sheet bed, ultimately being transported towards the ice sheet margin
104 (Evans et al., 2006; Powell and Cooper, 2002). At some point down flow, more sediments are melted
105 out from the ice than are eroded/incorporated into the ice, due to meltout and increased friction at
106 the ice/bed interface. As a result, the environment becomes dominated by depositional rather than
107 erosional processes (Evans et al., 2006; Spagnolo et al., 2016). Some of the sediment is transported
108 inside (englacially), or on top of (supraglacially) the ice and melts out directly at the ice margin.
109 Other sediment may be transported by subglacial meltwater, which drains the bed of the ice sheet
110 (Kleman et al., 2008; Krüger et al., 2009; Lønne, 1995; Thomas and Chiverrell, 2006). Glaciofluvial
111 (meltwater) sediments may be deposited in subglacial and englacial meltwater conduits (Burke et
112 al., 2015; Storrar et al., 2014) or beyond the ice margin as ice marginal or proglacial sediments
113 (Glückert, 1986; Zielinski and Van Loon, 2003; Zieliński and van Loon, 1998).

114 2.3 Glacial isostatic adjustment, eustatic and relative sea levels

115 Sea level changes are one of the major controls on the sediment distribution within most
116 sedimentary basins (Emery et al., 1996) and sedimentary systems typically respond to sea-level
117 changes. Ice sheets have a unique ability to change sea-level, both on local and global scales. There
118 are three major mechanisms by which ice sheets affect sea level fluctuations (Figure 2) (Lambeck,
119 1998; Milne et al., 2009; Peltier, 2002):

- 120 1. Ice sheets store vast amounts of water causing the eustatic sea level to fall during ice sheet
121 growth and rise during retreat when the stored water is released, via melting and iceberg
122 calving.
- 123 2. The weight of an ice sheet causes an isostatic depression of the pre-existing topography
124 resulting in a relative sea level rise in the vicinity of an ice sheet and a sea level fall where
125 the forebulge is present in front of the ice sheet.
- 126 3. The ice sheet mass locally perturbs the geoid and therefore affects the equipotential surface
127 of the ocean. As a result, the ocean surface rises proximal to the ice sheet.

128 Eustatic sea level rise and fall is most pronounced (Milne et al., 2009) when associated with both ice
129 sheet growth (glacials) and decay (interglacials), while lower amplitude oscillations of global and
130 local sea level may occur across stadials and interstadials (Spratt and Lisiecki, 2016).

131 2.4 Accommodation, and sediment supply

132

133 It is generally accepted that accommodation is essential for preservation of a sedimentary sequence
134 in the rock record (Jervey, 1988). Sedimentary basins provide this, and are affected, variously, by an
135 interplay between eustatic sea level and subsidence rate (Catuneanu, 2002; Catuneanu et al., 2011).
136 This relationship only partially holds in glacially-affected regions (Zecchin et al., 2015). Sedimentary
137 basins influenced by ice sheets may be intermittently (during a glaciation) affected by anomalously
138 high sediment fluxes resulting in rapid (in geological time scale) basin filling and increased
139 subsidence rates due to both sediment and ice loading, in comparison to other non-glacial
140 depositional environments (Eyles et al., 1993; Eyles, 1993). Moreover, sediment transport directions
141 and input points in glacially-affected sedimentary basins will change substantially over hundreds to
142 thousands of years as a response to ice advance and retreat (Nielsen and Rasmussen, 2018). The
143 efficacy with which ice and meltwaters erode, transport and deposit sediments in a basin will most
144 likely overprint other contemporary changes, including short wavelength sea level oscillations and
145 changes in fluvial input into the basin (Lawson, 1981).

146 3 Glacial landsystems

147 Glacial processes described in the previous section ultimately exert a controlling influence on the
148 distribution of glaciogenic sediments and landforms. A systematic approach to glacial landform-
149 sediment associations exists in the form of glacial landsystems (Benn and Evans, 2010; Evans, 2006).
150 To date, the application of the landsystems approach has mainly focused on qualitative landscape
151 characterisation (Evans, 2006) to develop landform-process associations in order to reconstruct the
152 dynamics of palaeoglaciations (Davies et al., 2013; Evans, 2006; Ingólfsson et al., 2016). A key benefit
153 of the landsystems methodology, from an exploration perspective, is the ability to divide
154 depositional environments into zones, with associated landforms and sediment types.

155 Ice sheet landsystems, which are the primary focus of this paper, describe processes, landforms and
156 sediments associated with continental scale ice masses. Modern analogues are the Antarctic and
157 Greenland Ice Sheets, although it must be stressed that these do not represent the full suite of ice
158 sheet landsystems that occur in the geological record. Specifically, they cannot act as analogues of
159 continental scale ice sheets that covered present day epicontinental seas (North Sea, Baltic), large
160 terrestrial terminating margins (e.g. Fennoscandian Ice Sheet (FIS), Laurentide Ice Sheet (LIS)) or ice
161 streams extending to the continental shelf edge (Margold et al., 2015; Patton et al., 2016; Rea et al.,
162 2018; Velichko et al., 1997).

163 Multiple landsystem models have been constructed (Evans, 2006), but the majority are limited to
164 surficial, short timeframe/snapshots, characterising a depositional system in a certain state, rather
165 than its full evolution over space and time (i.e. the landsystem observed at the earth surface and the
166 associated stratigraphy below, be it terrestrial or marine). It is important to note that a landsystem
167 can be described at different scales. For example, a fjord landsystem can be part of a bigger,
168 subaqueous landsystem when an ice sheet enters a water body. The landsystem models developed
169 from the investigation of relatively recent glacier dynamics, are of limited use when multiple,
170 stacked, deposits from glacial-interglacial cycles are analysed. When investigating ancient glaciations
171 from outcrops, well data or seismic surveys, it may be impossible to define a landsystem in the way
172 contemporary glacial landsystems are described. This is due to data limitations combined with the
173 complicating effects of post depositional reworking, compaction and diagenesis, varying ice sheet
174 thermal regimes and geometries and even transitions from submarine to terrestrial environments.

175 Sequence stratigraphy and the concept of system tracts is of practical use when interpreting
176 glaciogenic deposits (Boulton, 1990; Catuneanu, 2006; Lee, 2017; Pedersen, 2012; Powell and
177 Cooper, 2002; Zecchin et al., 2015). Unlike in traditional sequence stratigraphy, accommodation is
178 not linked to relative sea level changes. Instead it is the ice margin position that exerts the primary
179 control on accommodation and on mode of deposition (Boulton, 1990; Zecchin et al., 2015). In such
180 scenarios ice advance and retreat controls marine regression and transgression. The picture is
181 complicated further by glacial isostatic adjustment, forebulge collapse and eustatic sea level
182 changes, all of which have an effect on the final sedimentary assemblage (Powell and Cooper, 2002;
183 Zecchin et al., 2015). Finally, the erosional nature of glacial processes results in multiple, stacked
184 glacial erosional surfaces (known as GES) leading to difficulties in correlating glaciogenic packages
185 based on their stratigraphic relationships - the concept upon which the classical sequence is built
186 (Catuneanu et al., 2009; Lee, 2017; Van Wagoner et al., 1988). High lateral variability of deposition
187 requires an integrated interpretation approach utilizing high resolution, preferably 3D, seismic data
188 and wells (Zecchin et al., 2015).

189 4 Glaciogenic Deposition

190 Glaciogenic sedimentary sequences, whether ancient or contemporary, can be summarized using
191 the following key characteristics:

- 192 1. High flux and rapid deposition of sediments (decadal to millennial time scales) (Bellwald et
193 al., 2019; Ottesen et al., 2012).
- 194 2. Multiple erosional and depositional episodes, and frequent post-depositional reworking of
195 sediments (e.g. Boulton, 1979; Hodgson et al., 2014; Kleman et al., 2008).

- 196 3. Abrupt changes from subaqueous to subaerial conditions and sharp facies contacts (decadal
197 to millennial time scales) (e.g. Lamb et al., 2017; Thomas and Chiverrell, 2006).
- 198 4. Uneven distribution of glacial sediments through a glaciated terrain (e.g. Lopez-Gamundi
199 and Buatois, 2010; Marks, 2012; Martin, 1981).
- 200 5. distribution of sediments and landforms governed by the position of the ice margin (annual
201 to millennial time scales) (e.g. Ely et al., 2016; Lønne, 1995; Palmu, 1999).
- 202 6. High magnitude, extreme events (days to decades) (e.g. lake outburst floods, jökulauhps;
203 Gupta et al., 2017; Maizels, 1997).
- 204 7. Presence of large scale landforms/features characteristic of glacial processes only (e.g. Ely et
205 al., 2016; Haavik and Landrø, 2014; Kristensen et al., 2007; Ó Cofaigh et al., 2003).

206 All of the above elements may complicate evaluations of the reservoir potential of glaciogenic
207 successions and construction of a predictive facies model, when compared to those commonly
208 constructed for marine, fluvial or aeolian successions (e.g. Catuneanu et al., 2011; Kocurek, 1993;
209 Nichols and Fisher, 2007; Zecchin et al., 2015). However, some fundamental classifications are
210 possible and are presented here in a conceptual model to facilitate the interpretation of glacial
211 sediments (and landforms) that might act as oil and gas reservoirs.

212 5 Glaciogenic Reservoir Distribution – A Conceptual Model

213 5.1 Model framework

214 Multiple authors have presented glaciogenic depositional models (e.g. Brodzikowski and Loon, 1991;
215 Eyles et al., 1985; Lønne, 1995), describing in fine detail the distribution of landforms and sediments
216 over a specific area (Boulton, 1972) or related to a specific aspect of glaciogenic sedimentation (e.g.
217 sandar, grounding zones; Pisarska-Jamrozy, 2006; Powell and Alley, 1996).

218 The conceptual model of glaciogenic landforms and their sediments distribution presented here
219 (Figure 4) builds on these, and an extensive literature review of ancient and Pleistocene-to-
220 contemporary glaciogenic deposits (Tables 2, 3 and 4).

221 Glaciogenic deposition can be divided into three depositional zones controlled by the ice margin
222 position (1st order control on deposition):

- 223 1. Subglacial zone where glacial erosion and deposition is responsible for the formation of a
224 unique landform and sediment assemblage. It can be further subdivided in areas of slow-
225 moving and fast-moving ice.
- 226 2. Ice marginal zone, where a mix of subglacial and proglacial processes occur.

227 3. Proglacial zone, where no direct influence of ice contact on sediment deposition can be
228 seen.

229

230 Glaciogenic sedimentation is also affected by, and interacts with, the gross depositional
231 environment in which the ice sheet terminates (2nd order control) i.e. sedimentation in the ice
232 marginal zone of a marine grounded ice sheet will be significantly different to one terminating on
233 land. These depositional environments include:

- 234 1. Terrestrial - subaerially exposed land surface (including kettle hole and small proglacial
235 lakes).
- 236 2. Large proglacial lacustrine – continental-scale lakes.
- 237 3. Shallow marine – from the shore to the shelf break.
- 238 4. Deep marine - beyond the shelf break.

239 Finally, deposition is also controlled by ice sheet dynamics and can be further subdivided into:

- 240 1. Deposition during Ice advance when sediment incorporation and advection is dominant,
241 and less meltwater is released.
- 242 2. Deposition during Ice retreat when sediment release and meltwater processes are
243 dominant.

244 The influence of ice dynamics on sediment and landform assemblages is described and
245 discussed in detail below.

246 5.2 Landforms, sediments and their identification

247 Glacial landforms and their sediment associations are often described by their surface morphological
248 expression and studied to elucidate the glacial processes responsible for their formation (Hughes et
249 al., 2014; Klages et al., 2016; Phillips et al., 2002). The focus of this paper is on the reservoir potential
250 of glacial sedimentary sequences, so the abundance of landforms and the variations of
251 nomenclature was critically reviewed and re-grouped in our model, based on the potential to be: 1 -
252 preserved in the rock record and 2 - recognized in the subsurface. For example, landforms that have
253 been previously referred to as: grounding line fans (Powell, 1990), turbiditic outwash fans (Hirst,
254 2012), glaciomarine fans (Lajeunesse and Allard, 2002), subaqueous esker deltas (Thomas, 1984), ice
255 proximal fans (Batchelor and Dowdeswell, 2015), esker-fan complexes (Brennand, 2000); will be
256 described in our model as ice-contact subaqueous fans (Lønne, 1995). In all instances these will be
257 composed of sediments deposited at the ice margin (in the ice-marginal depositional zone in a
258 marine or lacustrine environment - Figure 3 and Figure 4) by channelized meltwater entering a water
259 body (ocean or lake). An alias table (Table 1) providing a synthesis of terms used to describe similar

260 glacial features, landforms and sediments from the published literature is provided to simplify the
261 terminology and enable easier use of Figures 3 and 4 (Table 1). A qualitative description of the
262 reservoir potential, based on published literature, wells and outcrop studies, of the landforms and
263 sediments assigned to the model is provided (Table 2, Table 3 Table 4). A traffic light system (green:
264 good/known reservoir; yellow: potential reservoir; red: non-reservoir/seal) is used to indicate the
265 potential reservoir quality. This simple scheme should improve predictability of reservoir quality
266 sediments within the glaciogenic depositional system.

267 It is crucial to emphasize that our conceptual model is a generalization which aims to represent the
268 majority of glaciogenic deposits found in nature. Therefore, there may be site-specific sediments or
269 landforms that do not conform to the reservoir quality assigned to them.

270 A systematic description of the major glaciogenic sediments and landforms, and their hydrocarbon
271 potential, with respect to depositional zones (subglacial, ice-marginal and proglacial) followed by
272 depositional environment (terrestrial/lacustrine/shallow marine/deep marine) and subdivided into
273 ice dynamic stages (ice advance and retreat), is now provided.

274 6 Subglacial zone

275 The bed in the interior of an ice sheet is generally marked by an erosional unconformity which
276 expands outwards as the ice advances. This is the subglacial erosional zone. Towards the ice margin,
277 under a warm-based ice sheet, the erosional unconformity is overlain by traction till composed of
278 mixed, unsorted material derived from overridden, pre-existing sediments, or eroded bedrock (Table
279 2) (Clarke, 1987). Such sediments described from the ancient (pre-Quaternary) rock record are
280 sometimes referred to as glacial diamictite. The diamictite category, however, comprises a broad
281 spectrum of sediments with bimodal or polymodal grainsize distributions, deposited by multiple
282 processes (e.g. mass wasting, rainout (dropstones) etc.). All the above processes need to be carefully
283 considered before interpreting diamicton/diamictite as a subglacial traction till or tillite. A broad
284 grainsize spectrum, lack of clear sedimentary structures and alignment of elongated clasts are
285 characteristics of subglacial traction tills (Evans et al., 2006). Micromorphology may also prove useful
286 when trying to distinguish between subglacial till and other similar-looking deposits (Busfield and Le
287 Heron, 2018).

288 Processes governing the subglacial depositional zone of a marine-terminating ice sheet (Figure 3 and
289 Figure 4) are similar to the subglacial depositional zone of a land terminating ice sheet, resulting in
290 similar landforms and sediments (Table 2, Table 3 and Table 4). A clear morphological division
291 between cross-shelf troughs eroded by ice streams and adjacent inter-ice stream areas is visible in
292 submarine settings (Ó Cofaigh et al., 2003).

293 6.1.1 Advance stage

294 Traction till could be deposited widely across the subglacial depositional zone or be confined to
295 specific topographic settings resulting in distinct landforms (e.g. Graham et al., 2009; Hughes et al.,
296 2014). Deposition may occur under the ice to form elongated landforms, although the genesis of
297 some of these is disputed. Amongst such landforms, the most common are (Table 2): drumlins and
298 Mega Scale Glacial Lineations (MSGSL) – elongated to extremely elongated features that are usually
299 found in areas of fast-flowing ice streams (Bingham et al., 2017; Clark et al., 2009; Spagnolo et al.,
300 2014; Stokes and Clark, 1999) . These landforms are easy to recognise in the subsurface records
301 because of their distinct shape and spatial arrangement. Well-sorted lenses and thin layers of sands
302 and gravel are often found between thick till sequences where subglacial meltwater flowed at the
303 ice-bed interface. Ice sheets advance and override landforms and deposits associated with either,
304 other sedimentary environments or, a previous stage of glaciation, reinitiating subglacial erosion and
305 deposition. All or part of the sediments deposited earlier will be cannibalized by the advancing ice
306 sheet and redeposited, down flow, as traction till (Table 2) covering older sediment packages
307 (Boulton, 1996). Preservation of pre-existing sedimentary packages largely depends on the depth of
308 glacial erosion (as a function of the duration of ice cover) and/or accommodation generated during
309 and since the previous retreat (e.g. Knutz et al., 2019).

310 Older, pre-existing bedforms are overridden and streamlined (Benn and Evans, 2010). In marine
311 environments, part of the sedimentary package will be eroded, entrained and transported more
312 distally to be deposited as traction till or released at the ice margin as meltout or carried off as ice
313 rafted debris in icebergs (IRD- Table 3) (Dowdeswell and Fugelli, 2012; Powell and Alley, 1996). Some
314 bedforms may survive overriding if they are sufficiently resistant to subglacial erosion or protective
315 material overlies them (Bellwald et al., 2019). In both cases, they can be only partially eroded or
316 streamlined and are preserved under a traction till carapace acting as a seal for fluid accumulation
317 (Ottesen et al., 2012). Such a mechanism is described for the Peon gas discovery (Ottesen et al.,
318 2012), where a large gas accumulation was found in a Pleistocene subaqueous outwash fan complex
319 (Figure 4 and Table 3). The ice-contact subaqueous fan deposit was subsequently overridden by the
320 fast-flowing Norwegian Channel ice stream which deposited an overlying traction till.

321 Glaciotectonic deformation (thrusting, folding and fracturing), erosion and streamlining of pre-
322 existing sediments occurs as the ice advances and the subglacial zone expands outwards (Krüger et
323 al., 2009; Phillips et al., 2002). If organic rich sediments are overridden by an advancing ice mass and
324 capped by traction till, they can be biologically (methanogens) or thermally (if burial depth is
325 sufficient) altered to produce gas accumulations (Holmes and Stoker, 2005; Laier et al., 1992).

326 From a petroleum reservoir perspective, sediments deposited in the subglacial zone during the ice
327 advance mostly have poor reservoir characteristics but may be considered as potential seals (Figure
328 4) (Bellwald et al., 2018; Clarke, 2018). However, careful evaluation is required when considering
329 traction till as a regional seal. A patchy or discontinuous distribution can hinder its sealing capacity as
330 can lenses of intra-till sand and gravel, deposited by subglacial meltwater drainage (Boulton, 1996).
331 Cross-shelf troughs (ice stream corridors) form elongated sub-basins which will most likely have a
332 distinctive sedimentary assemblage from parts of the shelf covered by a slow-moving ice (Knutz et
333 al., 2019; Ó Cofaigh et al., 2003; Stokes and Clark, 2001). This implies that reservoir properties will
334 vary between the two areas introducing regional scale heterogeneity as more erosion, but also more
335 meltwater derived sedimentation can be expected within the trough. Moreover, erosion of cross-
336 shelf troughs can juxtapose older, underlying sediments with the glaciogenic package and provide
337 fluid migration pathways. Present-day bathymetric data shows that cross shelf-troughs remain
338 largely underfilled following deglaciation (Batchelor and Dowdeswell, 2014; Hodgson et al., 2014;
339 Rütther et al., 2013; Swartz et al., 2015). Anoxic conditions and preservation of organic matter
340 (source rocks) may be facilitated in such settings during the post-glacial marine transgression (Le
341 Heron and Craig, 2012; Lüning et al., 2000).

342 6.1.2 Retreat stage

343 During ice retreat the subglacial zone migrates inwards, uncovering sediments and landforms
344 generated during the advance. As the ice sheet retreats, the warm-based subglacial zone migrates in
345 towards the ice divide where previously the ice sheet was cold-based and frozen to its bed. The
346 switch from a cold- to a warm-based thermal regime facilitates initiation of proximal subglacial
347 erosion and distal deposition of traction till (Table 2 and Figure 4). Rising atmospheric temperatures
348 generate melting and runoff, increasing ice and sediment fluxes. As a result, larger volumes of
349 glaciofluvial sediments will be deposited subglacially in meltwater conduits in the form of eskers
350 (Table 2, Figure 4 and Figure 5) - elongated, often curvilinear ridges, comprising silts, sands and
351 granule to boulder-sized gravels (Burke et al., 2015). Otherwise, the processes taking place in the
352 subglacial depositional zone (Figure 4) during retreat are similar to those during the ice advance.
353 Eskers, although having potential to be good reservoirs are rarely continuous and/or large enough to

354 constitute a stand-alone target. Anastomosing (amalgamated) eskers may provide significantly
355 greater reservoir volume and improve connectivity between otherwise discontinuous reservoirs.

356 7 Ice marginal zone

357 The ice marginal depositional zone migrates outwards as an ice sheet advances and inwards as it
358 retreats. It is relatively narrow but by far the most dynamic zone, with the most abrupt changes in
359 facies over relatively short distances. An interplay of subglacial and proglacial deposition,
360 glaciotectonic processes, large variations in meltwater energy and ice margin oscillations provide the
361 potential for complex sediment assemblages (e.g. Batchelor and Dowdeswell, 2015; Pedersen, 2014;
362 Vaughan-Hirsch and Phillips, 2017; Zieliński and Van Loon, 1998).

363 7.1 Terrestrial

364 Large moraine complexes (Table 2) are deposited where the ice margin stabilises for a sufficient
365 period (e.g. a stadial or glacial maxima), allowing sediments to accumulate in a relatively narrow
366 zone (e.g. Bennett, 2001; Krüger et al., 2009; 2016; Van der Wateren, 1995). Push moraines
367 comprise bulldozed and reworked sub-glacial to proglacial zone sediments and may include
368 glacialfluvial outwash, paraglacial and non-glacial sediments (Bennett, 2001). Thrust blocks can also
369 form large moraine complexes, sometimes even in bedrock (Pedersen, 2014; Phillips et al., 2018),
370 but are generally composed of proglacial outwash sands and gravels. Some of the largest examples
371 have a vertical relief of 150 m or more (Benn and Evans, 2010). Their composition may vary greatly
372 along the ice front depending on the available sediments (Bennett, 2001; Huuse and Lykke-
373 Andersen, 2000; Krüger et al., 2009; Le Heron et al., 2005). Moraine ridges may, in places, be
374 dissected by meltwater channels emanating from the ice sheet. Where meltwater exits the ice front
375 through portals, ice-contact fans (Table 2) may be formed (Zieliński and van Loon, 2000, 1999, 1998).
376 They are characterised by proximal cobble to boulder gravels, with sands and silts deposited distally
377 and laterally from the efflux location (Krzyszczkowski and Zielinski, 2002).

378 7.1.1 Advance

379 During an advance stage, ice-contact fans, moraines and sandar, or parts thereof, will be overridden
380 and at least partially cannibalized by the advancing ice sheet margin. Reservoir properties of land
381 terminating ice marginal deposits mainly depend on the type of sediment available for
382 remobilisation (Figure 4). Thrust-block moraines can have relatively good reservoir properties if
383 composed of proglacial outwash sands and gravels (van der Wateren, 1994; Van der Wateren, 1995).
384 Push moraines will typically exhibit poor reservoir quality as a result of mixing and homogenisation
385 during the bulldozing of the sediments by the ice margin (Phillips et al., 2002; Pisarska-Jamrozy,
386 2006). Ice-contact fans will have moderate to poor reservoir quality depending on the sediment

387 supply, stability of the ice margin and transport distance of the material (the longer the meltwater
388 transport the better the sorting and reservoir quality) (Zieliński and van Loon, 2000). Meltwater
389 deposited, ice marginal and proglacial sediments will generally be smaller in volume in this phase
390 than their retreat-stage counterparts, due to the lower meltwater discharge during the advance (van
391 der Wateren, 1994).

392 7.1.2 Retreat

393 Moraines (Table 2) composed of bulldozed outwash deposits and slope-failure/slump/meltout
394 sediments delineate back-stepping ice margin positions as the ice sheet periodically
395 stabilises/stillstands. Ice-contact fan size (Table 2) is a function of duration of the stillstand, the size
396 of the meltwater portal, subglacial catchment area, meltwater discharge and sediment availability. If
397 an ice-contact lake develops in a topographic low, subaqueous/ice-contact sediments will be
398 deposited. These landforms are described in section 7.2 and in Table 3. Reservoir properties of
399 moraines formed during retreat stillstands (de Geer moraines-Table 3) are poor (Figure 4) because
400 they are predominantly composed of traction till and gravity flow deposits (e.g. Reinardy et al.,
401 2013). During this stage occurrences of better sorted, meltwater-derived sediments increase in
402 volume and spatially coverage. The reservoir potential of ice-contact fans can be highly variable
403 depending upon, the sediment source and other factors (see above) (Zieliński and van Loon, 2000).

404 7.2 Water terminating

405 The style of deposition for a marine or freshwater terminating ice sheet largely depends on the
406 water depth in which the ice is grounded (i.e. ice is resting on the bed) (Glückert, 1995; Koch and
407 Isbell, 2013; Visser et al., 2003). If deposition occurs on the continental shelf, sediments delivered to
408 the ice front form a subaqueous analogue of a frontal moraine (Table 3) (Dowdeswell and Fugelli,
409 2012; Powell, 1990). Most of the sediments are deposited as gravity flows (debrites/turbidites) due
410 to slope instabilities at the ice front generated by a constant supply of water saturated sediments
411 and ice front oscillations. Grounding zone wedges (GZW) (Table 2, figure 4 and figure 6) are
412 deposited in cross-shelf troughs (figure 4) when ice stream grounding lines are stationary for a
413 period of time (Dowdeswell and Fugelli, 2012; Powell, 1990). GZWs are often transparent in
414 subsurface geophysical data (seismic), indicating little or no acoustic impedance (sediment bulk
415 density \times sonic velocity) contrast, reflecting glaciotectonic homogenisation of sediments
416 (Dowdeswell and Fugelli, 2012). Their geometries and location in ice stream troughs suggest that
417 glaciofluvial processes may play some role in the formation of GZWs (L. R. Bjarnadóttir et al., 2017;
418 Koch and Isbell, 2013), along with the deposition and reworking of traction till at the grounding line
419 (Table 3).

420 7.2.1 Advance

421 Most of the sediments deposited during an ice advance on the continental shelf have relatively low
422 preservation potential. The advancing ice sheet will most likely override and cannibalise ice marginal
423 deposits. Subaqueous ice-contact fans may be relatively well-sorted in comparison to sediments
424 bulldozed, melted out, squeezed and/or lodged by the ice movement (Table 3 and Figure 4). During
425 the ice advance, because of the lower supply of meltwater, the fans are likely to be small, short lived
426 and often overridden and/or eroded. When a fast-moving ice stream reaches the shelf edge,
427 deposition occurs primarily in the form of trough mouth fans (TMF) (Table 3, Figures 4 and 6), which
428 are very large, fan-shaped, debris flow complexes extending from the shelf edge down towards the
429 abyssal plain (Figure 4) (Dowdeswell et al., 2008; Gales et al., 2019; Ó Cofaigh et al., 2003; Vorren
430 and Laberg, 1997). Sediments are deposited by a mixture of mass wasting and glaciofluvial
431 processes. TMFs can extend for up to 200 km down the slope towards the abyssal plain with the
432 proximal thickness of sediments reaching 5 km offshore Alaska (Powell and Molnia, 1989).
433 Numerous examples, including the West Antarctica Belgica Fan (Dowdeswell et al., 2008), North Sea
434 Fan (Nygård et al., 2005; Ó Cofaigh et al., 2003) and the Barents Sea Bjørnøyerenna Fan (Laberg and
435 Dowdeswell, 2016; Vorren and Laberg, 1997), are clearly visible in bathymetry and seismic surveys of
436 formerly glaciated shelf margins.

437 From a reservoir perspective, large, subaqueous clastic fans are considered as a reservoir target, but
438 this might not apply to TMFs for three main reasons: (1) Most of the sediment is transported to the
439 shelf edge subglacially as a diamicton with limited selective sorting by meltwater; and (2) high
440 sedimentation rates and ice sheet oscillations result in oversteepening of slopes leading to
441 reworking of the material in gravity flows (Table 3); (3) Seismic data shows abundance of uniform or
442 chaotic seismic facies within the TMFs interpreted as landslide sediments which indicates mixing
443 and homogenisation. (Table 3 and Figure 6) (e.g. Bellwald et al., 2019; Olsen et al., 2013; Taylor et
444 al., 2002).

445 7.2.2 Retreat

446 Retreat of a grounded ice sheet margin, in response to climate warming involves intensified calving,
447 iceberg production and increased meltwater discharge. Higher basal meltwater pressure at the
448 ice/bed interface will facilitate faster ice flow, especially along ice streams (Benn and Evans, 2010;
449 Boulton et al., 1995), but recent observations from Greenland and arctic Russia suggest that this
450 picture may be more complex (Lane et al., 2014; Lea et al., 2014; Stokes et al., 2007; Zheng et al.,
451 2019) Sediment flux and deposition increases concomitantly as a response to the increase in
452 meltwater discharge.

453 Where ice is moving more slowly, in the inter-stream areas, morainal banks (ice-marginal moraines-
454 Table 2) usually delineate ice margin positions. They can be composed of older, cannibalised
455 sediments, traction till, well sorted proglacial subaqueous outwash and ice-contact delta deposits
456 (depending on water depth). Thin-skinned thrusting and glaciotectonic deformation (Table 3) of
457 underlying sediment has been reported from the Pleistocene succession in the North Sea and from
458 onshore Denmark and Germany (Vaughan-Hirsch and Phillips, 2017).

459 Densely spaced recessional moraines defined as sediment ridges delineating positions of short-lived
460 (possibly annual) re-advances during ice retreat (Dowdeswell et al., 2016b; Todd, 2014), are
461 frequently found on the seabed but are unlikely to be identifiable in the subsurface.

462 Grounding line fans are deposited where meltwater exits a portal across the grounding line and
463 enters a standing water body (Table 3 and Figure 4) (Mackiewicz et al., 1984; Powell and Molnia,
464 1989). Such fans form important reservoirs in the glaciogenic Ordovician succession in North Africa
465 (Lang et al., 2012; Le Heron et al., 2006). Powell (1990) described a relationship between the size of
466 the meltwater conduit, meltwater discharge, flow type (axi-symmetric or planar) and sediment
467 concentration. Gradual decrease in efflux jet energy (deceleration), distally from the meltwater
468 portal, results in proximal deposition of coarse fractions (boulders and cobbles). Sands and gravels
469 will be deposited along the length of the jet runout. From laboratory experiments it is known that a
470 high pressure jet may deposit most of its sediment load between the grounding line and a distance
471 up to 200 times the conduit diameter, where rapid flow deceleration occurs (Powell, 1990).
472 Laminations in glaciomarine sediments often reflect pulses (diurnal and/or seasonal) of meltwater
473 (Benn and Evans, 2010). Cyclopels (laminated clays and silts) and cyclopsams (laminated silts and
474 sands) (Powell and Cooper, 2002) are products of settling from turbid overflows and/or interflows.
475 Laminae are usually normally graded (fining upwards) reflecting density settling of suspended
476 sediments. Cyclopsams are usually deposited proximal to the efflux point (within 1 km from the
477 source) whereas cyclopels can be distributed over larger areas (several kilometres) (Mackiewicz et
478 al., 1984; Powell and Molnia, 1989). In lacustrine conditions laminated or varved sediments indicate
479 the transition between the warm season with meltwater input (bright and coarser laminae) and the
480 cold season with a frozen water surface, decreased sediment supply and temporary anoxia (dark,
481 finer laminae).

482 When an ice sheet is grounded in relatively shallow marine or lacustrine waters (10's of meters
483 rather than 100's) and meltwater transports abundant sediment to the ice margin, multiple
484 subaqueous fans and/or deltas may be constructed (Table 3 and Figure 4). Their location and size
485 will depend mainly on the period of ice margin stillstand (longer = bigger) and subglacial drainage

486 pattern. It appears that interlobate zones (confluence between ice lobes) can be associated with the
487 volumetrically largest sediment accumulations (Gruszka et al., 2012; Saarnisto and Saarinen, 2001).

488 Most of the well-sorted sediments will be deposited during this stage at, or proximal to, the ice
489 margin, as ice-contact deltas or fans (Table 3, Figure 4 and Figure 6)(Dietrich et al., 2017; Fyfe, 1990;
490 Lønne, 1995; Powell and Molnia, 1989). Large, reservoir-quality, sediment accumulations are usually
491 associated with periods when the ice margin stabilizes for longer during overall retreat. The well-
492 sorted sediments will most likely be blanketed by glaciomarine muds as the ice margin becomes
493 more distal. Glaciomarine and glaciolacustrine muds, often varved, have similar properties. These
494 lithotypes have a high seal capacity (Dahlgren et al., 2005; Eyles et al., 1985; Powell and Cooper,
495 2002). Some of the geotechnical properties of glaciomarine and deglacial muds have been discussed
496 in the context of slope stability by Kvalstad et al., (2005) and applied in a numerical model by
497 Bellwald et al., (2019).

498 8 Proglacial zone

499 8.1 Terrestrial

500 In the proglacial zone, deposition occurs mainly through glaciofluvial processes. After exiting the ice
501 sheet through portals, sediment-laden meltwater deposits broad sand and gravel-rich braidplains –
502 sandar (singular: sandur (Table 2)) (Magilligan et al., 2002; Maizels, 2007; Pisarska-Jamrozy, 2015;
503 Zielinski and Van Loon, 2003). Multiple meltwater input points, no identifiable fan apex and frequent
504 avulsions are characteristic of sandar (Zielinski and Van Loon, 2003). If the terrain constrains the
505 meltwater, a valley train, i.e. a valley-filling sediment belt, may be deposited. If the topography rises
506 away from the ice margin a proglacial lake may form (Martin et al., 2008). If a sandur is not in direct
507 connection with a water body, an ice marginal spillway network will ultimately drain the meltwater
508 away from the ice margin towards the nearest basin depocentre (Brodzikowski and van Loon, 1987).
509 Examples of both settings are known from Pleistocene glacial landsystems in Germany and Poland
510 (Pisarska-Jamrozy, 2015; Rinterknecht et al., 2012).

511 8.1.1 Advance

512 During the initial advance rivers may incise their valleys re-mobilising and removing part of the
513 sedimentary sequence of the proglacial zone as a response to sea level fall. It is important to re-
514 emphasize that meltwater discharge is lower during advance than retreat and will result in a reduced
515 area of active sandar deposition (Table 2). The proglacial drainage network will be re-arranged if ice
516 advances beyond an earlier terminal moraine. Vegetated areas in the proglacial deposition zone may
517 be partially blanketed by outwash sands and gravels. With decreasing distance from the ice margin
518 to the next sediment sink and a falling sea level, the angle of depositional slope increases, resulting

519 in upward coarsening facies and/or fluvial incision into the shelf and low stand delta progradation.
520 Proglacial glaciofluvial sediments have the best reservoir properties of all identified glaciogenic
521 landforms and sediments (Figure 4). They will likely reach their maximal lateral extent but not
522 maximal thickness during this stage. In general, glaciofluvial sediments of sandar deposited during
523 the ice advance can have good reservoir properties but they are often overridden by the advancing
524 ice sheet, which results in deformation and at least partial erosion of the sequence. Thin, sheeted
525 reservoir geometries are to be expected.

526 8.1.2 Retreat

527 As the melt increases and the ice margin retreats, a large amount of sediment is transported and
528 deposited by meltwater into the proglacial zone (Figure 4) as sandur deposits (Girard et al., 2012; Le
529 Heron, 2007; Magilligan et al., 2002; Pisarska-Jamrozy and Zieliński, 2014). Pitted sandar (Table 3)
530 develop where blocks of ice are completely, or partially, buried by glaciofluvial outwash and
531 subsequently melt away leaving a pitted kettle hole surface (dead ice topography)(Fleisher, 1986;
532 Thwaites, 1926). Some sandar may be deposited, or augmented, by periodic, high magnitude,
533 flooding events (jökulhlaup/glacial lake outburst floods) rather than by seasonal surface-melt driven
534 meltwater discharge (Girard et al., 2012; Gomez et al., 2000; Winsemann et al., 2016). An erosional
535 base and very large scale bedforms characterise deposits from such events (Marren, 2005). The
536 spatial extent and catastrophic nature of jökulhlaup deposits may be used to establish an isochron
537 for, at least part of, a glacial sedimentary sequence in the proglacial zone (Hanson and Clague, 2016).
538 One, or a series of, sub-basin/s may have been created between the moraine/s deposited during the
539 first stadial maximum advance, which are exposed on retreat providing accommodation space for
540 glaciofluvial sediments. This backfilling pattern is typical for glacial environments when space,
541 previously occupied by the ice sheet, is infilled by sediments released after the ice front retreats. Ice-
542 contact lakes, often developed between the ice margin and a moraine ridge/complex (García et al.,
543 2015), are typically infilled with sediment derived from a mixture of paraglacial and glaciofluvial
544 processes (Table 3 and Figure 5). Glacier-fed deltas (Table 3) may also develop in places where a
545 sandur terminates in a proglacial lake. The size the delta largely depends on landscape topography,
546 ice sheet geometry, and spillway elevations and size of the lake (a spillway is a pathway developed
547 when water from an ice-contact lake overflows the lowest point of the constraining topography)
548 (Benn and Evans, 2010). The seasonal nature of meltwater discharge (low in the winter and very high
549 in the summer) results in a large annual variation in the volume and grainsize of sediments being
550 deposited in proglacial lakes. When such a lake becomes infilled by outwash sediments sandur
551 deposition will re-commence (Pisarska-Jamrozy and Zieliński, 2014). On newly deglaciated terrain,
552 large exposures of fine-grained unconsolidated sediments, with little to no vegetation cover, are

553 highly susceptible to aeolian reworking (Chewings et al., 2014; Derbyshire and Owen, 2017;
554 Mountney and Russell, 2009). Fine fractions are entrained, transported and deposited by wind,
555 filling depressions from the small scale all the way up to large scale regional loess covers (Derbyshire
556 and Owen, 2017). Major sand dune systems may be present on sandur plains and other proglacial
557 areas (Ballantyne, 2002; Ballantyne, 2002; Maizels, 1997).

558 Distally, where the ice sheet had no direct influence on landform genesis, the only indication of ice
559 retreat may be found in deltaic or shoreline sedimentary records (Figure 5). During this time sea
560 level will generally rise, resulting in marine transgression. The regional sea level will be a function of
561 the eustatic sea level change, isostatic rebound, forebulge collapse (the kinematic response of the
562 lithosphere to off-loading following ice sheet retreat) and reduction in gravitational attraction. The
563 crest of the decaying Fennoscandian ice sheet forebulge, post Last Glacial Maximum at 15,000 ka BP
564 was estimated by Fjeldskaar (1994) to be 100 km beyond the ice margin and elevated by 60 m,
565 decreasing to 40 m by 11,000 years BP. High-discharge glacial rivers can transport large volumes of
566 sediment resulting in rapid progradation of marine and lacustrine deltas even at a significant
567 distance from the ice sheet margin (e.g. Pleistocene Mississippi River delta (Fildani et al., 2018)).

568 8.2 Marine/Lacustrine

569 Distal from the grounding line, beyond direct deposition from meltwater jets, muds and marine
570 diamictons are dominant (Table 3 and Figure 4, Figure 6) (Ó Cofaigh, 1996). Deposition occurs from
571 density currents and suspension settling, creating a fine grained, often laminated, package with
572 outsized clasts (dropstones, iceberg rafted debris (IRD - Table 4)) supplied by, and melted out from,
573 floating icebergs. This glacial marine diamicton (Table 3) is diagnostic for the presence of grounded ice
574 in the basin. Localised mass-wasting and slope processes associated with over-steepened slopes
575 occur (Clerc et al., 2013; Evans et al., 2012; Koch and Isbell, 2013). Proglacial muds often preserve
576 iceberg plough marks (Table 3) (Benn and Evans, 2010), which are formed when grounded icebergs
577 are pushed by the wind and ocean currents. They are typically v-shaped, linear or curvilinear furrows
578 in the seabed. In extreme cases, iceberg ploughing of sediments can destroy all primary sedimentary
579 structures leaving behind a structureless marine diamicton (Table 3 and Figure 4) (Benn and Evans,
580 2010). Length and depth of an individual plough mark largely depends on the water depth and
581 iceberg size (Dowdeswell and Bamber, 2007). The presence of iceberg plough marks preserved in
582 sediment packages requires grounded ice within the marine or lacustrine setting (Figure 4 and Figure
583 6).

584 8.2.1 Advance

585 Proglacial deposition occurring during ice advance has a limited preservation potential as it will be
586 subsequently overridden by the advancing ice sheet (Figure 6). Sedimentary packages will either be
587 eroded subsequently, creating an upper erosional unconformity, or deformed by overriding ice.
588 Some sediments may, however, be preserved if deposited in seabed depressions or larger basins.

589 Proglacial deposition occurs on the continental slope and into the abyss if the ice sheet extends all
590 the way to the continental shelf break and the grounding line is approximately collinear with the
591 shelf edge (Figure 4 and Figure 6) (Elmore et al., 2013; Ó Cofaigh et al., 2003; Powell and Alley, 1996).
592 Greater water depth, steep depositional slope and high accommodation, with respect to the
593 continental shelf, aids dispersal of the sedimentary package delivered by glaciofluvial processes
594 (Dowdeswell and Dowdeswell, 1989). Settling from suspension, mass-flows with long run-out
595 distances (distal turbidites from TMFs) and slope failures are the dominant depositional processes
596 on the slope. The final sediment assemblage in the abyss will consist mostly of laminated marine
597 shales with dropstones and iceberg dump deposits sometimes interbedded with density current
598 deposits and slump facies (Table 3) (Brodzikowski and van Loon, 1987). Sorted sandy sediments may
599 be deposited and/or reworked by contour currents forming contourites (Table 3) (Camerlenghi et al.,
600 2001; Lucchi and Rebesco, 2007; Stuart and Huuse, 2012). There is little potential for reservoir
601 quality packages to be deposited apart from TMFs and contourites (Figure 4) (Dowdeswell et al.,
602 2008; Laberg and Dowdeswell, 2016; Vorren and Laberg, 1997). Glaciomarine muds can be
603 considered as a good sealing lithology. Influence of iceberg plough marks on the pre-existing
604 sediments should be carefully considered; their keels can deform sediments to a significant depth.
605 The sealing properties of the glaciomarine muds may be degraded if ploughmarks are of sufficient
606 depth and are subsequently filled with more permeable sediments (Figure 4).

607 8.2.2 Retreat

608 The depositional zones (Figure 4) are linked to the grounding line/ice margin position, which changes
609 over the lifespan of the ice sheet (e.g. Andreassen *et al.*, 2014). As deglaciation commences, the
610 grounding line/ice margin retreats, revealing the seabed that was previously in the ice marginal or
611 subglacial depositional zone. The stratigraphic change in deposition from ice marginal to proglacial
612 may be gradual up-section if the ice margin retreat is slow (continuous annual retreat at a similar
613 rate), or abrupt, if retreat is rapid/catastrophic and it occurs over a significant distance (Sejrup et al.,
614 2016; Stokes et al., 2015). If the retreat is gradual ice-contact deltas may transition into glacier-fed
615 deltas (Table 3 and Figure 4, Figure 5 and Figure 6) as the ice sheet retreats and the ice margin
616 emerges from the water (Dietrich et al., 2017, 2016; Dietrich and Hofmann, 2019). Glacier-fed deltas
617 are one of the most prospective reservoir candidates as the sediments are commonly sand

618 dominated and the depositional processes are efficient at sorting and portioning the different
619 grainsizes, resulting in thick, laterally extensive packages with good reservoir properties.

620 In the marine proglacial zone, sediments may be transported offshore either in suspension or
621 trapped in icebergs that move with the ocean currents and winds. Sediments encased in icebergs are
622 subsequently melted out as dropstones and iceberg rafted debris (IRD -Table 3) (Benn and Evans,
623 2010), sometimes many hundreds of kilometres away from where they detached from the ice sheet.
624 The grain size distribution in glaciomarine sediments deposited from iceberg rainout varies greatly. It
625 is dependent upon the iceberg calving rate, debris concentrations in the ice sheet, meltwater
626 discharge, particle size of the parent sediment (lithology of the source area) and oceanographic
627 conditions including, but not limited to, water column density and bottom current winnowing,
628 transport and deposition (e.g. contourites –Table 3) (Benn and Evans, 2010). Dropstone
629 concentration appears to decrease with distance from the grounding zone (Dowdeswell and
630 Dowdeswell, 1989; Dowdeswell *et al.*, 2016). A bimodal grainsize distribution is a common
631 characteristic of glaciomarine diamicton (Table 3) where suspension settling, from buoyant sediment
632 plumes, is accompanied by coarser IRD deposition. Layers containing higher proportions of coarser
633 material may indicate increased calving due to rapid retreat of ice during deglaciation (Bond *et al.*,
634 1992; Hodell *et al.*, 2017). Dropstones and iceberg dump deposits are commonly used as a diagnostic
635 indicator of the proximity of ice sheets in the sedimentary basin (Bennett *et al.*, 1996). However, the
636 presence of dropstones in fine-grained sediments may also be explained by non-glacial processes
637 including deposition from floral mats (coarse material entangled in roots), volcanic bombs and
638 outrunner clasts from debris flows (Bennett *et al.*, 1996). Therefore, care must be taken when
639 investigating sediments of Carboniferous and younger age when flora was widespread. The presence
640 of iceberg dump deposits, in the form of massive, unsorted and structureless diamicton or
641 boulder/gravel lenses in otherwise fine marine muds allows for a more confident interpretation of
642 proximal glacial conditions. Sealing (rather than reservoir) lithologies can be expected to be
643 deposited in this zone. If ice flux is sufficiently high icebergs can locally supply coarser, moderately
644 sorted material into the marine environment. This iceberg-supplied package can be considered to
645 have moderate reservoir potential. Other than that, glaciomarine muds can be considered as a
646 regional seal candidate over a deglaciated area (Figure 4). The longevity and magnitude of the
647 highstand, coupled with the sediment supply, control probability of a regional seal being deposited.
648 Following the deglaciation of the Ordovician ice sheet in North Africa, such highstand conditions led
649 to the deposition of the Silurian hot shales, which act both as a source rock and a regional seal for
650 hydrocarbon accumulations in the region (Le Heron *et al.*, 2009; Lüning *et al.*, 2000).

651 8.2.3 Littoral reworking

652 The interplay of interglacial/postglacial sea level rise and glacial isostatic rebound often results in
653 marine/lacustrine regression and/or a transgression causing emergence or submergence of
654 deglaciaded landscapes (Mitrovica and Milne, 2002). Partial erosion and re-deposition of glacial
655 sediments and modification of glacial landforms by wave action and currents can be expected in
656 both cases (Dowdeswell and Ottesen, 2016) and a degree of postglacial reworking and re-deposition
657 of landforms and sediments is almost inevitable following deglaciation and should be considered a
658 normality rather than an exception. However, numerous examples of submerged or emerged glacial
659 landscapes with limited reworking are reported from the North Sea (Emery et al., 2019b, 2019a),
660 North America (Barrie and Conway, 2016; Ward et al., 2019) and Europe (Glückert, 1986;
661 Rinterknecht et al., 2004), suggesting that, in many instances, this has had little impact. This may be
662 due to the rapidity of relative sea level rise. Sorting related to littoral reworking may improve
663 reservoir properties of glaciogenic deposits.

664

665 8.2.4 Extreme scenarios

666 A melting ice sheet has the potential to produce very large volumes of water, that can be released in
667 a controlled manner through the subglacial drainage system, gradually supplying the marine,
668 proglacial zone. If meltwater is stored in an ice dammed lake, it may be released in a catastrophic
669 event which has the potential to scour the topography, erode and transport large volumes of
670 sediments far offshore. Examples include; breaching of the land connection between present-day
671 France and Great Britain, through the English Channel, sculpting large sandur areas in NE Poland
672 and breaching a topographic high in Germany (Gupta et al., 2017; Meinsen et al., 2011; Weckwerth
673 et al., 2019). An even more extreme example can be found between Labrador and Greenland in the
674 Labrador Sea; submarine channels originate at the shelf edge and extend all the way to the abyssal
675 plain in water depths of 3 - 4 km. A large submarine channel with a 200 m high levee complex is
676 present in the area. Outside the channel a coarse-grained braid plain with linguoidal bar forms has
677 been described by Hesse et al. (2001). The shape of the channel and barforms indicate extremely
678 high magnitude flows originating from the area of Hudson Bay and are linked to deglaciation of the
679 Laurentide ice sheet.

680 8.2.4.1 Tunnel valleys

681 Tunnel valleys (Table 4, Figure 4, Figure 5 and Figure 6) are elongated depressions eroded by
682 meltwater into underlying deposits and are best known from Pleistocene successions in the North
683 Sea, Western and Eastern Europe, Canada and ancient glacial deposits in Australia and North Africa
684 (Andersen *et al.*, 2012; Sandersen and Jørgensen, 2012). They can range from several to tens of

685 kilometers long, may be several kilometers wide and usually up to a couple of hundred meters deep.
686 The architecture of their infill is intimately linked to the landsystem in which they were created.
687 Some tunnel valleys, eroded beneath land terminating ice sheets, are subsequently infilled with
688 outwash sediments while others remain under-filled and become lakes following the ice margin
689 retreat (Thomas, 1984). When eroded at the seabed, they are subsequently infilled by either
690 subaqueous outwash sediments, glaciomarine diamicton, distal glaciomarine or marine muds,
691 associated with deglacial and interglacial conditions (L. R. Bjarnadóttir et al., 2017; Fichler et al.,
692 2005; Ghienne and Deynoux, 1998; Livingstone and Clark, 2016; Stewart et al., 2013; van der Vegt et
693 al., 2016). Slump deposits associated with wall collapse have been reported from several tunnel
694 valleys (van der Vegt et al., 2016). Tunnel valley fills may, or may not, be of glacial origin (Clerc et al.,
695 2013; Moreau and Huuse, 2014; Praeg, 2003) testifying to the complexity of processes governing
696 their infilling (e.g. Forbes et al., 2010; Stewart et al., 2013). Subglacial to proglacial tunnel valleys
697 (Table 3 and Figures 4, 5 and 6) are reported both from the Pleistocene section of the North Sea and
698 the Barents Sea (L. R. Bjarnadóttir et al., 2017; Praeg, 2003; van der Vegt et al., 2016). In the North
699 Sea they seem to be mainly of Middle to Late Pleistocene in age. Ancient tunnel valleys in marine
700 settings are reported from the Illizi Basin in Algeria where the Ordovician age reservoirs host
701 significant hydrocarbon reserves (Dixon et al., 2010; Hirst, 2012).

702 9 Discussion

703 The purpose of this paper is to provide an overview of current understanding of glacial
704 sedimentology from a hydrocarbon reservoir perspective. Glacial systems are extremely dynamic
705 and highly transient. The models described above are snap-shots of specific times in the history of an
706 idealised system and the final product that ends up in the rock record is a product of significant
707 reworking and over printing (Figure 7). In the following discussion we focus on the aspects of the
708 systems that produce the key components of hydrocarbon reservoir systems, especially the
709 architectural elements that have the potential to act as reservoirs for hydrocarbon, as aquifers for
710 water or sites for CO₂ storage.

711 9.1 Implications for hydrocarbon exploration

712 The description of landforms and sediments summarized in the conceptual model (Figures 3 and 4)
713 have a number of implications for hydrocarbon reservoir distribution: (1) the majority of subglacial
714 sediments and landforms, both in terrestrial and marine environments have poor reservoir
715 properties and are most likely to provide sealing lithologies on top of reservoirs or intraformational
716 barriers and baffles to fluid flow within reservoirs, (2) subglacial traction till is rarely continuous and
717 should not typically be considered as a regional seal, (3) in each ice sheet advance the subglacial
718 zone is marked by an extensive erosional surface which does not necessarily have to be overlain by

719 traction till. This implies that older, reservoir quality sediments may be partially or fully eroded
720 (Figure 7). When only partially eroded, they do not necessarily have to be covered (sealed) by a
721 traction till carapace. Lack of a sealing till layer on top results in older glacial sediments being in
722 connection with a subsequent, deglaciation sediment package (Figure 7) (4) eskers can add to the
723 volume of, and/or provide reservoir connectivity between, isolated, larger reservoir quality
724 sediment accumulations (ice-contact deltas, subaqueous outwash fans) deposited during ice margin
725 retreat, (5) sediments and landforms in the ice marginal zone have the most diverse composition
726 and show rapid changes over very short distances along the ice margin and their reservoir properties
727 depends on the mode of deposition (glaciofluvial may have moderate to good reservoir properties,
728 material bulldozed by ice or deposited from gravity flows at the ice margin will have poor to non-
729 reservoir properties), (6) proglacial zone sediments in terrestrial environments (sandar) have the
730 best reservoir properties and can be very extensive but their preservation over geological timescales
731 is uncertain if deposition occurs above the erosional baseline, (7) ice marginal-to-proglacial
732 glaciofluvial deposits (ice-contact deltas, glacier-fed deltas, subaqueous ice-contact fans) have both
733 good reservoir properties and high potential to be preserved in the rock record, and their deposition
734 is strictly associated with the ice margin (Figures 4 and 7), (9) glaciomarine or glaciolacustrine
735 diamicton has the potential to provide a regional seal if an ice sheet is marine or lake terminating
736 (Figures 4 and 7).

737 Some of the above points can be illustrated by hydrocarbon discoveries made in glaciogenic
738 sequences. In the North Sea the Peon gas discovery is interpreted to be hosted in a subaqueous
739 outwash fan deposited during ice margin retreat, which was subsequently overridden by ice margin
740 re-advance and sealed by a traction till carapace (Ottesen et al., 2012). The Aviat gas field, which has
741 also been interpreted as a subaqueous outwash fan is sealed by a thick package of glaciomarine
742 diamictons and marine muds (Rose et al., 2016). Gas fields in North Africa, including In Amenas and
743 Elephant fields, are hosted in glaciogenic rocks (Mamuniyat Formation) deposited over a glacial
744 erosional surface (GES) (e.g. Bataller et al., 2019; Hirst, 2012; Le Heron et al., 2009, 2006; Lüning et
745 al., 2000). The reservoir intervals show a broad spectrum of grainsizes, multiple minor internal
746 erosional contacts and at least two extensive GESs indicating two or more ice sheet re-advances
747 (Heron et al., 2015; Le Heron et al., 2009). They also fill valleys incised into older strata either, by
748 meltwater (tunnel valleys) or, ice streams (cross shelf troughs) (El-Ghali, 2005; Le Heron et al., 2018).
749 Recent studies indicate that ice streaming in ancient deposits is more common than previously
750 thought and can be recognized from glaciogenic successions of Ordovician and Late Palaeozoic age
751 (Andrews et al., 2019; Assine et al., 2018; Elhebery et al., 2019; Heron, 2018). Identification of such
752 features in the subsurface can aid understanding sediment transport mechanisms, mode of

753 deposition, resulting reservoir distribution and fluid migration pathways. Moreover, some
754 interpretations which describe large scale glaciogenic, erosional features as glacial valleys or palaeo-
755 valleys from ancient deposits may require re-evaluation (e.g. Clark-Lowes, 2005; Hirst et al., 2002;
756 Powell et al., 1994; Vaslet, 1990). The troughs may represent either palaeo-ice stream corridors or
757 tunnel valleys (Kehew et al., 2012; Ottesen et al., 2002; Stokes and Clark, 2001; van der Vegt et al.,
758 2016). The ability to discern them has significant implications for the understanding of their position
759 within the glacial environment and expected reservoir distribution. A careful morphometric study of
760 modern and ancient examples remains to be completed.

761 Sediments of the Hirnantian glaciation in North Africa are anomalous in that they are almost entirely
762 composed of sandy fractions (Deschamps et al., 2013; Hirst, 2012; Le Heron et al., 2009). This
763 phenomenon has been attributed to the Hirnantian ice sheet advecting, reworking and re-depositing
764 sandy shoreface sediments present in the region prior to the onset of glaciation (Le Heron et al.,
765 2009). For this reason, North African outcrops may be somewhat different to glaciogenic sequences
766 in the subsurface elsewhere. In Saudi Arabia the Hirnantian aged glaciogenic rocks are an important
767 target for gas exploration (Craigie et al., 2016; Ehlers et al., 2011; Melvin, 2019; Michael et al., 2018,
768 2015). In the south the Sanamah Formation includes sandar, glacier-fed deltas and/or ice-contact
769 deltas deposited over traction tills. In the north the Sarah Formation is comprised of marine, ice
770 marginal and proglacial deposits described as glacier-fed deltas, prodelta muds, shallow shelf and
771 deep marine facies (Michael et al., 2018). Time- equivalent facies in Jordan consist of subglacial,
772 glaciofluvial and glaciodeltaic deposits and proglacial turbidites and “sheet like lobe deposits”
773 (possible subaqueous outwash fans) in the south (Hirst and Khatatneh, 2019; Michael et al., 2018).
774 Common characteristics of all these areas is the occurrence of cross-cutting, incised valley networks
775 testifying to multiple phases of ice advance and retreat which can also be observed from Pleistocene
776 glaciations e.g. in the North Sea (Craigie et al., 2016; Kristensen et al., 2007; Le Heron, 2007;
777 Lonergan et al., 2006; Michael et al., 2018; Stewart and Lonergan, 2011). Here the glaciogenic
778 sequence is capped regionally by glaciomarine diamicton facies, with abundant dropstones,
779 illustrating deglaciation and post-glacial sea level rise (Fortuin, 1984; Ghienne, 2003; Le Heron et al.,
780 2010; Lüning et al., 2000). In Oman, the glaciogenic Al-Khlata Formation (late Carboniferous - early
781 Permian) forms an important reservoir target in the South Oman Salt Basin (e.g. Al-Abri et al., 2018;
782 Forbes et al., 2010; Hadley et al., 1991; Levell et al., 1988; Millson et al., 1996). It has been
783 interpreted to have been deposited by land terminating ice sheets as sandar, glacier-fed deltas and
784 ice-contact deltas deposited in glaciolacustrine environments during multiple phases of the ice sheet
785 advance (erosion and diamictic facies deposition) and retreat (reservoir quality glaciofluvial and

786 glacio-deltaic facies capped by glaciolacustrine muds) (Al-Abri et al., 2018; Heward and Penney,
787 2014; Osterloff et al., 2004b).

788 The conceptual model presented here offers a 2D, bird's eye view of a glaciated landsystem at any
789 given time. From this it is possible to trace the relative movement of the depositional zones in
790 response to ice sheet advance and retreat by plotting glacial sediments/landforms identified in
791 vertical succession from outcrops, wells or seismic data on the diagram (Figure 4). This allows
792 reconstruction of the depositional zones (subglacial, ice marginal and proglacial) and the
793 depositional environment (terrestrial, lacustrine, shallow marine, deep marine). This will aid in
794 correlation and ultimately prediction of potential reservoir-quality sediments up or down the
795 depositional dip.

796

797 9.2 Other considerations

798 Glaciogenic deposition is extremely dynamic (in relation to geologic time scales). An ice sheet margin
799 migrates in response to climate forcing and ice sheet dynamics, which may result in rapid spatial and
800 temporal changes of both the mode and location of deposition. A depocenter which was initially in
801 the ice-marginal depositional zone on land can be overridden by an advancing ice margin relatively
802 quickly and moved into the subglacial depositional zone. Alternatively, the subglacial zone may
803 rapidly give way to the proglacial depositional zone as the ice margin retreats. During retreat a land
804 terminating ice sheet margin can quickly become grounded in water due to rising sea level and/or
805 development of a large proglacial lake. This leads to different sediment and landform assemblages
806 being deposited, over the same area, in a very short period of time. It is crucial to emphasize that
807 such changes can be repeated multiple times in a vertical sedimentary succession. Although
808 dynamic, the basic geological laws of superposition (Steno) and lateral and vertical facies succession
809 (Walther), still hold true (Steno, 1671; Walther, 1893). Nonetheless, the series of events leading to
810 the deposition of a given succession maybe much more difficult to unravel.

811 The characteristics of the sedimentary sequence depends upon the sediment/bedrock present in the
812 subglacial zone, from where most of the sediment is advected. For example, an Ordovician marine
813 glaciogenic sediment sequence is described by Le Heron et al. (2009) as particularly sandy, as a result
814 of entrainment of overridden sandy aeolian and shoreface sediments, present in abundance at that
815 time on the northern margin of the palaeo-African continent. Alternatively, Pleistocene ice sheets
816 entering the North Sea basin from the W/NW (Shetland Platform and UK mainland) and E/NE
817 (present day Norway and Sweden) cannibalised fine grained sediments of deltaic and paralic origin
818 (Lamb et al., 2017; Rea et al., 2018; Stoker et al., 2011), re-working and re-depositing them as a finer

819 grained sediment package further into the basin. The diversity of sediment types emphasizes the
820 necessity to investigate glacial sedimentary sequences holistically, with respect to underlying and
821 overlying non-glacial sequences and available sediment sources in the area/region. Identification of
822 individual facies associations or morphological elements may not be sufficient to confidently
823 recognize glaciation. However, there are several diagnostic, non-depositional features and landforms
824 that have been included in the model (tunnel valleys, mega-scale glacial lineations, ploughmarks
825 etc., (Table 3, Figures 4, 5 and 6) explicitly to aid identification of a glacial succession.

826 An ice sheet is deemed land terminating when the majority of the ice margin is located on an
827 emerged surface above the mean sea level (Figure 4 and Figure 6) (Benn and Evans, 2010). If
828 accommodation is available terrestrially this will be filled with glaciofluvial and glaciolacustrine
829 deposits depending on: 1) meltwater discharge; 2) sediment availability; 3) topography; 4) ice sheet
830 geometry and 5) distance from the ice margin to the basin depocenter. Examples include Ordovician
831 sediments in intracratonic basins in Northern Africa and Carboniferous-to-Permian sediment basin-
832 fills in Oman and Saudi Arabia (Khalifa, 2015; Le Heron et al., 2009; Levell et al., 1988; Martin et al.,
833 2012). Glacial deposition may occur on land even when no accommodation is available by creating
834 positive topography or filling features eroded by the ice into the underlying bedrock and/or
835 sediments (Bennett, 2003; Deschamps et al., 2013; Le Heron et al., 2009; Swartz et al., 2015). This
836 can be seen, for example, from Pleistocene ice marginal and proglacial deposits associated with the
837 Fennoscandia ice sheet in Germany, Denmark, Poland, Latvia and Estonia (e.g. Andersen et al., 2012;
838 Marks, 2005; Rinterknecht et al., 2012). On longer timescales, the preservation of positive
839 topography is, at best, uncertain (Figure 6). Ice-contact and proglacial lake deposits are also included
840 in this depositional system. The distribution of sediments and landforms (Figure 4 and Figure 5)
841 associated with a land terminating ice sheet can be highly complex (Figure 6). Traction tills deposited
842 during ice advances dominate the subglacial depositional zone. During deglaciation, back stepping of
843 the ice front may result in partial erosion and remobilization of subglacial deposits and/or blanketing
844 by glaciofluvial deposits (sands and gravels). Backfilling of accommodation created by ice retreat is a
845 key characteristic of land terminating ice sheets (Figure 5). Subsequent ice sheet re-advance can
846 remove parts, or all, of the sediment packages deposited during previous glacial episodes, as well as
847 interglacial deposits. However, it has been demonstrated by Bellwald et al. (2019) that, under
848 favourable conditions, landforms associated with multiple ice flow episodes can be preserved in the
849 sedimentary record. In terms of reservoir potential, glaciofluvially sorted sediments in the proglacial
850 zone (sandur - Table 2, Figure 4 and Figure 5) most likely have the best reservoir quality. Sands and
851 gravels deposited in topographic lows have also the highest preservation potential. Finally,

852 sediments deposited during the final deglaciation are more likely to be preserved due to lack of
853 subsequent subglacial erosion and postglacial eustatic sea level rise.

854

855 Landforms and sediments associated with Pleistocene and older ice sheets indicate that, in many
856 instances, they extended across the continental shelf terminating in the ocean or terminated in a
857 large, fresh water body, for at least a part of their existence (Figure 6) (Dowdeswell et al., 2016b;
858 Eyles et al., 1985). Marine terminating ice sheets cannot extend beyond the shelf break. It is the
859 ultimate boundary, beyond which no ice sheet can remain grounded because of the increased
860 calving flux and submarine melting (Benn and Evans, 2010). This means that the ice flux can never be
861 high enough to sustain an advance into the ever-increasing water depths. In certain circumstances
862 ocean-scale ice shelves can form, which are up to a kilometre thick and ground on bathymetric highs
863 e.g. the Central Arctic Ocean on the Lomonosov Ridge (Jakobsson et al., 2010). Evidence of this is
864 widespread at high latitudes across the world (e.g. Dowdeswell et al., 2008; Ó Cofaigh et al., 2003),
865 where the bathymetry and sedimentology of continental shelves, all the way out to the shelf break,
866 reveals a rich assemblage of glacial landforms and sediments associated with proximal grounded ice
867 (e.g. Andreassen and Winsborrow, 2009; L. R. Bjarnadóttir et al., 2017; Bjarnadóttir and Andreassen,
868 2016; Dowdeswell and Fugelli, 2012; Esteves et al., 2017; Greenwood et al., 2018; Hodgson et al.,
869 2014; King et al., 2016; Kurjanski et al., 2019) (Bjarnadóttir and Andreassen, 2016; Greenwood et al.,
870 2018; Hodgson et al., 2014; King et al., 2016; Kurjanski et al., 2019). However, large volumes of
871 sediments delivered subglacially to the shelf break and deposited on the continental slope during
872 glaciation can cause the shelf to prograde basinward (Figure 6) (Eyles et al., 1985; Knutz et al., 2019;
873 Ottesen et al., 2012). This can be observed in seismic data on the north Norwegian continental
874 margin as well as the Norwegian, Danish, Dutch and German sectors of the North Sea (Ottesen et al.,
875 2012; Rea et al., 2018). Most coarse-grained sediments are deposited in the ice marginal zone
876 (Figure 4), proximal to the grounding line. Since ice can be grounded at depths exceeding several
877 hundred meters it is possible that coarse grained sediments will be deposited directly into deep
878 water. Sediment distribution in glaciomarine environments (Figure 4 and Figure 6) appears to be a
879 function of sediment input location, oceanographic conditions and distance from the grounding line.

880

881 Ice sheets terminating in, and interacting with, large lacustrine basins are also common (Carrivick
882 and Tweed, 2013; Murton et al., 2010; Patton et al., 2017). Generally, the interplay between crustal
883 isostatic response beneath, and beyond, an ice sheet margin promotes the formation of proglacial
884 lakes (Figure 2) (Carrivick and Tweed, 2013). For example, during the last glaciation (MIS 2-4, the

885 Wisconsinian) the Laurentide ice sheet was partially grounded along its southern margin in Lake
886 Agassiz and Lake Ojibway (Carrivick and Tweed, 2013; Levson et al., 2003; Thorleifson, 1996). The
887 lakes had a combined water volume of up to 163 000 km³ (Leverington et al., 2002), which equals
888 two times the volume of the, present-day, Caspian Sea and seven times the volume of the, present
889 day, Lake Baikal. In the South Salt Basin in Oman, the upper part of the Permo-Carboniferous Al
890 Khlata formation is interpreted as a large proglacial lake system (Martin et al., 2008; Osterloff et al.,
891 2004b). These large proglacial lakes may be intermittently connected to seas or oceans. For
892 example, the southern margin of the Fennoscandian ice sheet, during retreat from the Last Glacial
893 Maximum was grounded in the Baltic ice lake, which, at the time, had no connection to the global
894 ocean (Houmark-Nielsen, 2007; Uścińowicz, 2004; Vassiljev and Saarse, 2013).

895 It is crucial to emphasise that all the above environments can be interchangeably present over the
896 same area during the lifespan of one icehouse. Moreover, the final sediment assemblage is most
897 likely a result of multiple ice advance and retreat stages (glacial-interglacial cycles) superimposed on
898 each other with multiple erosional episodes (ice advance) removing a part or even a whole section
899 deposited during a previous glaciation. As a result, it is unlikely that the full sedimentary package
900 associated with an icehouse period will be preserved (Figure 6).

901 9.2.1 Improved imaging workflows, techniques and equipment

902

903 The typical offshore hydrocarbon workflow commences with gravity and magnetic surveys followed
904 by several widely spaced, long regional 2D (older standard) or large-scale 3D surveys aiming to
905 uncover the general structure of the basin (Alsadi, 2017; Nanda, 2016; Sengbush, 1983).
906 Subsequently a more targeted, densely spaced 2D (older standard) survey was performed or, more
907 likely now, part of a 3D cube is selected and often reprocessed over a prospective area. If the
908 prospective area is deemed worthy, a high-resolution, shallow-looking (higher frequency,) 2D or 3D
909 site survey, aiming to identify potential geotechnical and drilling hazards is contracted (Camargo et
910 al., 2019; Lane and Taylor, 2002; Shmatkova et al., 2015; Zhang et al., 2016).

911 This workflow, is not optimal for exploration in glaciogenic sequences for several reasons: (1) lower
912 frequencies resulting in poorer vertical resolution cannot image subtle, glaciogenic features (MSGL,
913 iceberg ploughmarks etc.) that are crucial for identification of a glaciogenic package and for
914 understanding its position within the glacial landsystem (Bellwald et al., 2018; Bellwald et al., 2019;
915 Bellwald and Planke, 2019). (2) Site-surveys of the shallow subsurface are almost exclusively focused
916 on identifying hazards and are not evaluating potential opportunities associated with shallow gas
917 accumulation (Huuse et al., 2012; Ottesen et al., 2012; Rose et al., 2016). The division between an
918 exploration survey versus a site-survey may result in missed opportunities.

919 Recent technological advances in processing workflows and equipment can often allow for a better
920 preservation of frequency bandwidth and better signal to noise ratio in seismic data (Brookshire et
921 al., 2015; Firth and Vinje, 2018; Soubaras and Whiting, 2011). Alternatively, surveys can be
922 performed with higher frequencies and smaller bin sizes resulting in better horizontal and vertical
923 resolution (Bellwald and Planke, 2019; Brookshire et al., 2015; Lebedeva-Ivanova et al., 2018). In
924 both cases imaging of the shallow (and deeper if frequencies are preserved) targets is improved.
925 Such high-resolution data can be used both for exploration and site risk assessment. The improved
926 imaging of the shallow section can yield additional, otherwise missed exploration opportunities and
927 contextualise it within a working petroleum system.

928

929

930 9.2.2 Shallow gas - a hazard or a missed opportunity?

931

932 Identification of shallow gas hazards in the subsurface is crucial to safely execute drilling operations.
933 Hazards, if volumes of hydrocarbons are sufficient, can be readily transformed into exploration
934 opportunities as demonstrated by the Aviat and Peon discoveries (Huuse et al., 2012; Ottesen et al.,
935 2012; Rose et al., 2016). In seismic data the interpretation of shallow gas in glaciogenic deposits
936 found offshore on glaciated continental margins is a direct indication of reservoir properties
937 (Bellwald and Planke, 2019; Haavik and Landrø, 2014). However, the complexity of these sequences
938 and limited/poor quality sealing lithologies requires improved understanding of the distribution and
939 properties of porous, permeable and impermeable packages within glaciogenic sequences. This is
940 crucial to ensure safe well abandonment, decommissioning and proposed carbon capture and
941 storage (CCS) activities. The conceptual model presented in this paper aims to support interpretation
942 efforts in all the above activities.

943

944 10 Conclusions

945 The conceptual model presented in this paper (Figure 3) is a synthesis and simplification of what can
946 be an extremely variable and complex depositional environment (Figure 4 and Figure 5). Therefore,
947 it should be used as a framework tool, enabling a first-pass interpretation of glacial landforms.
948 Subsequently, more detailed, interpretations to consider specific local conditions are required.

949 Several conclusions can be drawn:

- 950 1. Glaciofluvial sediments have the best reservoir properties since they are deposited by
951 meltwater, the implications for hydrocarbon exploration is that deglacial sediments (sands
952 and gravels) should be primarily targeted.
- 953 2. Landforms and sediments marked in yellow (potential reservoirs) in Figure 4 should be
954 investigated in further detail as they can comprise good reservoir quality sands and gravels,
955 fine sediments or a mixture of both. Local changes in the energy of the depositional system,
956 available sediments, substratum or local topography can all have a significant impact on
957 their composition e.g. moraines (push or thrust) can be composed of either, outwash sands
958 and gravels, or muds and diamictites, depending on the available substratum. A grounding
959 zone wedge could be either, predominantly composed of traction till (diamictite), or have a
960 significant proportion of well sorted sands and gravels, depending on meltwater discharge at
961 the grounding line and the distribution of meltwater portals (point sources).
- 962 3. Oscillations of the ice front can aid deposition of sealing lithologies on top of reservoir facies.
963 Reservoir quality sediments can be either overridden during ice advance and, if not eroded,
964 capped by a traction till carapace (e.g. Peon field) or, when ice retreats during deglaciation,
965 sea level rise may result in flooding of reservoir facies and deposition of a marine mud seal
966 on top.
- 967 4. Retreat of the ice front in a land terminating system can result in the deposition of triplets of
968 stacked subglacial tills and proglacial sandy and gravely outwash followed by a non-glacial
969 sediment assemblage, associated with interglacials.
- 970 5. Identification of characteristic glaciogenic landforms and/or sediments is crucial to
971 improving predictability of reservoir facies distribution and quality, within any basin.
- 972 6. The landsystem approach, is applicable for hydrocarbon exploration but may be of limited
973 use in development and production cases, where local complexities in sedimentary systems
974 become more important. All glaciogenic landsystems describe a “snapshot” view of a glacial
975 landscape rather than its evolution over time. Moreover, the landsystem approach is mainly
976 focused on ice dynamics (the processes) rather than the landforms and sediments (the
977 products).
- 978 7. Size, distribution and controls on emplacement of reservoir quality landforms in glaciogenic
979 depositional systems requires further research, of both modern and ancient analogues, with
980 the concept of preservation potential providing the, often overlooked, link between the
981 modern and ancient.

982 Acknowledgements

983

984 Authors would like to thank Benjamin Bellwald, Daniel Le Heron and one anonymous reviewer for
985 their insightful comments and suggestions which helped to improve the manuscript.

986 Funding

987

988 This manuscript contains work conducted during a PhD study undertaken as part of the Natural
989 Environment Research Council (NERC) Centre for Doctoral Training (CDT) in Oil & Gas [grant number
990 NEM00578X/1]. It is sponsored by The University of Aberdeen University via their Scholarship
991 Scheme

992 References

993

- 994 Aber, J.S., Croot, D.G., Fenton, M.M., 1989a. Large Composite-Ridges, in: *Glaciotectonic Landforms and*
995 *Structures*. pp. 29–46. https://doi.org/10.1007/978-94-015-6841-8_3
- 996 Aber, J.S., Croot, D.G., Fenton, M.M., 1989b. Small Composite-Ridges, in: *Glaciotectonic Landforms and*
997 *Structures*. pp. 47–69. https://doi.org/10.1007/978-94-015-6841-8_4
- 998 Al-Abri, F.G., Heward, A.P., Abbasi, I.A., 2018. Regional 3D Modeling of the Permo-Carboniferous Al Khlata
999 Formation in the Rima Area, Eastern Fflank of the South Ooman Salt Basin. *J. Pet. Geol.* 41, 29–46.
1000 <https://doi.org/10.1111/jpg.12691>
- 1001 Alsadi, H.N., 2017. *Seismic Hydrocarbon Exploration, Advances in Oil and Gas Exploration & Production*.
1002 Springer International Publishing, Cham. <https://doi.org/10.1007/978-3-319-40436-3>
- 1003 Andersen, T.R., Huuse, M., Jorgensen, F., Christensen, S., 2012. Seismic investigations of buried tunnel valleys
1004 on- and offshore Denmark. *Geol. Soc. London, Spec. Publ.* 129–144. <https://doi.org/10.1144/SP368.14>
- 1005 Anderson, J.B., Warny, S., Askin, R.A., Wellner, J.S., Bohaty, S.M., Kirshner, A.E., Livsey, D.N., Simms, A.R.,
1006 Smith, T.R., Ehrmann, W., Lawver, L.A., Barbeau, D., Wise, S.W., Kulhenek, D.K., Weaver, F.M., Majewski,
1007 W., 2011. Progressive Cenozoic cooling and the demise of Antarctica's last refugium. *Proc. Natl. Acad.*
1008 *Sci. U. S. A.* 108, 11356–11360. <https://doi.org/10.1073/pnas.1014885108>
- 1009 Andreassen, K., Winsborrow, M., 2009. Signature of ice streaming in Bjørnøyrenna, Polar North Atlantic,
1010 through the Pleistocene and implications for ice-stream dynamics. *Ann. Glaciol.* 50, 17–26.
- 1011 Andreassen, K., Winsborrow, M.C.M., Bjarnadóttir, L.R., Rütther, D.C., 2014. Ice stream retreat dynamics
1012 inferred from an assemblage of landforms in the northern Barents Sea. *Quat. Sci. Rev.* 92, 246–257.
1013 <https://doi.org/10.1016/j.quascirev.2013.09.015>

- 1014 Andrews, G.D., McGrady, A.T., Brown, S.R., Maynard, S.M., 2019. First description of subglacial megalineations
1015 from the late Paleozoic ice age in southern Africa. *PLoS One* 14, e0210673.
1016 <https://doi.org/10.1371/journal.pone.0210673>
- 1017 Ashley, G.M., 2002. Glaciolacustrine environments, in: *Modern and Past Glacial Environments*. Elsevier, pp.
1018 335–359. <https://doi.org/10.1016/B978-075064226-2/50014-3>
- 1019 Assine, M.L., de Santa Ana, H., Veroslavsky, G., Vesely, F.F., 2018. Exhumed subglacial landscape in Uruguay:
1020 Erosional landforms, depositional environments, and paleo-ice flow in the context of the late Paleozoic
1021 Gondwanan glaciation. *Sediment. Geol.* 369, 1–12. <https://doi.org/10.1016/j.sedgeo.2018.03.011>
- 1022 Ballantyne, C.K., 2002. A general model of paraglacial landscape response. *The Holocene* 12, 371–376.
1023 <https://doi.org/10.1191/0959683602hl553fa>
- 1024 Ballantyne, Colin K., 2002. Paraglacial geomorphology. *Quat. Sci. Rev.* 21, 1935–2017.
1025 [https://doi.org/10.1016/S0277-3791\(02\)00005-7](https://doi.org/10.1016/S0277-3791(02)00005-7)
- 1026 Barrie, J. V., Conway, K.W., 2016. Glacier-fed outwash plain on the Pacific margin of Canada. *Geol. Soc. Mem.*
1027 46, 225–226. <https://doi.org/10.1144/M46.54>
- 1028 Bataller, F.J., McDougall, N., Moscariello, A., 2019. Ordovician glacial paleogeography: Integration of seismic
1029 spectral decomposition, well sedimentological data, and glacial modern analogs in the Murzuq Basin,
1030 Libya. *Interpretation* 7, T383–T408. <https://doi.org/10.1190/INT-2018-0069.1>
- 1031 Batchelor, C.L., Dowdeswell, J.A., 2016. Lateral shear-moraines and lateral marginal-moraines of palaeo-ice
1032 streams. *Quat. Sci. Rev.* 151, 1–26. <https://doi.org/10.1016/j.quascirev.2016.08.020>
- 1033 Batchelor, C.L., Dowdeswell, J.A., 2015. Ice-sheet grounding-zone wedges (GZWs) on high-latitude continental
1034 margins. *Mar. Geol.* 363, 65–92. <https://doi.org/10.1016/J.MARGEO.2015.02.001>
- 1035 Batchelor, C.L., Dowdeswell, J.A., 2014. The physiography of High Arctic cross-shelf troughs. *Quat. Sci. Rev.* 92,
1036 68–96. <https://doi.org/10.1016/j.quascirev.2013.05.025>
- 1037 Bellwald, B., Planke, S., 2019. Shear margin moraine, mass transport deposits and soft beds revealed by high-
1038 resolution P-Cable three-dimensional seismic data in the Hoop area, Barents Sea. *Geol. Soc. London,*
1039 *Spec. Publ.* 477, 537–548. <https://doi.org/10.1144/sp477.29>
- 1040 Bellwald, Benjamin, Planke, S., Lebedeva-Ivanova, N., Piasecka, E.D., Andreassen, K., 2019. High-resolution
1041 landform assemblage along a buried glacio-erosive surface in the SW Barents Sea revealed by P-Cable 3D
1042 seismic data. *Geomorphology* 332, 33–50. <https://doi.org/10.1016/j.geomorph.2019.01.019>
- 1043 Bellwald, B., Planke, S., Polteau, S., Lebedeva-Ivanova, N., Hafeez, A., Faleide, J.I., Myklebust, R., 2018. Detailed
1044 Structure of Buried Glacial Landforms Revealed by High-resolution 3D Seismic Data in the SW Barents
1045 Sea. <https://doi.org/10.3997/2214-4609.201801161>

- 1046 Bellwald, B., Urlaub, M., Hjelstuen, B.O., Sejrup, H.P., Sørensen, M.B., Forsberg, C.F., Vanneste, M., 2019. NE
1047 Atlantic continental slope stability from a numerical modeling perspective. *Quat. Sci. Rev.* 203, 248–265.
1048 <https://doi.org/10.1016/J.QUASCIREV.2018.11.019>
- 1049 Benediktsson, Í.Ö., Longólfson, Ó., Schomacker, A., Kjaer, K.H., 2009. Formation of submarginal and proglacial
1050 end moraines: implications of ice-flow mechanism during the 1963–64 surge of Brúarjökull, Iceland.
1051 *Boreas* 38, 440–457. <https://doi.org/10.1111/j.1502-3885.2008.00077.x>
- 1052 Benn, D.I., Evans, D.J.A., 2010. *Glaciers and Glaciation*, 2nd ed. Hodder Education.
- 1053 Bennett, M.R., 2003. Ice streams as the arteries of an ice sheet: Their mechanics, stability and significance.
1054 *Earth-Science Rev.* 61, 309–339. [https://doi.org/10.1016/S0012-8252\(02\)00130-7](https://doi.org/10.1016/S0012-8252(02)00130-7)
- 1055 Bennett, M.R., 2001. The morphology, structural evolution and significance of push moraines. *Earth Sci. Rev.*
1056 53, 197–236. [https://doi.org/10.1016/S0012-8252\(00\)00039-8](https://doi.org/10.1016/S0012-8252(00)00039-8)
- 1057 Bennett, M.R., Doyle, P., Mather, A.E., 1996. Dropstones: Their origin and significance. *Palaeogeogr.*
1058 *Palaeoclimatol. Palaeoecol.* 121, 331–339. [https://doi.org/10.1016/0031-0182\(95\)00071-2](https://doi.org/10.1016/0031-0182(95)00071-2)
- 1059 Bennett, M.R., Glasser, N.F., 2009. Glacial Geology: Ice Sheets and Landforms, *Journal of Chemical Information*
1060 *and Modeling*. <https://doi.org/10.1017/CBO9781107415324.004>
- 1061 Bennett, M.R., Huddart, D., McCormick, T., 2000. An integrated approach to the study of glaciolacustrine
1062 landforms and sediments: a case study from Hagavatn, Iceland. *Quat. Sci. Rev.* 19, 633–665.
1063 [https://doi.org/10.1016/S0277-3791\(99\)00013-X](https://doi.org/10.1016/S0277-3791(99)00013-X)
- 1064 Berkson, M.J., Clay, C.S., 1973. Microphysiography and Possible Iceberg Grooves on the Floor of Western Lake
1065 Superior. *Geol. Soc. Am. Bull.* 84, 1315. [https://doi.org/10.1130/0016-7606\(1973\)84<1315:MAPIGO>2.0.CO;2](https://doi.org/10.1130/0016-7606(1973)84<1315:MAPIGO>2.0.CO;2)
- 1067 Bingham, R.G., Vaughan, D.G., King, E.C., Davies, D., Cornford, S.L., Smith, A.M., Arthern, R.J., Brisbourne, A.M.,
1068 De Rydt, J., Graham, A.G.C., Spagnolo, M., Marsh, O.J., Shean, D.E., 2017. Diverse landscapes beneath
1069 Pine Island Glacier influence ice flow. *Nat. Commun.* 8, 1618. <https://doi.org/10.1038/s41467-017-01597-y>
- 1071 Bjarnadóttir, L.R., Andreassen, K., 2016. Ice-stream landform assemblage in Kveithola, western Barents Sea
1072 margin. *Geol. Soc. London, Mem.* 46, 325–328. <https://doi.org/10.1144/m46.145>
- 1073 Bjarnadóttir, L.R., Winsborrow, M.C.M., Andreassen, K., 2017. Large subglacial meltwater features in the
1074 central Barents Sea. *Geology* 45, 159–162. <https://doi.org/10.1130/G38195.1>
- 1075 Bjarnadóttir, L.R., Winsborrow, M.C.M., Andreassen, K., 2017. Large subglacial meltwater features in the
1076 central Barents Sea. *Geology* 45, 159–162. <https://doi.org/10.1130/G38195.1>
- 1077 Bogen, J., Xu, M., Kennie, P., 2015. The impact of pro-glacial lakes on downstream sediment delivery in

- 1078 Norway. *Earth Surf. Process. Landforms* 40, 942–952. <https://doi.org/10.1002/esp.3669>
- 1079 Bond, G., Heinrich, H., Broecker, W., Labeyrie, L., McManus, J., Andrews, J., Huon, S., Jantschik, R., Clasen, S.,
1080 Simet, C., Tedesco, K., Klas, M., Bonani, G., Ivy, S., 1992. Evidence for massive discharges of icebergs into
1081 the North Atlantic ocean during the last glacial period. *Nature* 360, 245–249.
1082 <https://doi.org/10.1038/360245a0>
- 1083 Boulton, G.S., 1996. Theory of glacial erosion, transport and deposition as a consequence of subglacial
1084 sediment deformation. *J. Glaciol.* 42, 43–62. <https://doi.org/10.3189/S0022143000030525>
- 1085 Boulton, G.S., 1990. Sedimentary and sea level changes during glacial cycles and their control on glacial
1086 facies architecture. *Geol. Soc. Spec. Publ.* 53, 15–52. <https://doi.org/10.1144/GSL.SP.1990.053.01.02>
- 1087 Boulton, G.S., 1979. Processes of Glacier Erosion on Different Substrata. *J. Glaciol.* 23, 15–38.
1088 <https://doi.org/10.3189/S0022143000029713>
- 1089 Boulton, G.S., 1972. Modern Arctic glaciers as depositional models for former ice sheets. *J. Geol. Soc. London*
1090 128, 361–393. <https://doi.org/10.1144/gsjgs.128.4.0361>
- 1091 Boulton, G.S., Caban, P.E., Van Gijssel, K., 1995. Groundwater Flow Beneath Ice Sheets : Part I - Patterns. *Quat.*
1092 *Sci. Rev.* 14, 545–562. [https://doi.org/10.1016/0277-3791\(95\)00039-r](https://doi.org/10.1016/0277-3791(95)00039-r)
- 1093 Boulton, G.S., Deynoux, M., 1981. Sedimentation in glacial environments and the identification of tills and
1094 tillites in ancient sedimentary sequences. *Precambrian Res.* 15, 397–422. [https://doi.org/10.1016/0301-9268\(81\)90059-0](https://doi.org/10.1016/0301-9268(81)90059-0)
- 1095
- 1096 Bradley, R.S., 2015. Climate and Climatic Variation. *Paleoclimatology* 13–54. <https://doi.org/10.1016/B978-0-12-386913-5.00002-8>
- 1097
- 1098 Brennand, T.A., 2000. Deglacial meltwater drainage and glaciodynamics: inferences from Laurentide eskers,
1099 Canada. *Geomorphology* 32, 263–293. [https://doi.org/10.1016/S0169-555X\(99\)00100-2](https://doi.org/10.1016/S0169-555X(99)00100-2)
- 1100 Brodzikowski, K., Loon, A.J. van, 1991. *Glacigenic sediments*. Elsevier Science.
- 1101 Brodzikowski, K., van Loon, A.J., 1987. A systematic classification of glacial and periglacial environments, facies
1102 and deposits. *Earth Sci. Rev.* 24, 297–381. [https://doi.org/10.1016/0012-8252\(87\)90061-4](https://doi.org/10.1016/0012-8252(87)90061-4)
- 1103 Brookshire, B.N., Landers, F.P., Stein, J.A., 2015. Applicability of ultra-high-resolution 3D seismic data for
1104 geohazard identification at mid-slope depths in the Gulf of Mexico: Initial results. *Underw. Technol.* 32,
1105 271–278. <https://doi.org/10.3723/ut.32.271>
- 1106 Burke, M.J., Brennand, T.A., Sjogren, D.B., 2015. The role of sediment supply in esker formation and ice tunnel
1107 evolution. *Quat. Sci. Rev.* 115, 50–77. <https://doi.org/10.1016/J.QUASCIREV.2015.02.017>
- 1108 Busfield, M.E., Le Heron, D.P., 2018. Snowball Earth Under the Microscope. *J. Sediment. Res.* 88, 659–677.
1109 <https://doi.org/10.2110/jsr.2018.34>

- 1110 Camargo, J.M.R., Silva, M.V.B., Júnior, A.V.F., Araújo, T.C.M., 2019. Marine geohazards: A bibliometric-based
1111 review. *Geosci.* <https://doi.org/10.3390/geosciences9020100>
- 1112 Camerlenghi, A., Domack, E., Rebesco, M., Gilbert, R., Ishman, S., Leventer, A., Brachfeld, S., Drake, A., 2001.
1113 Glacial morphology and post-glacial contourites in northern Prince Gustav Channel (NW Weddell Sea,
1114 Antarctica). *Mar. Geophys. Res.* 22, 417–443. <https://doi.org/10.1023/A:1016399616365>
- 1115 Canals, M., Amblas, D., Casamor, J.L., 2016. Cross-shelf troughs in Central Bransfield Basin, Antarctic Peninsula.
1116 *Geol. Soc. Mem.* 46, 171–172. <https://doi.org/10.1144/M46.138>
- 1117 Carrivick, J.L., Tweed, F.S., 2013. Proglacial Lakes: Character, behaviour and geological importance. *Quat. Sci.*
1118 *Rev.* 78, 34–52. <https://doi.org/10.1016/j.quascirev.2013.07.028>
- 1119 Catuneanu, O., 2006. *Principles of sequence stratigraphy*. Elsevier.
- 1120 Catuneanu, O., 2002. Sequence stratigraphy of clastic systems: Concepts, merits, and pitfalls. *J. African Earth*
1121 *Sci.* 35, 1–43. [https://doi.org/10.1016/S0899-5362\(02\)00004-0](https://doi.org/10.1016/S0899-5362(02)00004-0)
- 1122 Catuneanu, O., Abreu, V., Bhattacharya, J.P., Blum, M.D., Dalrymple, R.W., Eriksson, P.G., Fielding, C.R., Fisher,
1123 W.L., Galloway, W.E., Gibling, M.R., Giles, K.A., Holbrook, J.M., Jordan, R., Kendall, C.G.S.C., Macurda, B.,
1124 Martinsen, O.J., Miall, A.D., Neal, J.E., Nummedal, D., Pomar, L., Posamentier, H.W., Pratt, B.R., Sarg, J.F.,
1125 Shanley, K.W., Steel, R.J., Strasser, A., Tucker, M.E., Winker, C., 2009. Towards the standardization of
1126 sequence stratigraphy. *Earth-Science Rev.* <https://doi.org/10.1016/j.earscirev.2008.10.003>
- 1127 Catuneanu, O., Galloway, W.E., Kendall, C.G.S.C., Miall, A.D., Posamentier, H.W., Strasser, A., Tucker, M.E.,
1128 2011. *Sequence Stratigraphy: Methodology and Nomenclature*. *Newsletters Stratigr.* 44, 173–245.
1129 <https://doi.org/10.1127/0078-0421/2011/0011>
- 1130 Chewings, J.M., Atkins, C.B., Dunbar, G.B., Golledge, N.R., 2014. Aeolian sediment transport and deposition in a
1131 modern high-latitude glacial marine environment. *Sedimentology* 61, 1535–1557.
1132 <https://doi.org/10.1111/sed.12108>
- 1133 Clark-Lowes, D.D., 2005. Arabian glacial deposits: Recognition of palaeovalleys within the Upper Ordovician
1134 Sarah Formation, Al Qasim district, Saudi Arabia. *Proc. Geol. Assoc.* [https://doi.org/10.1016/S0016-](https://doi.org/10.1016/S0016-7878(05)80051-3)
1135 [7878\(05\)80051-3](https://doi.org/10.1016/S0016-7878(05)80051-3)
- 1136 Clark, C.D., Hughes, A.L.C., Greenwood, S.L., Spagnolo, M., Ng, F.S.L., 2009. Size and shape characteristics of
1137 drumlins, derived from a large sample, and associated scaling laws. *Quat. Sci. Rev.* 28, 677–692.
1138 <https://doi.org/10.1016/j.quascirev.2008.08.035>
- 1139 Clark, C.D., Spagnolo, M., 2016. Glacially eroded cross-shelf troughs surrounding Iceland from Olex data. *Geol.*
1140 *Soc. Mem.* 46, 165–166. <https://doi.org/10.1144/M46.86>
- 1141 Clarke, B.G., 2018. The engineering properties of glacial tills. *Geotech. Res.* 5, 262–277.
1142 <https://doi.org/10.1680/jgere.18.00020>

- 1143 Clarke, G.K.C., 1987. Subglacial till: A physical framework for its properties and processes. *J. Geophys. Res.* 92,
1144 9023. <https://doi.org/10.1029/JB092iB09p09023>
- 1145 Clerc, S., Buoncristiani, J.F., Guiraud, M., Vennin, E., Desaubliaux, G., Portier, E., 2013. Subglacial to proglacial
1146 depositional environments in an Ordovician glacial tunnel valley, Alnif, Morocco. *Palaeogeogr.*
1147 *Palaeoclimatol. Palaeoecol.* 370, 127–144. <https://doi.org/10.1016/j.palaeo.2012.12.002>
- 1148 Craig, J., Thurow, J., Thusu, B., Whitham, A., Abutarruma, Y., 2009. Global Neoproterozoic petroleum systems:
1149 the emerging potential in North Africa. *Glob. Neoproterozoic Pet. Syst. Emerg. Potential North Africa*
1150 326, 1–25. <https://doi.org/10.1144/sp326.1>
- 1151 Craigie, N.W., Rees, A., MacPherson, K., Berman, S., 2016. Chemostratigraphy of the Ordovician Sarah
1152 Formation, North West Saudi Arabia: An integrated approach to reservoir correlation. *Mar. Pet. Geol.* 77,
1153 1056–1080. <https://doi.org/10.1016/J.MARPETGEO.2016.07.009>
- 1154 Dahlgren, K.I.T., Vorren, T.O., Stoker, M.S., Nielsen, T., Nygård, A., Petter Sejrup, H., 2005. Late Cenozoic
1155 prograding wedges on the NW European continental margin: their formation and relationship to
1156 tectonics and climate. *Mar. Pet. Geol.* 22, 1089–1110. <https://doi.org/10.1016/j.marpetgeo.2004.12.008>
- 1157 Davies, B.J., Glasser, N.F., Carrivick, J.L., Hambrey, M.J., Smellie, J.L., Nyvlt, D., 2013. Landscape evolution and
1158 ice-sheet behaviour in a semi-arid polar environment: James Ross Island, NE Antarctic Peninsula. *Geol.*
1159 *Soc. London, Spec. Publ.* 381, 1–43. <https://doi.org/10.1144/SP381.1>
- 1160 Derbyshire, E., Owen, L.A., 2017. *Glacioaeolian Processes, Sediments, and Landforms, Past Glacial*
1161 *Environments: Second Edition.* Elsevier Ltd. <https://doi.org/10.1016/B978-0-08-100524-8.00008-7>
- 1162 Deschamps, R., Eschard, R., Roussé, S., 2013. Architecture of Late Ordovician glacial valleys in the Tassili N'Ajjer
1163 area (Algeria). *Sediment. Geol.* 289. <https://doi.org/10.1016/j.sedgeo.2013.02.012>
- 1164 Dietrich, P., Ghienne, J.-F., Normandeau, A., Lajeunesse, P., 2016. Upslope-Migrating Bedforms In A Proglacial
1165 Sandur Delta: Cyclic Steps From River-Derived Underflows? *J. Sediment. Res.* 86, 113–123.
1166 <https://doi.org/10.2110/jsr.2016.4>
- 1167 Dietrich, P., Ghienne, J.-F.F., Normandeau, A., Lajeunesse, P., 2017. Reconstructing ice-margin retreat using
1168 delta morphostratigraphy. *Sci. Rep.* 7, 16936. <https://doi.org/10.1038/s41598-017-16763-x>
- 1169 Dietrich, P., Hofmann, A., 2019. Ice-margin fluctuation sequences and grounding zone wedges: The record of
1170 the Late Palaeozoic Ice Age in the eastern Karoo Basin (Dwyka Group, South Africa). *Depos. Rec.* 5, 247–
1171 271. <https://doi.org/10.1002/dep2.74>
- 1172 Dixon, R.J., Moore, J.K.S., Bourne, M., Dunn, E., Haig, D.B., Hossack, J., Roberts, N., Simmons, C.J., 2010.
1173 *Petroleum Geology Conference series Integrated petroleum systems and play fairway analysis in a*
1174 *complex Palaeozoic basin : Ghadames-Illizi Basin , North Africa Integrated petroleum systems and play*
1175 *fairway analysis in a complex Palaeozoic basin : Ghadames.* *Pet. Geol. Conf. Ser.* 7, 735–760.

- 1176 <https://doi.org/10.1144/0070735>
- 1177 Domack, E.W., 1982. Sedimentology of glacial and glacial marine deposits on the George V-Adelie continental
1178 shelf, East Antarctica. *Boreas* 11, 79–97. <https://doi.org/10.1111/j.1502-3885.1982.tb00524.x>
- 1179 Domack, E.W., Lawson, D.E., 1985. Pebble Fabric in an Ice-Rafted Diamicton. *J. Geol.* 93, 577–591.
1180 <https://doi.org/10.1086/628982>
- 1181 Dowdeswell, J.A., Bamber, J.L., 2007. Keel depths of modern Antarctic icebergs and implications for sea-floor
1182 scouring in the geological record. *Mar. Geol.* 243, 120–131.
1183 <https://doi.org/10.1016/j.margeo.2007.04.008>
- 1184 Dowdeswell, J.A., Canals, M., Jakobsson, M., Todd, B.J., Dowdeswell, E.K., Hogan, K.A., 2016a. Introduction: an
1185 *Atlas of Submarine Glacial Landforms*. *Geol. Soc. London, Mem.* 46, 3–14.
1186 <https://doi.org/10.1144/M46.171>
- 1187 Dowdeswell, J.A., Canals, M., Jakobsson, M., Todd, B.J., Dowdeswell, E.K., Hogan, K.A., 2016b. The variety and
1188 distribution of submarine glacial landforms and implications for ice-sheet reconstruction. *Geol. Soc.*
1189 *London, Mem.* 46, 519–552. <https://doi.org/10.1144/M46.183>
- 1190 Dowdeswell, J.A., Cofaigh, C.Ó., 2002. Glacier-influenced sedimentation on high-latitude continental margins:
1191 introduction and overview. *Geol. Soc. London, Spec. Publ.* 203, 1–9.
1192 <https://doi.org/10.1144/GSL.SP.2002.203.01.01>
- 1193 Dowdeswell, J.A., Dowdeswell, E.K., 1989. Debris in Icebergs and Rates of Glaci-Marine Sedimentation:
1194 Observations from Spitsbergen and a Simple Model. *J. Geol.* <https://doi.org/10.2307/30065541>
- 1195 Dowdeswell, J.A., Fugelli, E.M.G., 2012. The seismic architecture and geometry of grounding-zone wedges
1196 formed at the marine margins of past ice sheets. *Bull. Geol. Soc. Am.* 124, 1750–1761.
1197 <https://doi.org/10.1130/B30628.1>
- 1198 Dowdeswell, J.A., Ó Cofaigh, C., Pudsey, C.J., 2004. Continental slope morphology and sedimentary processes
1199 at the mouth of an Antarctic palaeo-ice stream. *Mar. Geol.* 204, 203–214.
1200 [https://doi.org/10.1016/S0025-3227\(03\)00338-4](https://doi.org/10.1016/S0025-3227(03)00338-4)
- 1201 Dowdeswell, J.A., Ottesen, D., 2016. Current-modified recessional-moraine ridges on the NW Spitsbergen
1202 shelf. *Geol. Soc. Mem.* 46, 255–256. <https://doi.org/10.1144/M46.68>
- 1203 Dowdeswell, J.A.A., Bamber, J.L.L., 2007. Keel depths of modern Antarctic icebergs and implications for sea-
1204 floor scouring in the geological record. *Mar. Geol.* 243, 120–131.
1205 <https://doi.org/10.1016/j.margeo.2007.04.008>
- 1206 Dowdeswell, J.A.A., O’Cofaigh, C., Noormets, R., Larter, R.D.D., Hillenbrand, C.-D.D., Benetti, S., Evans, J.,
1207 Pudsey, C.J.J., 2008. A major trough-mouth fan on the continental margin of the Bellingshausen Sea,
1208 West Antarctica: The Belgica Fan. *Mar. Geol.* 252, 129–140.

- 1209 <https://doi.org/10.1016/j.margeo.2008.03.017>
- 1210 Dunlop, P., Clark, C.D., 2006. The morphological characteristics of ribbed moraine. *Quat. Sci. Rev.* 25, 1668–
1211 1691. <https://doi.org/10.1016/j.quascirev.2006.01.002>
- 1212 Ehlers, J., Gibbard, P.L., Hughes, P.D., 2011. *Quaternary glaciations - extent and chronology : a closer look.*
1213 Elsevier.
- 1214 El-Ghali, M.A.K., 2005. Depositional environments and sequence stratigraphy of paralic glacial, paraglacial and
1215 postglacial Upper Ordovician siliciclastic deposits in the Murzuq Basin, SW Libya. *Sediment. Geol.* 177,
1216 145–173. <https://doi.org/10.1016/j.sedgeo.2005.02.006>
- 1217 Elhebiry, M.S., Sultan, M., Abu El-Leil, I., Kehew, A.E., Bekiet, M.H., Abdel Shahid, I., Soliman, N.M.A., Abotalib,
1218 A.Z., Emil, M., 2019. Paleozoic glaciation in NE Africa: field and remote sensing-based evidence from the
1219 South Eastern Desert of Egypt. *Int. Geol. Rev.* <https://doi.org/10.1080/00206814.2019.1636416>
- 1220 Elmore, C.R., Gulick, S.P.S., Willems, B., Powell, R., 2013. Seismic stratigraphic evidence for glacial expanse
1221 during glacial maxima in the Yakutat Bay Region, Gulf of Alaska. *Geochemistry, Geophys. Geosystems* 14,
1222 1294–1311. <https://doi.org/10.1002/ggge.20097>
- 1223 Ely, J.C., Clark, C.D., Spagnolo, M., Stokes, C.R., Greenwood, S.L., Hughes, A.L.C., Dunlop, P., Hess, D., 2016. Do
1224 subglacial bedforms comprise a size and shape continuum? *Geomorphology* 257, 108–119.
1225 <https://doi.org/10.1016/j.geomorph.2016.01.001>
- 1226 Emery, A.R., Hodgson, D.M., Barlow, N.L.M., Carrivick, J.L., Cotterill, C.J., Mellett, C.L., Booth, A.D., 2019a.
1227 Topographic and hydrodynamic controls on barrier retreat and preservation: An example from Dogger
1228 Bank, North Sea. *Mar. Geol.* 416. <https://doi.org/10.1016/j.margeo.2019.105981>
- 1229 Emery, A.R., Hodgson, D.M., Barlow, N.L.M., Carrivick, J.L., Cotterill, C.J., Phillips, E., 2019b. Left High and Dry:
1230 Deglaciation of Dogger Bank, North Sea, Recorded in Proglacial Lake Evolution. *Front. Earth Sci.* 7.
1231 <https://doi.org/10.3389/feart.2019.00234>
- 1232 Emery, D., Myers, K., Bertram, G.T., 1996. *Sequence stratigraphy.* Blackwell Science.
- 1233 Esteves, M., Bjarnadóttir, L.R., Winsborrow, M.C.M., Shackleton, C.S., Andreassen, K., 2017. Retreat patterns
1234 and dynamics of the Sentralbankrenna glacial system, central Barents Sea. *Quat. Sci. Rev.* 169, 131–147.
1235 <https://doi.org/10.1016/J.QUASCIREV.2017.06.004>
- 1236 Evans, D.J.A., 2006. Glacial Landsystems, in: *Glacier Science and Environmental Change.* Blackwell Publishing,
1237 Malden, MA, USA, pp. 83–88. <https://doi.org/10.1002/9780470750636.ch18>
- 1238 Evans, D.J.A., Hiemstra, J.F., Cofaigh, C.O., 2012. Stratigraphic architecture and sedimentology of a Late
1239 Pleistocene subaqueous moraine complex, southwest Ireland. *J. Quat. Sci.* 27, 51–63.
1240 <https://doi.org/10.1002/jqs.1513>

- 1241 Evans, D.J.A., Phillips, E.R., Hiemstra, J.F., Auton, C.A., 2006. Subglacial till: Formation, sedimentary
1242 characteristics and classification. *Earth-Science Rev.* 78, 115–176.
1243 <https://doi.org/10.1016/j.earscirev.2006.04.001>
- 1244 Evans, D.J.A., Thomson, S.A., 2010. Glacial sediments and landforms of Holderness, eastern England: A glacial
1245 depositional model for the North Sea Lobe of the British-Irish Ice Sheet. *Earth-Science Rev.* 101, 147–
1246 189. <https://doi.org/10.1016/j.earscirev.2010.04.003>
- 1247 Eyles, C.H., Eyles, N., Franca, A.B., 1993. Glaciation and tectonics in an active intracratonic basin: the late
1248 Palaeozoic Itarare Group, Parana Basin, Brazil. *Sedimentology* 40, 1–25.
1249 <https://doi.org/https://doi.org/10.1111/j.1365-3091.1993.tb01087.x>
- 1250 Eyles, C.H., Eyles, N., Miall, A.D., 1985. Models of glaciomarine sedimentation and their application to the
1251 interpretation of ancient glacial sequences. *Palaeogeogr. Palaeoclimatol. Palaeoecol.* 51, 15–84.
1252 [https://doi.org/10.1016/0031-0182\(85\)90080-X](https://doi.org/10.1016/0031-0182(85)90080-X)
- 1253 Eyles, N., 2008. Glacio-epochs and the supercontinent cycle after ~ 3.0 Ga: Tectonic boundary conditions for
1254 glaciation. *Palaeogeogr. Palaeoclimatol. Palaeoecol.* 258, 89–129.
1255 <https://doi.org/10.1016/j.palaeo.2007.09.021>
- 1256 Eyles, N., 1993. Earth's glacial record and its tectonic setting. *Earth Sci. Rev.* 35, 1–248.
1257 [https://doi.org/10.1016/0012-8252\(93\)90002-O](https://doi.org/10.1016/0012-8252(93)90002-O)
- 1258 Farmer, G.T., Cook, J., 2013. Pleistocene Glaciations, in: *Climate Change Science: A Modern Synthesis*. Springer
1259 Netherlands, Dordrecht, pp. 407–427. https://doi.org/10.1007/978-94-007-5757-8_21
- 1260 Fichler, C., Henriksen, S., Rueslaatten, H., Hovland, M., 2005. North Sea Quaternary morphology from seismic
1261 and magnetic data: indications for gas hydrates during glaciation? . *Pet. Geosci.* 11, 331–337.
1262 <https://doi.org/10.1144/1354-079304-635>
- 1263 Fildani, A., Hessler, A.M., Mason, C.C., McKay, M.P., Stockli, D.F., 2018. Late Pleistocene glacial transitions in
1264 North America altered major river drainages, as revealed by deep-sea sediment. *Sci. Rep.* 8, 13839.
1265 <https://doi.org/10.1038/s41598-018-32268-7>
- 1266 Firth, J., Vinje, V., 2018. On top of the spread. *Oilf. Technol.*
- 1267 Fjeldskaar, W., 1994. The amplitude and decay of the glacial forebulge in Fennoscandia. *Nor. Geol. Tidsskr.* 74,
1268 2–8.
- 1269 Fleisher, P.J., 1986. Dead-ice sinks and moats: environments of stagnant ice deposition. *Geology* 14, 39–42.
1270 [https://doi.org/10.1130/0091-7613\(1986\)14<39:DSAMEO>2.0.CO;2](https://doi.org/10.1130/0091-7613(1986)14<39:DSAMEO>2.0.CO;2)
- 1271 Forbes, G.A., Janseni, H.S.M., Schreurs, J., 2010. Lexicon of oman subsurface stratigraphy. *GeoArabia* 15, 210–
1272 215.

- 1273 Fortuin, A.R., 1984. Late ordovician glaciomarine deposits (orea shale) in the sierra de albarracin, Spain.
1274 Palaeogeogr. Palaeoclimatol. Palaeoecol. 48, 245–261. [https://doi.org/10.1016/0031-0182\(84\)90047-6](https://doi.org/10.1016/0031-0182(84)90047-6)
- 1275 Fyfe, G.J., 1990. The effect of water depth on ice-proximal glaciolacustrine sedimentation: Salpausselkä I,
1276 southern Finland. *Boreas* 19, 147–164. <https://doi.org/10.1111/j.1502-3885.1990.tb00576.x>
- 1277 Gales, J., Hillenbrand, C.-D., Larter, R., Laberg, J.S., Melles, M., Benetti, S., Passchier, S., 2019. Processes
1278 influencing differences in Arctic and Antarctic trough mouth fan sedimentology. *Geol. Soc. London, Spec.*
1279 *Publ.* 475. <https://doi.org/10.1144/SP475.7>
- 1280 García, J.L., Strelin, J.A., Vega, R.M., Hall, B.L., Stern, C.R., 2015. Ambientes glaciolacustres y construcción
1281 estructural de morrenas frontales tardiglaciales en Torres del Paine, Patagonia austral chilena. *Andean*
1282 *Geol.* 42, 190–212. <https://doi.org/10.5027/andgeoV42n2-a03>
- 1283 Ghienne, J.F., 2003. Late Ordovician sedimentary environments, glacial cycles, and post-glacial transgression in
1284 the Taoudeni Basin, West Africa. *Palaeogeogr. Palaeoclimatol. Palaeoecol.* 189, 117–145.
1285 [https://doi.org/10.1016/S0031-0182\(02\)00635-1](https://doi.org/10.1016/S0031-0182(02)00635-1)
- 1286 Ghienne, J.F., Deynoux, M., 1998. Large-scale channel fill structures in Late Ordovician glacial deposits in
1287 Mauritania, western Sahara. *Sediment. Geol.* 119, 141–159. [https://doi.org/10.1016/S0037-](https://doi.org/10.1016/S0037-0738(98)00045-1)
1288 [0738\(98\)00045-1](https://doi.org/10.1016/S0037-0738(98)00045-1)
- 1289 Girard, F., Ghienne, J.-F., Rubino, J.-L., 2012. Channelized sandstone bodies ('cordons') in the Tassili N'Ajjer
1290 (Algeria & Libya): snapshots of a Late Ordovician proglacial outwash plain. *Geol. Soc. London, Spec. Publ.*
1291 368, 355–379. <https://doi.org/10.1144/sp368.3>
- 1292 Glückert, G., 1995. The Baltic Ice Lake in south Finland and its outlets. *Quat. Int.* 27, 47–51.
1293 [https://doi.org/10.1016/1040-6182\(94\)00059-E](https://doi.org/10.1016/1040-6182(94)00059-E)
- 1294 Glückert, G., 1986. The First Salpausselkä at Lohja, southern Finland. *Bull. Geol. Soc. Finl.* 58, 45–55.
- 1295 Gold, C., 2009. Varves in lacustrine sediments – an overview. *Www.Geo.Tu-Freiberg.De* 11.
- 1296 Gomez, B., Smith, L.C., Magilligan, F.J., Mertes, L.A.K., Smith, N.D., 2000. Glacier outburst floods and outwash
1297 plain development: Skeiðarársandur, Iceland. *Terra Nov.* 12, 126–131. [https://doi.org/10.1111/j.1365-](https://doi.org/10.1111/j.1365-3121.2000.00277.x)
1298 [3121.2000.00277.x](https://doi.org/10.1111/j.1365-3121.2000.00277.x)
- 1299 Graham, A.G.C., Larter, R.D., Gohl, K., Hillenbrand, C.-D., Smith, J.A., Kuhn, G., 2009. Bedform signature of a
1300 West Antarctic palaeo-ice stream reveals a multi-temporal record of flow and substrate control. *Quat.*
1301 *Sci. Rev.* 28, 2774–2793. <https://doi.org/10.1016/j.quascirev.2009.07.003>
- 1302 Graham, A.G.C., Lonergan, L., Stoker, M.S., 2007. Evidence for Late Pleistocene ice stream activity in the Witch
1303 Ground Basin, central North Sea, from 3D seismic reflection data. *Quat. Sci. Rev.* 26, 627–643.
1304 <https://doi.org/10.1016/j.quascirev.2006.11.004>

- 1305 Greenwood, S.L., Simkins, L.M., Halberstadt, A.R.W., Prothro, L.O., Anderson, J.B., 2018. Holocene
1306 reconfiguration and readvance of the East Antarctic Ice Sheet. *Nat. Commun.* 9, 3176.
1307 <https://doi.org/10.1038/s41467-018-05625-3>
- 1308 Griffiths, J.S., Martin, C.J., 2017. Engineering Geology and Geomorphology of Glaciated and Periglaciated
1309 Terrains: Engineering Group Working Party Report, Volume 28. ed, Geological Society, London,
1310 Engineering Geology Special Publications. The Geological Society of London. [https://doi.org/DOI:](https://doi.org/DOI:https://doi.org/10.1144/EGSP28)
1311 <https://doi.org/10.1144/EGSP28>
- 1312 Gruszka, B., Morawski, W., Zieliński, T., 2012. Sedimentary record of a Pleistocene ice-sheet interlobate zone
1313 (NE Poland). *Geologos* 18, 65–81. <https://doi.org/10.2478/v10118-012-0005-1>
- 1314 Gupta, S., Collier, J.S., Garcia-Moreno, D., Oggioni, F., Trentesaux, A., Vanneste, K., De Batist, M., Camelbeeck,
1315 T., Potter, G., Van Vliet-Lanoë, B., Arthur, J.C.R., 2017. Two-stage opening of the Dover Strait and the
1316 origin of island Britain. *Nat. Commun.* 8, 15101. <https://doi.org/10.1038/ncomms15101>
- 1317 Haavik, K.E., Landrø, M., 2014. Iceberg ploughmarks illuminated by shallow gas in the central North Sea. *Quat.*
1318 *Sci. Rev.* 103, 34–50. <https://doi.org/10.1016/j.quascirev.2014.09.002>
- 1319 Hadley, D., Ain, a, Focke, J., 1991. Old Sandstones, New Horizons. *Middle East Well Eval. Rev.* 11, 10–26.
- 1320 Hanson, M.A., Clague, J.J., 2016. Record of glacial Lake Missoula floods in glacial Lake Columbia, Washington.
1321 *Quat. Sci. Rev.* 133, 62–76. <https://doi.org/10.1016/j.quascirev.2015.12.009>
- 1322 Heron, D.P. Le, 2018. An exhumed Paleozoic glacial landscape in Chad. *Geology* 46, 91–94.
1323 <https://doi.org/10.1130/G39510.1>
- 1324 Heron, D.P. Le, Meinhold, G., Elgadry, M., Abutarruma, Y., Boote, D., 2015. Early Palaeozoic evolution of Libya:
1325 perspectives from Jabal Eghei with implications for hydrocarbon exploration in Al Kufrah Basin. *Basin*
1326 *Res.* 27, 60–83. <https://doi.org/10.1111/bre.12057>
- 1327 Hesse, R., Klauke, I., Khodabakhsh, S., Piper, D.J.W., Ryan, W.B.F., Hesse, R., 2001. Potential deep-water
1328 reservoirs 8, 1499–1521.
- 1329 Heward, A.P., Penney, R.A., 2014. Al Khata glacial deposits in the Oman Mountains and their implications.
1330 *Geol. Soc. London, Spec. Publ.* 392, 279–301. <https://doi.org/10.1144/SP392.15>
- 1331 Hirst, J.P.P., 2012. Ordovician proglacial sediments in Algeria: insights into the controls on hydrocarbon
1332 reservoirs in the In Amenas field, Illizi Basin. *Geol. Soc. London, Spec. Publ.* 368, 319–353.
1333 <https://doi.org/10.1144/SP368.17>
- 1334 Hirst, J.P.P., Benbakir, A., Payne, D.F., Westlake, I.R., 2002. Tunnel valleys and density flow processes in the
1335 Upper Ordovician glacial succession, Illizi Basin, Algeria: Influence on reservoir quality. *J. Pet. Geol.* 25,
1336 297–324. <https://doi.org/10.1111/j.1747-5457.2002.tb00011.x>

- 1337 Hirst, J.P.P., Khatatneh, M., 2019. Depositional model for the distal Ordovician glaciated margin of Jordan;
1338 implications for the reservoir potential of the Risha Formation. *Geol. Soc. London, Spec. Publ.* 475, 109–
1339 129. <https://doi.org/10.1144/SP475.4>
- 1340 Hodell, D.A., Nicholl, J.A., Bontognali, T.R.R., Danino, S., Dorador, J., Dowdeswell, J.A., Einsle, J., Kuhlmann, H.,
1341 Martrat, B., Mleneck-Vautravers, M.J., Rodríguez-Tovar, F.J., Röhl, U., 2017. Anatomy of Heinrich Layer 1
1342 and its role in the last deglaciation. *Paleoceanography* 32, 284–303.
1343 <https://doi.org/10.1002/2016PA003028>
- 1344 Hodgson, D.A., Graham, A.G.C., Griffiths, H.J., Roberts, S.J., Cofaigh, C.Ó., Bentley, M.J., Evans, D.J.A., 2014.
1345 Glacial history of sub-Antarctic South Georgia based on the submarine geomorphology of its fjords. *Quat.*
1346 *Sci. Rev.* 89, 129–147. <https://doi.org/10.1016/j.quascirev.2013.12.005>
- 1347 Holmes, R., Stoker, S.J., 2005. Investigation of the origin of shallow gas in outer Moray Firth open blocks
1348 15/20c and 15/25d.
- 1349 Houmark-Nielsen, M., 2007. Extent and age of Middle and Late Pleistocene glaciations and periglacial episodes
1350 in southern Jylland, Denmark. *Bull. Geol. Soc. Denmark* 55, 9–35.
- 1351 Hughes, A.L.C., Clark, C.D., Jordan, C.J., 2014. Flow-pattern evolution of the last British Ice Sheet. *Quat. Sci.*
1352 *Rev.* 89, 148–168. <https://doi.org/10.1016/j.quascirev.2014.02.002>
- 1353 Huuse, M., Le Heron, D.P., Dixon, R., Redfern, J., Moscariello, a., Craig, J., 2012. Glaciogenic reservoirs and
1354 hydrocarbon systems: an introduction. *Geol. Soc. London, Spec. Publ.* 368, 1–28.
1355 <https://doi.org/10.1144/SP368.19>
- 1356 Huuse, M., Lykke-Andersen, H., 2000. Large-scale glaciotectonic thrust structures in the eastern Danish North
1357 Sea. *Geol. Soc. London, Spec. Publ.* 176, 293–305. <https://doi.org/10.1144/GSL.SP.2000.176.01.22>
- 1358 Ingólfsson, Ó., Benediktsson, Í.Ö., Schomacker, A., Kjær, K.H., Brynjólfsson, S., Jónsson, S.A., Korsgaard, N.J.,
1359 Johnson, M.D., 2016. Glacial geological studies of surge-type glaciers in Iceland - Research status and
1360 future challenges. *Earth-Science Rev.* 152, 37–69. <https://doi.org/10.1016/j.earscirev.2015.11.008>
- 1361 Jamieson, S.S.R., Hulton, N.R.J., Hagdorn, M., 2008. Modelling landscape evolution under ice sheets.
1362 *Geomorphology* 97, 91–108. <https://doi.org/10.1016/J.GEOMORPH.2007.02.047>
- 1363 Jamieson, S.S.R., Stokes, C.R., Livingstone, S.J., Vieli, A., Cofaigh, C., Hillenbrand, C.D., Spagnolo, M., 2016.
1364 Subglacial processes on an Antarctic ice stream bed. 2: Can modelled ice dynamics explain the
1365 morphology of mega-scale glacial lineations? *J. Glaciol.* 62, 285–298.
1366 <https://doi.org/10.1017/jog.2016.19>
- 1367 Jervey, M.T., 1988. Quantitative geological modeling of siliciclastic rock sequences and their seismic
1368 expression. *Sea-Level Chang.* 42, 47–69. <https://doi.org/10.2110/pec.88.01.0047>
- 1369 Jones, B.G., Fergusson, C.L., Zambelli, P.F., 1993. Ordovician contourites in the Lachlan Fold Belt, eastern

- 1370 Australia. *Sediment. Geol.* 82, 257–270. [https://doi.org/10.1016/0037-0738\(93\)90125-0](https://doi.org/10.1016/0037-0738(93)90125-0)
- 1371 Kehew, A.E., Piotrowski, J.A., Jørgensen, F., 2012. Tunnel valleys: Concepts and controversies - A review. *Earth-*
1372 *Science Rev.* 113, 33–58. <https://doi.org/10.1016/j.earscirev.2012.02.002>
- 1373 Khalifa, M.A., 2015. Glacial and post-glacial deposits of the Unayzah Formation (Carboniferous-Permian), Saudi
1374 Arabia: facies analysis and sequence stratigraphy. *Carbonates and Evaporites* 30, 207–227.
1375 <https://doi.org/10.1007/s13146-014-0206-5>
- 1376 King, E.L., Rise, L., Bellec, V.K., 2016. Crescentic submarine hills and holes produced by iceberg calving and
1377 rotation. *Geol. Soc. London, Mem.* 46, 267–268. <https://doi.org/10.1144/M46.119>
- 1378 Klages, J.P., Kuhn, G., Graham, A.G.C., Hillenbrand, C.-D., Smith, J.A., Nitsche, F.O., Larter, R.D., Gohl, K., 2015.
1379 Palaeo-ice stream pathways and retreat style in the easternmost Amundsen Sea Embayment, West
1380 Antarctica, revealed by combined multibeam bathymetric and seismic data. *Geomorphology* 245, 207–
1381 222. <https://doi.org/10.1016/J.GEOMORPH.2015.05.020>
- 1382 Klages, J.P., Kuhn, G., Hillenbrand, C.-D., Graham, A.G.C., Smith, J.A., Larter, R.D., Gohl, K., 2016. A glacial
1383 landform assemblage from an inter-ice stream setting in the eastern Amundsen Sea Embayment, West
1384 Antarctica. *Geol. Soc. London, Mem.* 46, 349–352. <https://doi.org/10.1144/M46.147>
- 1385 Kleman, J., Stroeve, A.P., Lundqvist, J., 2008. Patterns of Quaternary ice sheet erosion and deposition in
1386 Fennoscandia and a theoretical framework for explanation. *Geomorphology* 97, 73–90.
1387 <https://doi.org/10.1016/j.geomorph.2007.02.049>
- 1388 Klett, T., 2000. Total Petroleum Systems of the Illizi Province , Algeria and Libya — Tanezzuft-Illizi U . S .
1389 Department of the Interior. *U. S. Geol. Surv.* 1.
- 1390 Knutz, P.C., Newton, A.M.W., Hopper, J.R., Huuse, M., Gregersen, U., Sheldon, E., Dybkjær, K., 2019. Eleven
1391 phases of Greenland Ice Sheet shelf-edge advance over the past 2.7 million years. *Nat. Geosci.* 12, 361–
1392 368. <https://doi.org/10.1038/s41561-019-0340-8>
- 1393 Koch, Z.J., Isbell, J.L., 2013. Processes and products of grounding-line fans from the Permian Pagoda Formation,
1394 Antarctica: Insight into glacial conditions in polar Gondwana. *Gondwana Res.* 24, 161–172.
1395 <https://doi.org/10.1016/j.gr.2012.10.005>
- 1396 Kocurek, G., Havholm, K.G., 1993. Eolian sequence stratigraphy - A conceptual framework, in: *Siliclastic*
1397 *Sequence Stratigraphy: Recent Developments and Applications*. AAPG Special Volumes, pp. 393–409.
- 1398 Kristensen, T.B., Huuse, M., Piotrowski, J. a, Clausen, O.R., 2007. A morphometric analysis of tunnel valleys in
1399 the eastern North Sea based on 3D seismic data. *J. Quat. Sci.* 22, 801–815. <https://doi.org/10.1002/jqs>
- 1400 Krüger, J., Schomacker, A., Örn Benediktsson, Í., 2009. 6 Ice-Marginal Environments: Geomorphic and
1401 Structural Genesis of Marginal Moraines at Mýrdalsjökull. *Dev. Quat. Sci.* 13, 79–104.
1402 [https://doi.org/10.1016/S1571-0866\(09\)01306-2](https://doi.org/10.1016/S1571-0866(09)01306-2)

- 1403 Krzyszkowski, D., Zielinski, T., 2002. The Pleistocene end moraine fans: Controls on their sedimentation and
1404 location. *Sediment. Geol.* 149, 73–92. [https://doi.org/10.1016/S0037-0738\(01\)00245-7](https://doi.org/10.1016/S0037-0738(01)00245-7)
- 1405 Kurjanski, B., Rea, B.R., Spagnolo, M., Winsborrow, M., Cornwell, D.G., Andreassen, K., Howell, J., 2019.
1406 Morphological evidence for marine ice stream shutdown, central Barents Sea. *Mar. Geol.* 414, 64–76.
1407 <https://doi.org/10.1016/j.margeo.2019.05.001>
- 1408 Kvalstad, T.J., Andresen, L., Forsberg, C.F., Berg, K., Bryn, P., Wangen, M., 2005. The Storegga slide: Evaluation
1409 of triggering sources and slide mechanics. *Mar. Pet. Geol.* 22, 245–256.
1410 <https://doi.org/10.1016/j.marpetgeo.2004.10.019>
- 1411 Laberg, J.S., Dowdeswell, J.A., 2016. Glacigenic debris-flows on the Bear Island Trough-Mouth Fan, Barents Sea
1412 margin. *Geol. Soc. London, Mem.* 46, 367–368. <https://doi.org/10.1144/M46.77>
- 1413 Laier, T., Jørgensen, N.O., Buchardt, B., Cederberg, T., Kuijpers, A., 1992. Accumulation and seepages of
1414 biogenic gas in northern Denmark. *Cont. Shelf Res.* 12, 1173–1186. [https://doi.org/10.1016/0278-4343\(92\)90077-W](https://doi.org/10.1016/0278-4343(92)90077-W)
- 1416 Lajeunesse, P., Allard, M., 2002. Sedimentology of an ice-contact glaciomarine fan complex, Nastapoka Hills,
1417 eastern Hudson Bay, northern Québec. *Sediment. Geol.* 152, 201–220. [https://doi.org/10.1016/S0037-0738\(02\)00069-6](https://doi.org/10.1016/S0037-0738(02)00069-6)
- 1419 Lamb, R.M., Harding, R., Huuse, M., Stewart, M., Brocklehurst, S.H., 2017. The early Quaternary North Sea
1420 Basin. *J. Geol. Soc. London.* jgs2017-057. <https://doi.org/10.1144/jgs2017-057>
- 1421 Lambeck, K., 1998. Sea-level change, flacial rebound and mantle viscosity for northern Europe. *Geophys* 134,
1422 102–144.
- 1423 Lane, A., Taylor, A., 2002. Geohazards: Are We Looking at Them the Right Way? View From Down Under, in:
1424 Offshore Technology Conference. Offshore Technology Conference. <https://doi.org/10.4043/14106-MS>
- 1425 Lane, T.P., Roberts, D.H., Rea, B.R., Cofaigh, C., Vieli, A., Rodés, A., 2014. Controls upon the Last Glacial
1426 Maximum deglaciation of the northern Uummannaq Ice Stream System, West Greenland. *Quat. Sci. Rev.*
1427 92, 324–344. <https://doi.org/10.1016/j.quascirev.2013.09.013>
- 1428 Lang, J., Dixon, R.J., Le Heron, D.P., Winsemann, J., 2012. Depositional architecture and sequence stratigraphic
1429 correlation of Upper Ordovician glaciogenic deposits, Illizi Basin, Algeria. *Geol. Soc. London, Spec. Publ.*
1430 368, 293–317. <https://doi.org/10.1144/SP368.1>
- 1431 Lawson, D.E., 1981. Sedimentological characteristics and classification of depositional processes and deposits
1432 in the glacial environment 81–27, 22 p.
- 1433 Le Heron, D.P., 2007. Late Ordovician glacial record of the Anti-Atlas, Morocco. *Sediment. Geol.* 201, 93–110.
1434 <https://doi.org/10.1016/j.sedgeo.2007.05.004>

- 1435 Le Heron, D.P., Armstrong, H.A., Wilson, C., Howard, J.P., Gindre, L., 2010. Glaciation and deglaciation of the
1436 Libyan Desert: The Late Ordovician record. *Sediment. Geol.* 223, 100–125.
1437 <https://doi.org/10.1016/j.sedgeo.2009.11.002>
- 1438 Le Heron, D.P., Craig, J., 2012. Neoproterozoic deglacial sediments and their hydrocarbon source rock
1439 potential. *Geol. Soc. Spec. Publ.* 368, 381–393. <https://doi.org/10.1144/SP368.16>
- 1440 Le Heron, D.P., Craig, J., Etienne, J.L., 2009. Ancient glaciations and hydrocarbon accumulations in North Africa
1441 and the Middle East. *Earth-Science Rev.* 93, 47–76. <https://doi.org/10.1016/j.earscirev.2009.02.001>
- 1442 Le Heron, D.P., Craig, J., Sutcliffe, O.E., Whittington, R., 2006. Late Ordovician glaciogenic reservoir
1443 heterogeneity: An example from the Murzuq Basin, Libya. *Mar. Pet. Geol.* 23, 655–677.
1444 <https://doi.org/10.1016/j.marpetgeo.2006.05.006>
- 1445 Le Heron, D.P., Hogan, K.A., Phillips, E.R., Huuse, M., Busfield, M.E., Graham, A.G.C., 2019. An introduction to
1446 glaciated margins: the sedimentary and geophysical archive. *Geol. Soc. London, Spec. Publ.* 475.
1447 <https://doi.org/10.1144/SP475.12>
- 1448 Le Heron, D.P., Sutcliffe, O.E., Whittington, R.J., Craig, J., 2005. The origins of glacially related soft-sediment
1449 deformation structures in Upper Ordovician glaciogenic rocks: Implication for ice-sheet dynamics.
1450 *Palaeogeogr. Palaeoclimatol. Palaeoecol.* 218, 75–103. <https://doi.org/10.1016/j.palaeo.2004.12.007>
- 1451 Le Heron, D.P.P., Tofaif, S., Melvin, J., 2017. The Early Palaeozoic Glacial Deposits of Gondwana: Overview,
1452 Chronology, and Controversies, *Past Glacial Environments: Second Edition*. Elsevier Ltd.
1453 <https://doi.org/10.1016/B978-0-08-100524-8.00002-6>
- 1454 Lea, J.M., Mair, D.W.F., Nick, F.M., Rea, B.R., van As, D., Morlighem, M., Nienow, P.W., Weidick, A., 2014.
1455 Fluctuations of a Greenlandic tidewater glacier driven by changes in atmospheric forcing: observations
1456 and modelling of Kangiata Nunaata Sermia, 1859–present. *Cryosph.* 8, 2031–2045.
1457 <https://doi.org/10.5194/tc-8-2031-2014>
- 1458 Lebedeva-Ivanova, N., Polteau, S., Bellwald, B., Planke, S., Berndt, C., Stokke, H.H., 2018. Toward one-meter
1459 resolution in 3D seismic. *Lead. Edge* 37, 818–828. <https://doi.org/10.1190/tle37110818.1>
- 1460 Lee, J., 2017. *Glacial Lithofacies and Stratigraphy, Past Glacial Environments: Second Edition*. Elsevier Ltd.
1461 <https://doi.org/10.1016/B978-0-08-100524-8.00011-7>
- 1462 Levell, B.K., Braakman, J.H., Rutten, K.W., 1988. Oil-bearing sediments of Gondwana glaciation in Oman. *Am.*
1463 *Assoc. Pet. Geol. Bull.* 72, 775–796.
- 1464 Leverington, D.W., Mann, J.D., Teller, J.T., 2002. Changes in the bathymetry and volume of glacial Lake Agassiz
1465 between 9200 and 7700 ¹⁴C yr B.P. *Quat. Res.* 57, 244–252. <https://doi.org/10.1006/qres.2001.2311>
- 1466 Levson, B.V.M., Ferbey, T., Kerr, B., Johnsen, T., Bednarski, J.M., Smith, R., Blackwell, J., Jonnes, S., 2003.
1467 *Quaternary Geology and Aggregate Mapping in Northeast British Columbia : Applications for Oil and Gas*

- 1468 Exploration and Development 29–40.
- 1469 Lewis, M. a., Cheney, C.S., O Dochartaigh, B.E., 2006. Guide to Permeability Indices.
- 1470 Lisiecki, L.E., Raymo, M.E., 2005. A Pliocene-Pleistocene stack of 57 globally distributed benthic $\delta^{18}\text{O}$ records.
1471 Paleoclimatology 20, 1–17. <https://doi.org/10.1029/2004PA001071>
- 1472 Livingstone, S.J., Clark, C.D., 2016. Morphological properties of tunnel valleys of the southern sector of the
1473 Laurentide Ice Sheet and implications for their formation. Earth Surf. Dyn. 4, 567–589.
1474 <https://doi.org/10.5194/esurf-4-567-2016>
- 1475 Lonergan, L., Maidment, S.C.R., Collier, J.S., 2006. Pleistocene subglacial tunnel valleys in the central North Sea
1476 basin: 3-D morphology and evolution. J. Quat. Sci. 21, 891–903. <https://doi.org/10.1002/jqs.1015>
- 1477 Lønne, I., 1995. Sedimentary facies and depositional architecture of ice-contact glaciomarine systems.
1478 Sediment. Geol. 98, 13–43. [https://doi.org/10.1016/0037-0738\(95\)00025-4](https://doi.org/10.1016/0037-0738(95)00025-4)
- 1479 Lønne, I., Nemec, W., 2004. High-arctic fan delta recording deglaciation and environment disequilibrium.
1480 Sedimentology 51, 553–589. <https://doi.org/10.1111/j.1365-3091.2004.00636.x>
- 1481 Lopez-Gamundi, O.R., Buatois, L. a, 2010. Introduction: Late Paleozoic glacial events and postglacial
1482 transgressions in Gondwana. Geol. Soc. Am. Spec. Pap. 468, v–viii.
1483 [https://doi.org/10.1130/2010.2468\(00\)](https://doi.org/10.1130/2010.2468(00)).
- 1484 Lovell, H., Boston, C.M., 2017. Glacitectonic composite ridge systems and surge-type glaciers: an updated
1485 correlation based on Svalbard, Norway. Arktos 3, 2. <https://doi.org/10.1007/s41063-017-0028-5>
- 1486 Lucchi, R.G., Rebesco, M., 2007. Glacial contourites on the Antarctic Peninsula margin: insight for
1487 palaeoenvironmental and palaeoclimatic conditions. Geol. Soc. London, Spec. Publ. 276, 111–127.
1488 <https://doi.org/10.1144/GSL.SP.2007.276.01.06>
- 1489 Lüning, S., Craig, J., Loydell, D., Štorch, P., Fitches, B., 2000. Lower Silurian 'hot shales' in North Africa and
1490 Arabia: regional distribution and depositional model. Earth-Science Rev. 49, 121–200.
1491 [https://doi.org/10.1016/S0012-8252\(99\)00060-4](https://doi.org/10.1016/S0012-8252(99)00060-4)
- 1492 Mackiewicz, N.E., Powell, R.D., Carlson, P.R., Molnia, B.F., 1984. Interlaminated ice-proximal glaciomarine
1493 sediments in Muir Inlet, Alaska. Mar. Geol. 57, 113–147. [https://doi.org/10.1016/0025-3227\(84\)90197-X](https://doi.org/10.1016/0025-3227(84)90197-X)
- 1494 Magilligan, F.J., Gomez, B., Mertes, L. a K., Smith, L.C., Smith, N.D., Finnegan, D., Garvin, J.B., 2002.
1495 Geomorphic effectiveness, sandur development, and the pattern of landscape response during
1496 jökulhlaups: Skeidarársandur, southeastern Iceland. Geomorphology 44, 95–113.
1497 [https://doi.org/10.1016/S0169-555X\(01\)00147-7](https://doi.org/10.1016/S0169-555X(01)00147-7)
- 1498 Maizels, J., 2007. Sediments and landforms of modern proglacial terrestrial environments. Mod. Past Glacial
1499 Environ. 279–316. <https://doi.org/10.1016/b978-075064226-2/50012-x>

- 1500 Maizels, J., 1997. Jokulhlaup deposits in proglacial areas. *Quat. Sci. Rev.* 16, 793–819.
1501 [https://doi.org/10.1016/S0277-3791\(97\)00023-1](https://doi.org/10.1016/S0277-3791(97)00023-1)
- 1502 Margold, M., Stokes, C.R., Clark, C.D., 2015. Ice streams in the Laurentide Ice Sheet: Identification,
1503 characteristics and comparison to modern ice sheets. *Earth-Science Rev.* 143, 117–146.
1504 <https://doi.org/10.1016/j.earscirev.2015.01.011>
- 1505 Maries, G., Ahokangas, E., Mäkinen, J., Pasanen, A., Malehmir, A., 2017. Architecture et caractéristiques
1506 hydrogéologiques associées d'eskers interlobés basées sur une combinaison de sismique réflexion à
1507 haute résolution et de tomographie par réfraction, Virttaankangas, Sud-Ouest de la Finlande. *Hydrogeol.*
1508 *J.* 25, 829–845. <https://doi.org/10.1007/s10040-016-1513-9>
- 1509 Marks, L., 2012. Timing of the Late Vistulian (Weichselian) glacial phases in Poland. *Quat. Sci. Rev.* 44, 81–88.
1510 <https://doi.org/10.1016/J.QUASCIREV.2010.08.008>
- 1511 Marks, L., 2005. Pleistocene glacial limits in the territory of Poland. *Prz. Geol.* 53, 988–993.
1512 [https://doi.org/http://dx.doi.org/10.1016/S1571-0866\(04\)80079-4](https://doi.org/http://dx.doi.org/10.1016/S1571-0866(04)80079-4)
- 1513 Marren, P.M., 2005. Magnitude and frequency in proglacial rivers: a geomorphological and sedimentological
1514 perspective. *Earth-Science Rev.* 70, 203–251. <https://doi.org/10.1016/j.earscirev.2004.12.002>
- 1515 Martin, H., 1981. The late Palaeozoic Gondwana glaciation. *Geol. Rundschau* 70, 480–496.
1516 <https://doi.org/10.1007/BF01822128>
- 1517 Martin, J.R., Redfern, J., Aitken, J.F., 2008. A regional overview of the late Paleozoic glaciation in Oman. *Resolv.*
1518 *Late Paleoz. Ice Age Time Space, Geol. Soc. Am. Spec. Publ.* 441 80301, 175–186.
1519 [https://doi.org/10.1130/2008.2441\(12\)](https://doi.org/10.1130/2008.2441(12)).
- 1520 Martin, J.R., Redfern, J., Williams, B.P.J., 2012. Evidence for multiple ice centres during the late Palaeozoic ice
1521 age in Oman: Outcrop sedimentology and provenance of the late Carboniferous-Early Permian Al Khilata
1522 Formation. *Geol. Soc. Spec. Publ.* 368, 229–256. <https://doi.org/10.1144/SP368.18>
- 1523 Meinsen, J., Winsemann, J., Weitkamp, A., Landmeyer, N., Lenz, A., Dölling, M., 2011. Middle Pleistocene
1524 (Saalian) lake outburst floods in the Münsterland Embayment (NW Germany): Impacts and magnitudes.
1525 *Quat. Sci. Rev.* 30, 2597–2625. <https://doi.org/10.1016/j.quascirev.2011.05.014>
- 1526 Melvin, J., 2019. Zarqa megafacies: widespread subglacial deformation in the Sarah Formation of Saudi Arabia
1527 and implications for the sequence stratigraphy of the Hirnantian glaciation. *Geol. Soc. London, Spec.*
1528 *Publ.* 475, 53–80. <https://doi.org/10.1144/SP475.6>
- 1529 Michael, N.A., Shammari, S., LePain, D., Abubshait, A., Guy, M., Van Dijk, C., Zühlke, R., 2015. The Sarah
1530 Formation: A Glaciogenic Reservoir Analogue in Saudi Arabia. *AAPG Annu. Conv. Exhib.* 51167.
- 1531 Michael, N.A., Zühlke, R., Hayton, S., 2018. The palaeo-valley infilling glaciogenic Sarah Formation, an example
1532 from Rahal Dhab palaeo-valley, Saudi Arabia. *Sedimentology* 65, 851–876.

- 1533 <https://doi.org/10.1111/sed.12408>
- 1534 Millson, J.A., Mercadier, C.G.L., Livera, S.E., Peters, J.M., 1996. The Lower Palaeozoic of Oman and its context
1535 in the evolution of a Gondwanan continental margin. *J. Geol. Soc. London.* 153, 213–230.
1536 <https://doi.org/10.1144/gsjgs.153.6.1021>
- 1537 Milne, G.A., Gehrels, W.R., Hughes, C.W., Tamisiea, M.E., 2009. Identifying the causes of sea-level change. *Nat.*
1538 *Geosci.* 2, 471–478. <https://doi.org/10.1038/ngeo544>
- 1539 Mitrovica, J.X., Milne, G.A., 2002. On the origin of late Holocene sea-level highstands within equatorial ocean
1540 basins. *Quat. Sci. Rev.* 21, 2179–2190. [https://doi.org/10.1016/S0277-3791\(02\)00080-X](https://doi.org/10.1016/S0277-3791(02)00080-X)
- 1541 Moreau, J., Huuse, M., 2014. Infill of tunnel valleys associated with landward-flowing ice sheets: The missing
1542 Middle Pleistocene record of the NW European rivers? *Geochemistry, Geophys. Geosystems* 15, 1–9.
1543 <https://doi.org/10.1002/2013GC005007>
- 1544 Mountney, N.P., Russell, A.J., 2009. Aeolian dune-field development in a water table-controlled system:
1545 Skeiðarársandur, Southern Iceland. *Sedimentology* 56, 2107–2131. <https://doi.org/10.1111/j.1365-3091.2009.01072.x>
- 1547 Murton, J.B., Bateman, M.D., Dallimore, S.R., Teller, J.T., Yang, Z., 2010. Identification of Younger Dryas
1548 outburst flood path from Lake Agassiz to the Arctic Ocean. *Nature* 464, 740–743.
1549 <https://doi.org/10.1038/nature08954>
- 1550 Nanda, N.C., 2016. *Seismic Data Interpretation and Evaluation for Hydrocarbon Exploration and Production.*
1551 Springer International Publishing, Cham. <https://doi.org/10.1007/978-3-319-26491-2>
- 1552 Nemeč, W., 2009. *Aspects of Sediment Movement on Steep Delta Slopes, Coarse-Grained Deltas.* Blackwell
1553 Publishing Ltd., Oxford, UK. <https://doi.org/10.1002/9781444303858.ch3>
- 1554 Nichols, G.J., Fisher, J.A., 2007. Processes, facies and architecture of fluvial distributary system deposits.
1555 *Sediment. Geol.* 195, 75–90. <https://doi.org/10.1016/J.SEDGEO.2006.07.004>
- 1556 Nielsen, T., Rasmussen, T.L., 2018. Reconstruction of ice sheet retreat after the Last Glacial maximum in
1557 Storfjorden, southern Svalbard. *Mar. Geol.* 402, 228–243.
1558 <https://doi.org/10.1016/J.MARGEO.2017.12.003>
- 1559 Nygård, A., Sejrup, H.P., Haflidason, H., Bryn, P., 2005. The glacial North Sea Fan, southern Norwegian Margin:
1560 Architecture and evolution from the upper continental slope to the deep-sea basin. *Mar. Pet. Geol.* 22,
1561 71–84. <https://doi.org/10.1016/j.marpetgeo.2004.12.001>
- 1562 Ó Cofaigh, C., 1996. Tunnel valley genesis. *Prog. Phys. Geogr. Earth Environ.* 20, 1–19.
1563 <https://doi.org/10.1177/030913339602000101>
- 1564 Ó Cofaigh, C., Dowdeswell, J.A., Grobe, H., 2001. Holocene glacial marine sedimentation, inner Scoresby Sund,

- 1565 East Greenland: the influence of fast-flowing ice-sheet outlet glaciers. *Mar. Geol.* 175, 103–129.
1566 [https://doi.org/10.1016/S0025-3227\(01\)00117-7](https://doi.org/10.1016/S0025-3227(01)00117-7)
- 1567 Ó Cofaigh, C., Taylor, J., Dowdeswell, J.A., Pudsey, C.J., 2003. Palaeo-ice streams, trough mouth fans and high-
1568 latitude continental slope sedimentation. *Boreas* 32, 37–55. <https://doi.org/10.1080/03009480310001858>
1569
- 1570 Olsen, L., Sveian, H., Ottesen, D., Rise, L., 2013. Quaternary glacial, interglacial and interstadial deposits of
1571 Norway and adjacent onshore and offshore areas. *Quat. Geol. Norw.* 13, 79–144.
- 1572 Osterloff, P., Al-Harthy, A., Penney, R., Spaak, P., Williams, G., Al-Zadjali, F., Jones, N., Knox, R., Stephenson,
1573 M.H., Oliver, G., Al-Husseini, M.I., 2004a. Depositional sequences of the Gharif and Khuff Formations,
1574 subsurface interior Oman, *GeoArabia*. ed, Carboniferous, Permian and Early Triassic Arabian stratigraphy.
1575 *GeoArabia*.
- 1576 Osterloff, P., Penney, R., Aitken, J., Clark, N., Al-Husseini, M.I., 2004b. Depositional sequences of the Al Khlata
1577 Formation, subsurface interior Oman, *GeoArabia*. ed, Carboniferous, Permian and Early Triassic Arabian
1578 stratigraphy. *GeoArabia*.
- 1579 Ottesen, D., Dowdeswell, J. a., Rise, L., Rokoengen, K., Henriksen, S., 2002. Large-scale morphological evidence
1580 for past ice-stream flow on the mid-Norwegian continental margin. *Geol. Soc. London, Spec. Publ.* 203,
1581 245–258. <https://doi.org/10.1144/GSL.SP.2002.203.01.13>
- 1582 Ottesen, D., Dowdeswell, J.A., Bellec, V.K., Bjarnadóttir, L.R., 2017. The geomorphic imprint of glacier surges
1583 into open-marine waters: Examples from eastern Svalbard. *Mar. Geol.* 392, 1–29.
1584 <https://doi.org/10.1016/J.MARGEO.2017.08.007>
- 1585 Ottesen, D., Dowdeswell, J.A., Rise, L., Bugge, T., 2012. Large-scale development of the mid-Norwegian shelf
1586 over the last three million years and potential for hydrocarbon reservoirs in glacial sediments. *Geol. Soc.*
1587 *London, Spec. Publ.* 53–73. <https://doi.org/10.1144/SP368.6>
- 1588 Palmu, J.P., 1999. Sedimentary environment of the second salpausselkä ice marginal deposits in the karkkila-
1589 loppi area in Southwestern Finland, Tutkimusraportti - Geologian Tutkimuskeskus.
- 1590 Patton, H., Hambrey, M.J., 2009. Ice-marginal sedimentation associated with the Late Devensian Welsh Ice Cap
1591 and the Irish Sea Ice Stream: Tonfanau, West Wales. *Proc. Geol. Assoc.* 120, 256–274.
1592 <https://doi.org/10.1016/j.pgeola.2009.10.004>
- 1593 Patton, H., Hubbard, A., Andreassen, K., Auriac, A., Whitehouse, P.L., Stroeven, A.P., Shackleton, C.,
1594 Winsborrow, M., Heyman, J., Hall, A.M., 2017. Deglaciation of the Eurasian ice sheet complex. *Quat. Sci.*
1595 *Rev.* 169, 148–172. <https://doi.org/10.1016/J.QUASCIREV.2017.05.019>
- 1596 Patton, H., Hubbard, A., Andreassen, K., Winsborrow, M., Stroeven, A.P., 2016. The build-up, configuration,
1597 and dynamical sensitivity of the Eurasian ice-sheet complex to Late Weichselian climatic and oceanic

- 1598 forcing. *Quat. Sci. Rev.* 153, 97–121. <https://doi.org/10.1016/j.quascirev.2016.10.009>
- 1599 Pedersen, S., 2014. Architecture of Glaciotectonic Complexes. *Geosciences* 4, 269–296.
1600 <https://doi.org/10.3390/geosciences4040269>
- 1601 Pedersen, S.A.S., 2012. Glaciodynamic sequence stratigraphy Glaciodynamic sequence stratigraphy 29–51.
1602 <https://doi.org/10.1144/SP368.2>
- 1603 Peltier, W.R., 2002. On eustatic sea level history: Last Glacial Maximum to Holocene. *Quat. Sci. Rev.* 21, 377–
1604 396. [https://doi.org/10.1016/S0277-3791\(01\)00084-1](https://doi.org/10.1016/S0277-3791(01)00084-1)
- 1605 Phillips, E., Cotterill, C., Johnson, K., Crombie, K., James, L., Carr, S., Ruiter, A., 2018. Large-scale glacitectonic
1606 deformation in response to active ice sheet retreat across Dogger Bank (southern central North Sea)
1607 during the Last Glacial Maximum. *Quat. Sci. Rev.* 179, 24–47.
1608 <https://doi.org/10.1016/j.quascirev.2017.11.001>
- 1609 Phillips, E.R., Evans, D.J.A., Auton, C.A., 2002. Polyphase deformation at an oscillating ice margin following the
1610 Loch Lomond Readvance, central Scotland, UK. *Sediment. Geol.* 149, 157–182.
1611 [https://doi.org/10.1016/S0037-0738\(01\)00250-0](https://doi.org/10.1016/S0037-0738(01)00250-0)
- 1612 Piasecka, E.D., Winsborrow, M.C.M., Andreassen, K., Stokes, C.R., 2016. Reconstructing the retreat dynamics of
1613 the Bjørnøyrenna Ice Stream based on new 3D seismic data from the central Barents Sea. *Quat. Sci. Rev.*
1614 151, 212–227. <https://doi.org/10.1016/j.quascirev.2016.09.003>
- 1615 Pisarska-Jamrozy, M., 2015. Factors controlling sedimentation in the Toru??-Eberswalde ice-marginal valley
1616 during the Pomeranian phase of the Weichselian glaciation: An overview. *Geologos* 21, 1–29.
1617 <https://doi.org/10.1515/logos-2015-0001>
- 1618 Pisarska-Jamrozy, M., 2006. Transitional deposits between the end moraine and outwash plain in the
1619 Pomeranian glaciomarginal zone of NW Poland: a missing component of ice-contact sedimentary
1620 models. *Boreas* 35, 126–141. <https://doi.org/10.1080/03009480500359038>
- 1621 Pisarska-Jamrozy, M., Weckwerth, P., 2013. Soft-sediment deformation structures in a Pleistocene
1622 glaciolacustrine delta and their implications for the recognition of subenvironments in delta deposits.
1623 *Sedimentology* 60, 637–665. <https://doi.org/10.1111/j.1365-3091.2012.01354.x>
- 1624 Pisarska-Jamrozy, M., Zieliński, T., 2014. Pleistocene sandur rhythms, cycles and megacycles: Interpretation of
1625 depositional scenarios and palaeoenvironmental conditions. *Boreas* 43, 330–348.
1626 <https://doi.org/10.1111/bor.12041>
- 1627 Postma, G., 1990. An analysis of the variation in delta architecture. *Terra Nov.* 2, 124–130.
1628 <https://doi.org/10.1111/j.1365-3121.1990.tb00052.x>
- 1629 Powell, J.H., Moh'd, B.K., Masri, A., 1994. Late ordovician-early silurian glaciofluvial deposits preserved in
1630 palaeovalleys in South Jordan. *Sediment. Geol.* [https://doi.org/10.1016/0037-0738\(94\)90099-X](https://doi.org/10.1016/0037-0738(94)90099-X)

- 1631 Powell, R.D., 1990. Glacimarine processes at grounding-line fans and their growth to ice-contact deltas. *Geol.*
1632 *Soc. London, Spec. Publ.* 53, 53–73. <https://doi.org/10.1144/GSL.SP.1990.053.01.03>
- 1633 Powell, R.D., Alley, R.B., 1996. Grounding-Line Systems: Processes, Glaciological Inferences and the
1634 Stratigraphic Record. *American Geophysical Union*, pp. 169–187. <https://doi.org/10.1029/AR071p0169>
- 1635 Powell, R.D., Cooper, J.M., 2002. A glacial sequence stratigraphic model for temperate, glaciated continental
1636 shelves. *Geol. Soc. London, Spec. Publ.* 203, 215–244. <https://doi.org/10.1144/GSL.SP.2002.203.01.12>
- 1637 Powell, R.D., Domack, E., 1995. Modern glaciomarine environments. *Mod. Past Glacial Environ.* 1, 445–486.
- 1638 Powell, R.D., Molnia, B.F., 1989. Glacimarine sedimentary processes, facies and morphology of the south-
1639 southeast Alaska shelf and fjords. *Mar. Geol.* 85, 359–390. [https://doi.org/10.1016/0025-
1640 3227\(89\)90160-6](https://doi.org/10.1016/0025-3227(89)90160-6)
- 1641 Praeg, D., 2003. Seismic imaging of mid-Pleistocene tunnel-valleys in the North Sea Basin-high resolution from
1642 low frequencies. *J. Appl. Geophys.* 53, 273–298. <https://doi.org/10.1016/j.jappgeo.2003.08.001>
- 1643 Rea, B.R., Newton, A.M.W., Lamb, R.M., Harding, R., Bigg, G.R., Rose, P., Spagnolo, M., Huuse, M., Cater, J.M.L.,
1644 Archer, S., Buckley, F., Halliyeva, M., Huuse, J., Cornwell, D.G., Brocklehurst, S.H., Howell, J.A., 2018.
1645 Extensive marine-terminating ice sheets in Europe from 2.5 million years ago. *Sci. Adv.* 4, eaar8327.
1646 <https://doi.org/10.1126/sciadv.aar8327>
- 1647 Reading, H.G., 2002. *Sedimentary environments : processes, facies, and stratigraphy.* Blackwell Science.
- 1648 Reinardy, B.T.I., Leighton, I., Marx, P.J., 2013. Glacier thermal regime linked to processes of annual moraine
1649 formation at Midtdalsbreen, southern Norway. *Boreas* 42, 896–911. <https://doi.org/10.1111/bor.12008>
- 1650 Rinterknecht, V., Braucher, R., Böse, M., Bourlès, D., Mercier, J.L., 2012. Late Quaternary ice sheet extents in
1651 northeastern Germany inferred from surface exposure dating. *Quat. Sci. Rev.* 44, 89–95.
1652 <https://doi.org/10.1016/j.quascirev.2010.07.026>
- 1653 Rinterknecht, V.R., Clark, P.U., Raisbeck, G.M., Yiou, F., Brook, E.J., Tschudi, S., Lunkka, J.P., 2004. Cosmogenic
1654 ¹⁰Be dating of the Salpausselkä I Moraine in southwestern Finland. *Quat. Sci. Rev.* 23, 2283–2289.
1655 <https://doi.org/10.1016/J.QUASCIREV.2004.06.012>
- 1656 Rose, P., Byerley, G., Vaughan, O., Cater, J., Rea, B.R., Spagnolo, M., Archer, S., 2016. Aviat: a Lower Pleistocene
1657 shallow gas hazard developed as a fuel gas supply for the Forties Field. *Geol. Soc. London, Pet. Geol.*
1658 *Conf. Ser.* 8, 485–505. <https://doi.org/10.1144/pgc8.16>
- 1659 Rust, B.R., 1965. The sedimentology and diagenesis of Silurian turbidites in south-east Wigtownshire, Scotland.
1660 *Scottish J. Geol.* 1 Part 3, 231–246. <https://doi.org/>
- 1661 Rust, B.R., Romanelli, Ri., 1975. Late Quaternary ubaqueous Outwash Deposits Near Ottawa, Canada, in:
1662 *Glaciofluvial and Glaciolacustrine Sedimentation.* SEPM (Society for Sedimentary Geology), pp. 177–192.

- 1663 <https://doi.org/10.2110/pec.75.23.0177>
- 1664 Rütther, D.C., Andreassen, K., Spagnolo, M., 2013. Aligned glaciotectionic rafts on the central Barents Sea
1665 seafloor revealing extensive glaciotectionic erosion during the last deglaciation. *Geophys. Res. Lett.* 40,
1666 6351–6355. <https://doi.org/10.1002/2013GL058413>
- 1667 Rütther, D.C., Mattingsdal, R., Andreassen, K., Forwick, M., Husum, K., 2011. Seismic architecture and
1668 sedimentology of a major grounding zone system deposited by the Bjørnøyrenna Ice Stream during Late
1669 Weichselian deglaciation. *Quat. Sci. Rev.* 30, 2776–2792.
1670 <https://doi.org/10.1016/j.quascirev.2011.06.011>
- 1671 Saarnisto, M., Saarinen, T., 2001. Deglaciation chronology of the Scandinavian Ice Sheet from the Lake Onega
1672 Basin to the Salpausselkä End Moraines. *Glob. Planet. Change* 31, 387–405.
1673 [https://doi.org/10.1016/S0921-8181\(01\)00131-X](https://doi.org/10.1016/S0921-8181(01)00131-X)
- 1674 Sandersen, P.B.E., Jørgensen, F., 2012. Substratum control on tunnel valley formation in Denmark 145–157.
1675 <https://doi.org/10.1144/SP368.12#The>
- 1676 Sejrup, H.P., Clark, C.D., Hjelstuen, B.O., 2016. Rapid ice sheet retreat triggered by ice stream debuttressing:
1677 Evidence from the North Sea. *Geology* 44, 355–358. <https://doi.org/10.1130/G37652.1>
- 1678 Sengbush, R.L., 1983. *Seismic Exploration Methods*. Springer Netherlands, Dordrecht.
1679 <https://doi.org/10.1007/978-94-011-6397-2>
- 1680 Shmatkova, A.A., Shmatkov, A.A., Gainanov, V.G., Buenz, S., 2015. Identification of geohazards based on the
1681 data of marine high-resolution 3D seismic observations in the Norwegian Sea. *Moscow Univ. Geol. Bull.*
1682 70, 53–61. <https://doi.org/10.3103/S0145875215010068>
- 1683 Simkins, L.M., Greenwood, S.L., Anderson, J.B., 2018. Diagnosing ice sheet grounding line stability from
1684 landform morphology. *Cryosph.* 2707–2726. <https://doi.org/10.5194/tc-2018-44>
- 1685 Soubaras, R., Whiting, P., 2011. Variable depth streamer — The new broadband acquisition system, in: *SEG*
1686 *Technical Program Expanded Abstracts 2011*. Society of Exploration Geophysicists, pp. 4349–4353.
1687 <https://doi.org/10.1190/1.3628115>
- 1688 Spagnolo, M., Clark, C.D., Ely, J.C., Stokes, C.R., Anderson, J.B., Andreassen, K., Graham, A.G.C., King, E.C., 2014.
1689 Size, shape and spatial arrangement of mega-scale glacial lineations from a large and diverse dataset.
1690 *Earth Surf. Process. Landforms* n/a-n/a. <https://doi.org/10.1002/esp.3532>
- 1691 Spagnolo, M., Phillips, E., Piotrowski, J.A., Rea, B.R., Clark, C.D., Stokes, C.R., Carr, S.J., Ely, J.C., Ribolini, A.,
1692 Wysota, W., Szuman, I., 2016. Ice stream motion facilitated by a shallow-deforming and accreting bed.
1693 *Nat. Commun.* 7, 10723. <https://doi.org/10.1038/ncomms10723>
- 1694 Spratt, R.M., Lisiecki, L.E., 2016. A Late Pleistocene sea level stack. *Clim. Past* 12, 1079–1092.
1695 <https://doi.org/10.5194/cp-12-1079-2016>

- 1696 Steno, N., 1671. Nicolai Stenonis De solido intra solidum naturaliter contento dissertationis prodromus. The
1697 Macmillan Company.
- 1698 Stewart, M.A., Lonergan, L., 2011. Seven glacial cycles in the middle-late Pleistocene of northwest Europe:
1699 Geomorphic evidence from buried tunnel valleys. *Geology* 39, 283–286.
1700 <https://doi.org/10.1130/G31631.1>
- 1701 Stewart, M.A., Lonergan, L., Hampson, G., 2013. 3D seismic analysis of buried tunnel valleys in the central
1702 North Sea: Morphology, cross-cutting generations and glacial history. *Quat. Sci. Rev.* 72, 1–17.
1703 <https://doi.org/10.1016/j.quascirev.2013.03.016>
- 1704 Stoker, M.S., Balson, P.S., Long, D., Tappin, D.R., 2011. An overview of the lithostratigraphical framework for
1705 the Quaternary deposits on the United Kingdom continental shelf 48.
- 1706 Stokes, C.R., Clark, C.D., 2002. Ice stream shear margin moraines. *Earth Surf. Process. Landforms* 27, 547–558.
1707 <https://doi.org/10.1002/esp.326>
- 1708 Stokes, C.R., Clark, C.D., 2001. Palaeo-ice streams 20, 1437–1457. [https://doi.org/10.1016/S0277-](https://doi.org/10.1016/S0277-3791(01)00003-8)
1709 3791(01)00003-8
- 1710 Stokes, C.R., Clark, C.D., 1999. Geomorphological criteria for identifying Pleistocene ice streams. *Ann. Glaciol.*
1711 28, 67–74. <https://doi.org/10.3189/172756499781821625>
- 1712 Stokes, C.R., Clark, C.D., Lian, O.B., Tulaczyk, S., 2007. Ice stream sticky spots: A review of their identification
1713 and influence beneath contemporary and palaeo-ice streams. *Earth-Science Rev.* 81, 217–249.
1714 <https://doi.org/10.1016/j.earscirev.2007.01.002>
- 1715 Stokes, C.R., Tarasov, L., Blomdin, R., Cronin, T.M., Fisher, T.G., Gyllencreutz, R., Hättestrand, C., Heyman, J.,
1716 Hindmarsh, R.C.A., Hughes, A.L.C., Jakobsson, M., Kirchner, N., Livingstone, S.J., Margold, M., Murton,
1717 J.B., Noormets, R., Peltier, W.R., Peteet, D.M., Piper, D.J.W., Preusser, F., Renssen, H., Roberts, D.H.,
1718 Roche, D.M., Saint-Ange, F., Stroeven, A.P., Teller, J.T., 2015. On the reconstruction of palaeo-ice sheets:
1719 Recent advances and future challenges. *Quat. Sci. Rev.* 125, 15–49.
1720 <https://doi.org/10.1016/j.quascirev.2015.07.016>
- 1721 Storrar, R.D., Ewertowski, M., Tomczyk, A.M., Barr, I.D., Livingstone, S.J., Ruffell, A., Stoker, B.J., Evans, D.J.A.,
1722 2019. Equifinality and preservation potential of complex eskers. *Boreas* bor.12414.
1723 <https://doi.org/10.1111/bor.12414>
- 1724 Storrar, R.D., Stokes, C.R., Evans, D.J.A., 2014. Morphometry and pattern of a large sample (>20,000) of
1725 Canadian eskers and implications for subglacial drainage beneath ice sheets. *Quat. Sci. Rev.* 105, 1–25.
1726 <https://doi.org/10.1016/J.QUASCIREV.2014.09.013>
- 1727 Strand, K., 2012. Global and continental-scale glaciations on the Precambrian earth. *Mar. Pet. Geol.* 33, 69–79.
1728 <https://doi.org/10.1016/j.marpetgeo.2012.01.011>

- 1729 Stroeven, A.P., Hättestrand, C., Kleman, J., Heyman, J., Fabel, D., Fredin, O., Goodfellow, B.W., Harbor, J.M.,
1730 Jansen, J.D., Olsen, L., Caffee, M.W., Fink, D., Lundqvist, J., Rosqvist, G.C., Strömberg, B., Jansson, K.N.,
1731 2016. Deglaciation of Fennoscandia. *Quat. Sci. Rev.* 147, 91–121.
1732 <https://doi.org/10.1016/j.quascirev.2015.09.016>
- 1733 Stuart, J.Y., Huuse, M., 2012. 3D seismic geomorphology of a large Plio-Pleistocene delta - “Bright spots” and
1734 contourites in the Southern North Sea. *Mar. Pet. Geol.* 38, 143–157.
1735 <https://doi.org/10.1016/j.marpetgeo.2012.06.003>
- 1736 Stumm, D., 2012. A review on tunnel valleys in northern Europe. *Quat. Int.* 279–280, 474.
1737 <https://doi.org/10.1002/esp.1668>.Nagra
- 1738 Swartz, J.M., Gulick, S.P.S., Goff, J.A., 2015. Gulf of Alaska continental slope morphology: Evidence for recent
1739 trough mouth fan formation. *Geochemistry, Geophys. Geosystems* 16, 165–177.
1740 <https://doi.org/10.1002/2014GC005594>
- 1741 Taylor, J., Dowdeswell, J. a., Kenyon, N.H., O’Cofaigh, C.S., 2002. Late Quaternary compositional architecture of
1742 trough-mouth fans: debris flows and suspended sediments on the Norwegian margin. *Glacier-Influenced*
1743 *Sediment. High-Latitude Cont. Margins* 55–71. <https://doi.org/10.1144/GSL.SP.2002.203.01.04>
- 1744 Thomas, G.S.P., 1984. Sedimentation of a sub-aqueous esker-delta at Strabathie, Aberdeenshire. *Scottish J.*
1745 *Geol.* 20, 9–20. <https://doi.org/10.1144/sjg20010009>
- 1746 Thomas, G.S.P., Chiverrell, R.C., 2006. A model of subaqueous sedimentation at the margin of the Late
1747 Midlandian Irish Ice Sheet, Connemara, Ireland, and its implications for regionally high isostatic sea-
1748 levels. *Quat. Sci. Rev.* 25, 2868–2893. <https://doi.org/10.1016/j.quascirev.2006.04.002>
- 1749 Thorleifson, L.H., 1996. Review of Lake Agassiz history. *Geol. Assoc. Canada* 55–84.
- 1750 Thwaites, F.T., 1926. The Origin and Significance of Pitted Outwash. *J. Geol.* 34, 308–319.
1751 <https://doi.org/10.1086/623315>
- 1752 Todd, B.J., 2016. The Laurentian Channel: A major cross-shelf trough in Atlantic Canada. *Geol. Soc. Mem.* 46,
1753 161–162. <https://doi.org/10.1144/M46.124>
- 1754 Todd, B.J., 2014. De Geer moraines on German Bank , southern Scotian Shelf of Atlantic Canada 1–2.
1755 <https://doi.org/10.1144/M46.112>
- 1756 Uścińowicz, S., 2004. Rapid sea level changes in the Southern Baltic during late glacial and early Holocene.
1757 *Polish Geol. Inst. Spec. Pap.* 11, 9–18.
- 1758 van der Vegt, P., Janszen, A., Moscariello, A., Janszen, A., Moscariello, A., 2016. Tunnel valleys : current
1759 knowledge and future perspectives. *Geol. Soc. London, Spec. Publ.* 368, 75–97.
1760 <https://doi.org/10.1144/SP368.13>

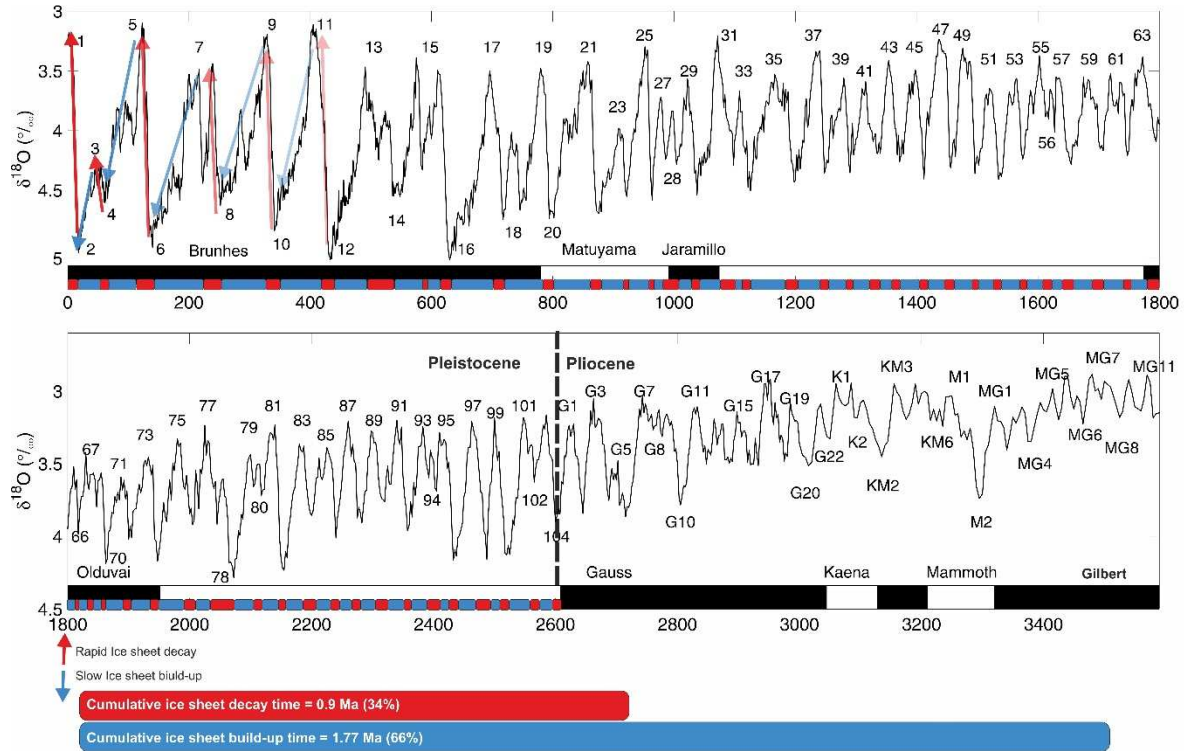
- 1761 van der Wateren, F.M., 1994. Proglacial subaquatic outwash fan and delta sediments in push moraines—
1762 indicators of subglacial meltwater activity. *Sediment. Geol.* 91, 145–172. <https://doi.org/10.1016/0037->
1763 0738(94)90127-9
- 1764 Van der Wateren, F.M., 1995. Structural Geology and Sedimentology of Push Moraines - Processes of soft
1765 sediment deformation in a glacial environment and the distribution of glaciotectonic styles. *Meded. Rijks*
1766 *Geol. Dienst.* 54, 1–168.
- 1767 Van Landeghem, K.J.J., Wheeler, A.J., Mitchell, N.C., 2009. Seafloor evidence for palaeo-ice streaming and
1768 calving of the grounded Irish Sea Ice Stream: Implications for the interpretation of its final deglaciation
1769 phase. *Boreas* 38, 111–131. <https://doi.org/10.1111/j.1502-3885.2008.00041.x>
- 1770 Van Loon, A.J. (Tom), Pisarska-Jamroży, M., 2017. Changes in the Heavy-Mineral Spectra on Their Way From
1771 Various Sources to Joint Sinks. *Sediment Proven.* 49–62. [https://doi.org/10.1016/B978-0-12-803386-](https://doi.org/10.1016/B978-0-12-803386-9.00004-6)
1772 9.00004-6
- 1773 Van Wagoner, J.C., Posamentier, H.W., Mitchum, R.M., Vail, P.R., Sarg, J.F., Loutit, T.S., Hardenbol, J., 1988. An
1774 Overview of the Fundamentals of Sequence Stratigraphy and Key Definitions, in: *Sea-Level Changes.*
1775 *SEPM (Society for Sedimentary Geology)*, pp. 39–45. <https://doi.org/10.2110/pec.88.01.0039>
- 1776 Vaslet, D., 1990. Upper Ordovician glacial deposits in Saudi Arabia. *Episodes* 13, 147–162.
- 1777 Vassiljev, J.J., Saarse, L., 2013. Timing of the Baltic ice lake in the eastern Baltic. *Bull. Geol. Soc. Finl.* 85, 9–18.
1778 <https://doi.org/10.1016/j.quaint.2008.10.005>
- 1779 Vaughan-Hirsch, D.P., Phillips, E.R., 2017. Mid-Pleistocene thin-skinned glaciotectonic thrusting of the
1780 Aberdeen Ground Formation, Central Graben region, central North Sea. *J. Quat. Sci.* 32, 196–212.
1781 <https://doi.org/10.1002/jqs.2836>
- 1782 Velichko, A.A., Kononov, Y.M., Faustova, M.A., 1997. The last glaciation of earth: Size and volume of ice-sheets.
1783 *Quat. Int.* 41–42, 43–51. [https://doi.org/10.1016/S1040-6182\(96\)00035-3](https://doi.org/10.1016/S1040-6182(96)00035-3)
- 1784 Visser, J.N.J., Loock, W.P., Colliston, W.P., 2003. Subaqueous Outwash Fan and Esker Sandstones in the Permo-
1785 Carboniferous Dwyka Formation of South Africa. *SEPM J. Sediment. Res. Vol.* 57, 467–478.
1786 <https://doi.org/10.1306/212f8b66-2b24-11d7-8648000102c1865d>
- 1787 Vorren, T.O., Laberg, J.S., 1997. Trough mouth fans - Palaeoclimate and ice-sheet monitors. *Quat. Sci. Rev.* 16,
1788 865–881. [https://doi.org/10.1016/S0277-3791\(97\)00003-6](https://doi.org/10.1016/S0277-3791(97)00003-6)
- 1789 Walther, J., 1893. *Einleitung in die Geologie als historische Wissenschaft.* Jena, G. Fischer.
- 1790 Wang, D., Helmy, M., Rawnsley, K., 2011. Glacial Sedimentological Interpretation from Microresistivity Images ,
1791 Al Khata Formation , Oman. *AAPG Search Discov. Artic.* 50511.
- 1792 Ward, L.G., Grizzle, R., Johnson, P., 2019. High Resolution Seafloor Bathymetry, Surficial Sediment Maps, and

- 1793 Interactive Database: Jeffreys Ledge and Vicinity. University of New Hampshire Center for Coastal and
1794 Ocean Mapping and Joint Hydrographic Center, Durham. [WWW Document]. URL
1795 <http://ccom.unh.edu/project/jeffreys-ledge> (accessed 10.26.19).
- 1796 Weckwerth, P., Wysota, W., Piotrowski, J.A., Adamczyk, A., Krawiec, A., Dąbrowski, M., 2019. Late Weichselian
1797 glacier outburst floods in North-Eastern Poland: Landform evidence and palaeohydraulic significance.
1798 *Earth-Science Rev.* <https://doi.org/10.1016/j.earscirev.2019.05.006>
- 1799 Westoby, M.J., Glasser, N.F., Brasington, J., Hambrey, M.J., Quincey, D.J., Reynolds, J.M., 2014. Modelling
1800 outburst floods from moraine-dammed glacial lakes. *Earth-Science Rev.* 134, 137–159.
1801 <https://doi.org/10.1016/j.earscirev.2014.03.009>
- 1802 Winsborrow, M., Andreassen, K., Hubbard, A., Plaza-Faverola, A., Gudlaugsson, E., Patton, H., 2016. Regulation
1803 of ice stream flow through subglacial formation of gas hydrates. *Nat. Geosci.* 9, 370–374.
1804 <https://doi.org/10.1038/ngeo2696>
- 1805 Winsemann, J., Alho, P., Laamanen, L., Goseberg, N., Lang, J., Klostermann, J., 2016. Flow dynamics,
1806 sedimentation and erosion of glacial lake outburst floods along the Middle Pleistocene Scandinavian Ice
1807 Sheet (northern central Europe). *Boreas* 45, 260–283. <https://doi.org/10.1111/bor.12146>
- 1808 Zecchin, M., Catuneanu, O., Rebesco, M., 2015. High-resolution sequence stratigraphy of clastic shelves IV:
1809 High-latitude settings. *Mar. Pet. Geol.* 68, 427–437. <https://doi.org/10.1016/j.marpetgeo.2015.09.004>
- 1810 Zhang, Z., Wardlaw, S., Haneberg, W.C., 2016. Seismic AVO Analysis for Shallow Hazard Assessments in
1811 Stratigraphically Complicated Areas in Onshore Alaska Locations, in: SPE Western Regional Meeting.
1812 Society of Petroleum Engineers. <https://doi.org/10.2118/180455-MS>
- 1813 Zheng, W., Pritchard, M.E., Willis, M.J., Stearns, L.A., 2019. The Possible Transition From Glacial Surge to Ice
1814 Stream on Vavilov Ice Cap. *Geophys. Res. Lett.* 2019GL084948. <https://doi.org/10.1029/2019GL084948>
- 1815 Zielinski, T., Van Loon, A.J., 2003. Pleistocene sandur deposits represent braidplains, not alluvial fans. *Boreas*
1816 32, 590–611. <https://doi.org/10.1111/j.1502-3885.2003.tb01238.x>
- 1817 Zieliński, T., van Loon, A.J., 2000. Subaerial terminoglacial fans III: overview of sedimentary characteristics and
1818 depositional model. *Netherlands J. Geosci. - Geol. en Mijnb.* 79, 93–107.
1819 <https://doi.org/10.1017/S0016774600021600>
- 1820 Zieliński, T., van Loon, A.J.J., 1999. Subaerial terminoglacial fans II: A semi-quantitative sedimentological
1821 analysis of the middle and distal environments. *Geol. en Mijnb.* 78, 73–85.
1822 <https://doi.org/10.1023/A:1003862730530>
- 1823 Zieliński, T., van Loon, A.J.J., 1998. Subaerial terminoglacial fans I: A semi-quantitative sedimentological
1824 analysis of the proximal environment. *Geol. en Mijnbouw/Netherlands J. Geosci.* 77, 1–15.
1825 <https://doi.org/https://doi.org/10.1023/A:1003535101480>

1826

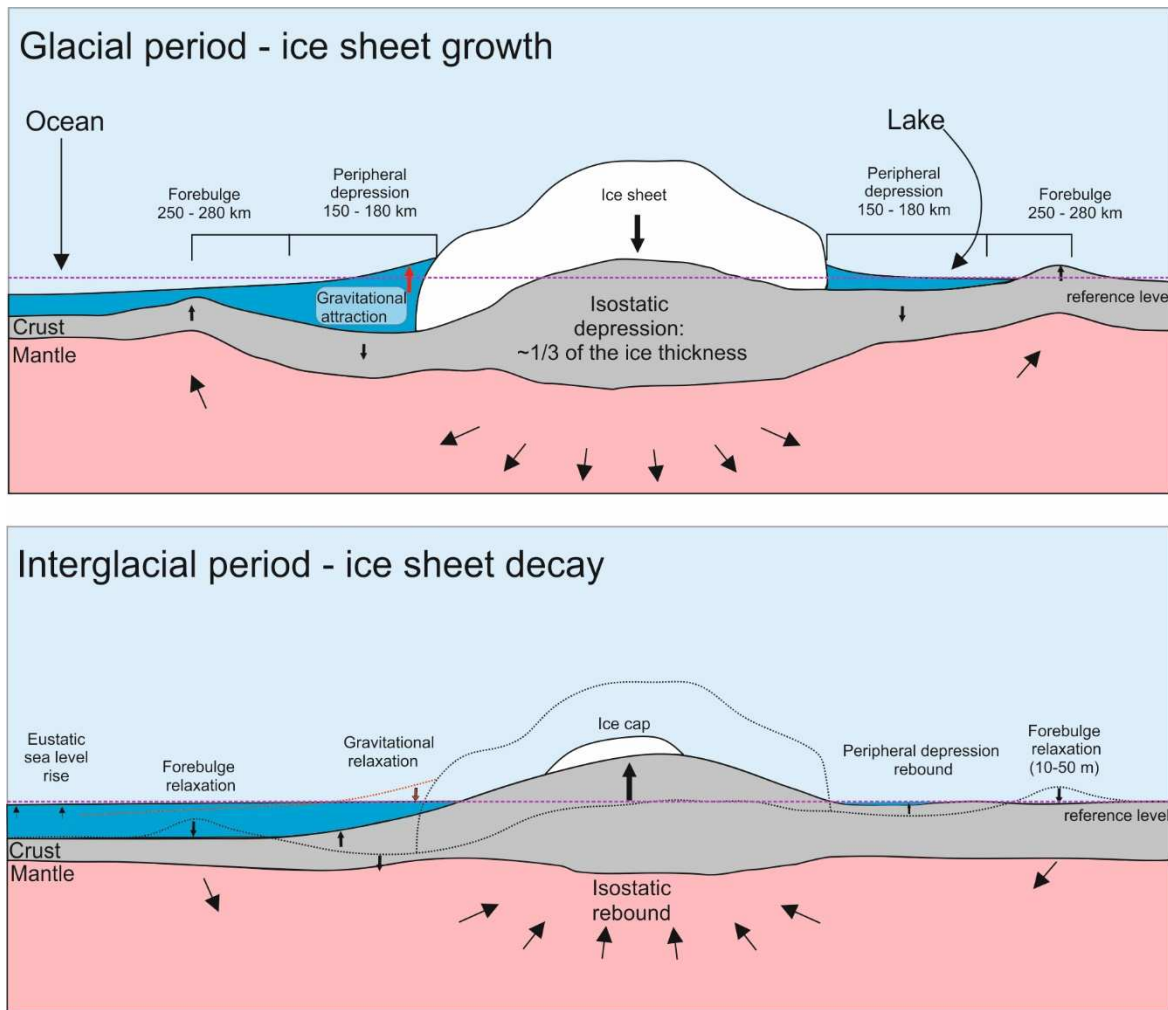
1827 Figures

1828



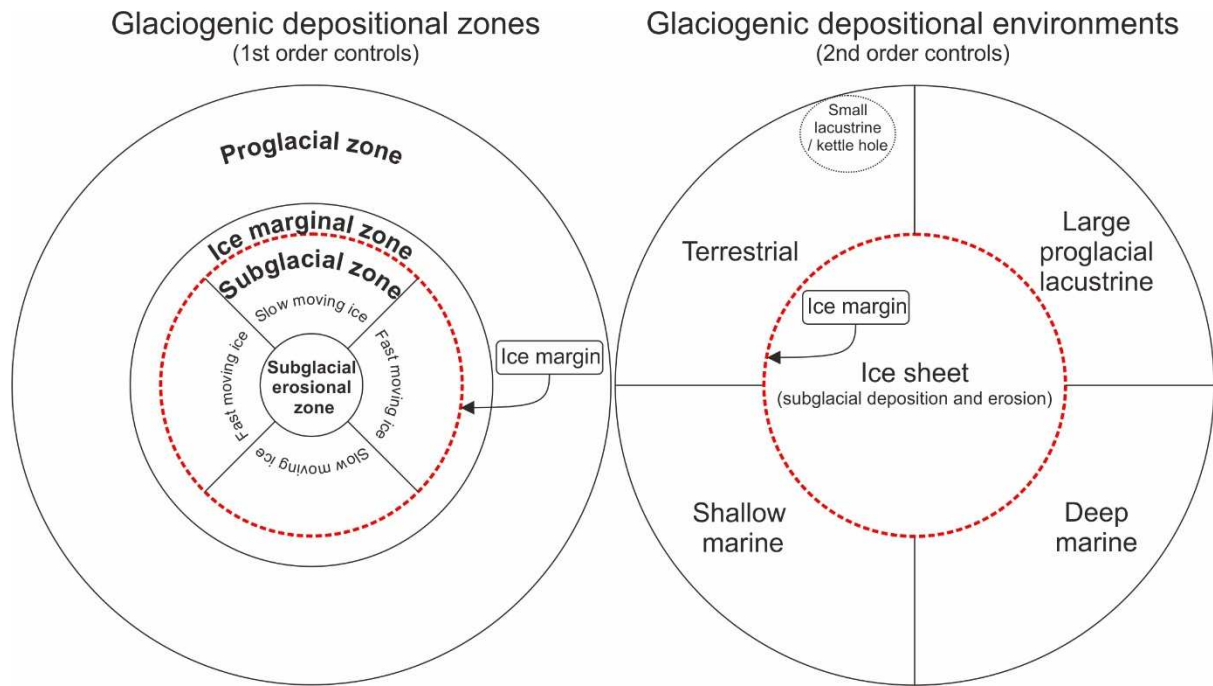
1829

1830 Figure 1: $\delta^{18}\text{O}$ (‰) Marine oxygen isotope (MIS) stages for the past 3.6 Ma, modified from Lisiecki &
 1831 Raymo (2005). Note the asymmetry in time between global ice build-up and decay (termination).
 1832 This is most pronounced for the last four cycles, but a similar pattern is visible through the entire
 1833 Pleistocene. Time is shown in kilo-years and the magnetic reversal timescale is shown as the black
 1834 (normal polarity) and white (reversed polarity) bars.



1835

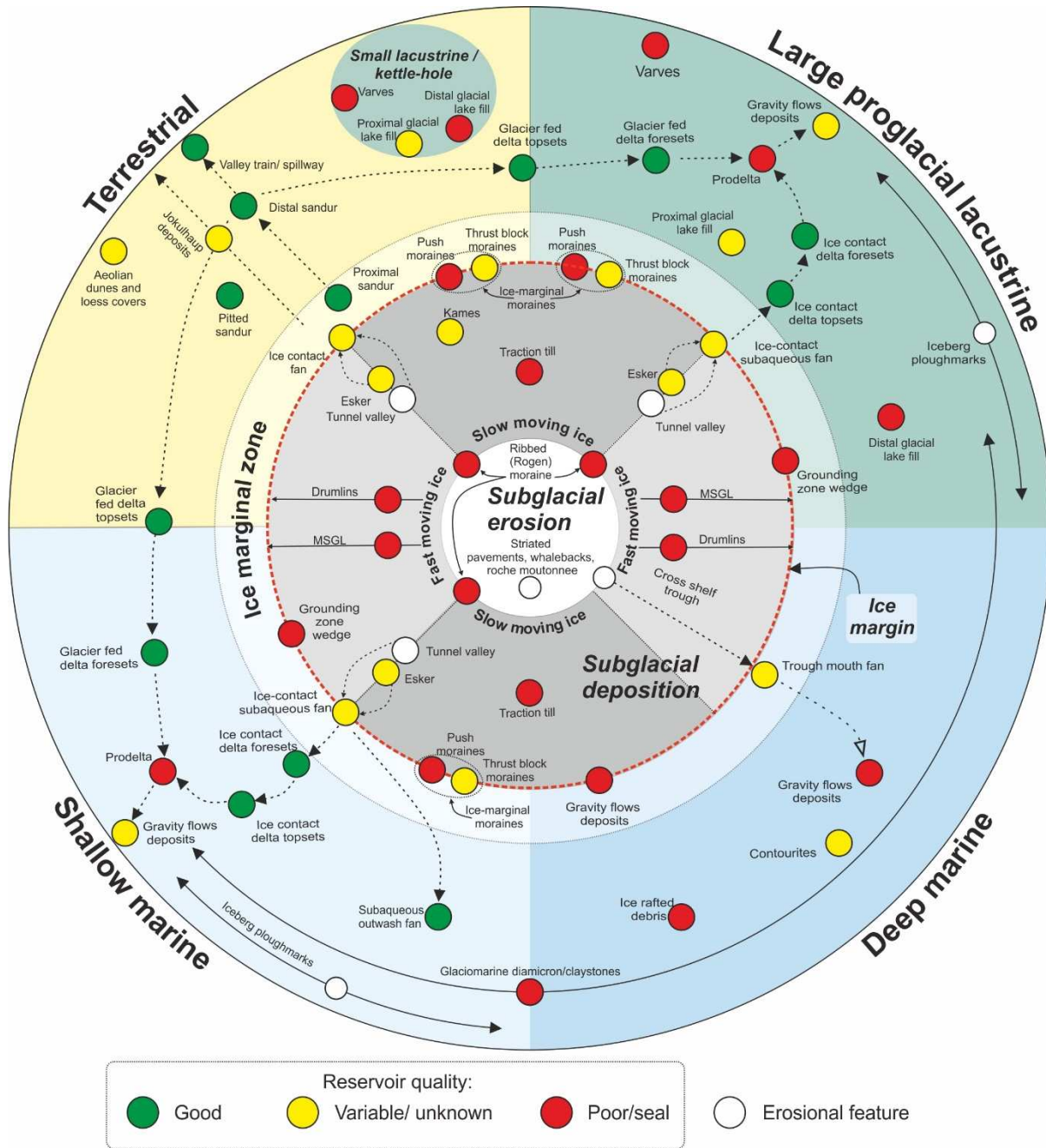
1836 Figure 2: Crust and mantle response to growth (top) and decay (bottom) of ice sheets during glacial -
 1837 interglacial cycles. Note the changes to the ocean/lake level proximally and distally to the ice sheet.
 1838 Approximated distances and elevation changes based on Fjeldskaar (1994)



1839

1840 Figure 3: Schematic representation of the model framework. Left: the model is divided into three
 1841 major depositional zones: proglacial, ice marginal and subglacial. The subglacial zone is further
 1842 subdivided into an erosional zone, spreading from the ice sheet centre (ice divide) where erosion >
 1843 deposition, and the subglacial depositional zone, where the opposite is true. Subglacial deposition is
 1844 differentiated into zones of fast-moving ice (ice streams or lobes) and slow moving ice (ice divides
 1845 and inter-stream areas). Right: the model is divided into depositional environments in which the ice
 1846 sheet terminates, which exerts a second order control on sediment and landform distributions.

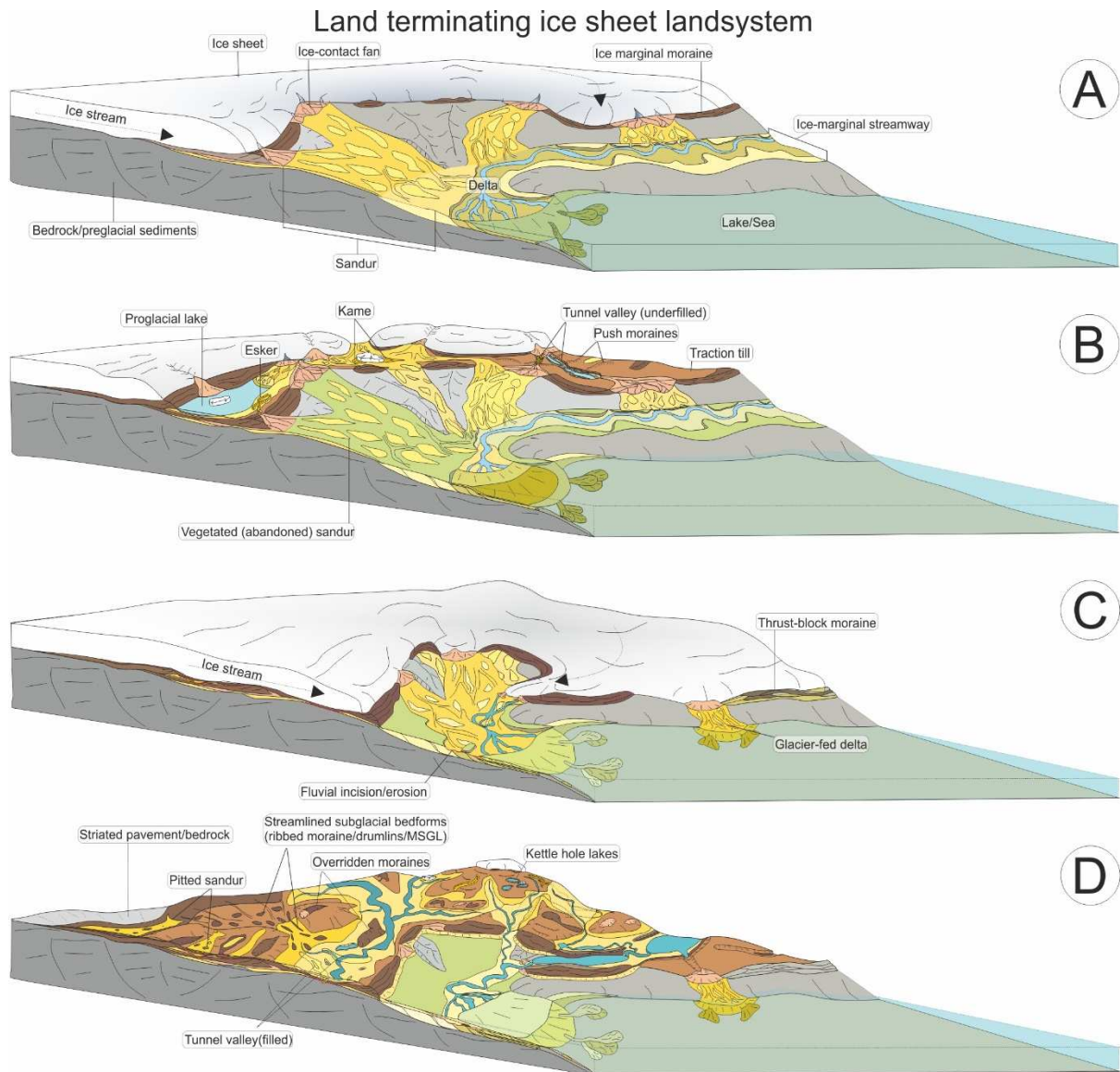
1847



1848

1849 Figure 4: Conceptual diagram generalizing the planform (bird eye view) sediment and landform distribution
 1850 for ice sheet depositional systems. The diagram is centred on the ice sheet which is located within the inner
 1851 circle (delineated by the ice margin, i.e. the red, dashed line) and “covers” the subglacial erosional zone and
 1852 the subglacial depositional zone and ignores cold based ice. Landforms are positioned radially (proximal-distal)
 1853 relative to the ice sheet divide, which is located at the very centre of the diagram (subglacial erosional zone).
 1854 Where possible, sediments and landforms are positioned in relative position, for example proximal sandur,
 1855 distal sandur, glacier-fed delta, indicated by dotted black arrows. Landforms/sediments with attached solid
 1856 black arrows can be found across the environment. A traffic light system is used to highlight
 1857 landforms/sediment reservoir potential : Green - good reservoir, yellow - variable/unknown, red - poor
 1858 reservoir/seal. White dots represent major, recognizable glaciogenic erosional features that are extremely
 1859 useful, or even diagnostic, for identification of the location within a glaciated palaeo landscape.

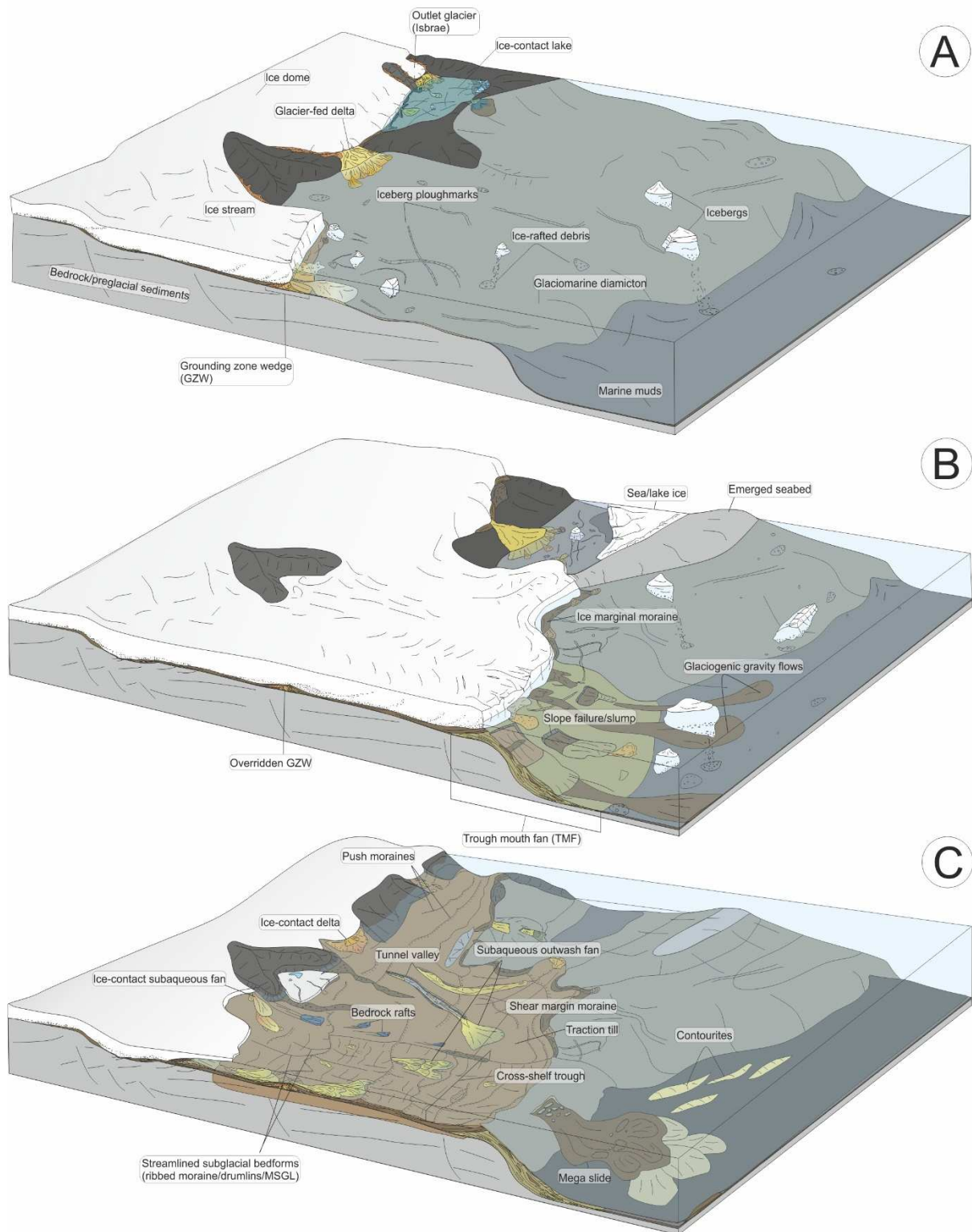
1860



1861

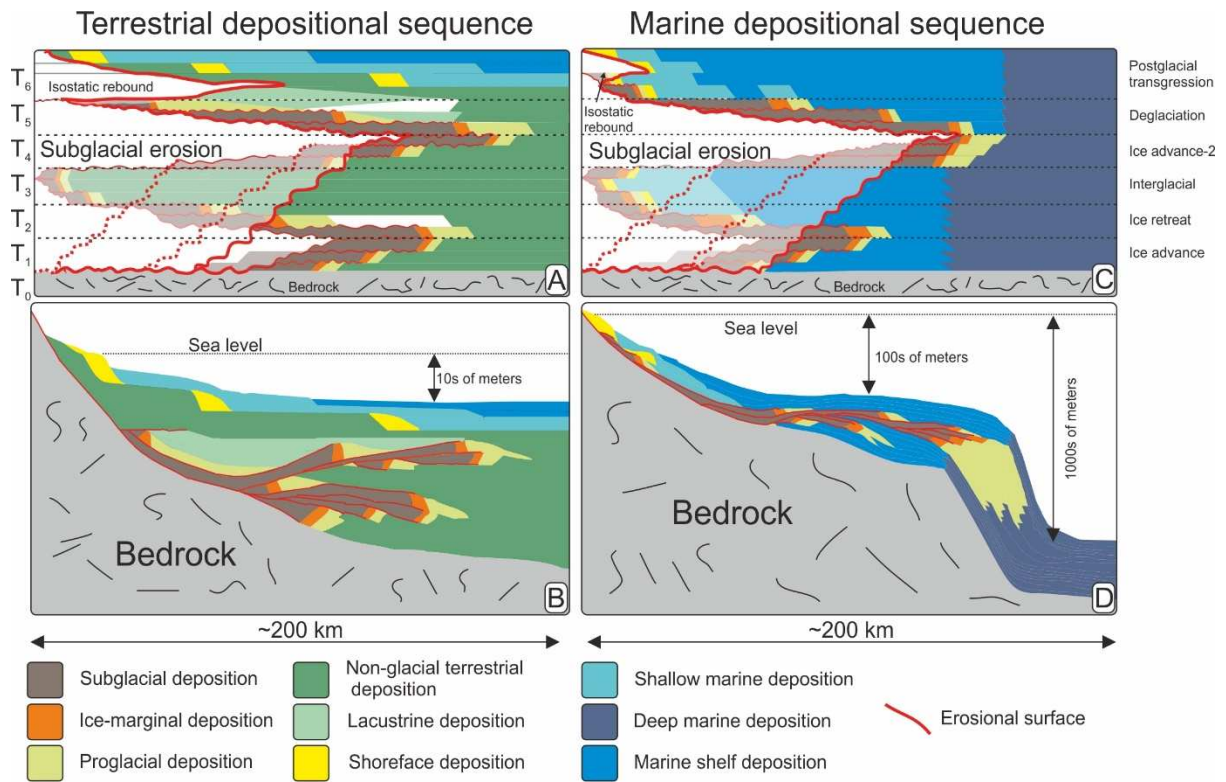
1862 Figure 5: Land terminating ice sheet depositional system across a glacial cycle. A: First ice sheet
 1863 advance - stadial 1, B: Ice sheet retreat — interstadial 1, C: Second ice sheet advance — stadial 2, D:
 1864 Final ice sheet retreat – transition from glacial to interglacial conditions. A - C can happen
 1865 repeatedly, within a single glaciation, before D.

Marine/lacustrine terminating ice sheet landssystem



1866

1867 Figure 6: Water terminating ice sheet depositional system across a glacial cycle. A: First ice sheet
 1868 advance into a basin - Stadial 1, B: Ice advance to the shelf break – maximum ice extent, C: Ice sheet
 1869 retreat – transition from glacial to interglacial conditions.



1870

1871 Figure 7: Simplified conceptual sections through terrestrial (A and B) and marine (C and D)
 1872 depositional sequences, illustrating multiple phases of ice advance and retreat. Subglacial erosion is
 1873 responsible for removal of previous glacial and interglacial deposits. The missing section is visible on
 1874 chronostratigraphic cross-sections A and C as the faded area. The extent and depth of subglacial
 1875 erosion is dependent on numerous factors, including the duration of glaciation, subsidence rate,
 1876 basal thermal regime and initial thickness of the underlying sediments.

1877

1878

1879

1880

1881

1882

1883

1884

1885

1886

1887

1888

1889

1890 Tables

1891

1892 Table 1: Alias table of some of the glaciogenic features, landforms and sediments

Glacial feature	Also known as	References
Ice marginal streamway	urstromtal, spillway, pradolina, valley train, ice marginal valley	(Brodzikowski and van Loon, 1987; Pisarska-Jamrozy, 2015)
Sandur	glacial outwash, outwash plain, fluvio-glacial outwash, sander plateau, braided outwash, proglacial braided river, glacial braidplain, sandur plain, sandar (plural)	(Girard et al., 2012; Gomez et al., 2000; Khalifa, 2015; Marren, 2005; Martin et al., 2008; Zielinski and Van Loon, 2003)
Glacier-fed delta	sandur delta, glacial outwash delta, glacio-lacustrine delta, sandur/delta system, proglacial delta, braid-delta	(Benn and Evans, 2010; Dietrich et al., 2017, 2016)
Ice-contact delta	kame delta, glacial delta, esker delta, ice-marginal delta, glacio-lacustrine delta, glacier delta	(Benn and Evans, 2010; Glückert, 1986; Lønne, 1995; Powell and Molnia, 1989)
Jökulhlaup	glacial lake outburst flood (GLOF), outburst flood, megaflood	(Gomez et al., 2000; Maizels, 1997; Westoby et al., 2014)
Traction till	subglacial diamicton, comminution till, lodgement till, melt-out till, deformation till, boulder clay, tillite (if lithified)	(Batchelor and Dowdeswell, 2015; Benn and Evans, 2010; Deschamps et al., 2013; Eyles, 1993; Lewis et al., 2006)
Ice marginal moraine	terminal moraine, retreat moraine, frontal moraine???, moraine ridges, terminoglacial fans	(Benediktsson et al., 2009; Benn and Evans, 2010; Bennett et al., 2000; Krüger et al., 2009; Krzyszowski and Zielinski, 2002; Lønne, 1995)
Push moraines	recessional moraines, de Geer moraines, transverse ridges, annual moraine ridges, push and squeeze moraines, morainal bank (subaqueous)	(Benn and Evans, 2010; Bennett, 2001; Todd, 2014)
Thrust block moraines	composite ridges, push moraines, end moraine marginal moraine, end moraine, terminal moraine, morainal bank (subaqueous)	(Aber et al., 1989a, 1989b; Benn and Evans, 2010; Lovell and Boston, 2017; Patton et al., 2016; Pedersen, 2014; Phillips et al., 2018, 2002; Van der Wateren, 1995; Vaughan-Hirsch and Phillips, 2017)
Ice-contact fan	proglacial fan, terminoglacial subaerial fan, latero-frontal fan, end moraine fans	(Benn and Evans, 2010; Zieliński and van Loon, 1998)
Esker	subglacial tunnel fill, serpent kame, complex eskers, interlobate esker	(Burke et al., 2015; Maries et al., 2017; Storrar et al., 2019, 2014)
Grounding zone wedge	till delta	(Batchelor and Dowdeswell, 2015; Benn and Evans, 2010; Powell and Alley, 1996; Rütger et al., 2011; Simkins et al., 2018)
Ice-contact subaqueous fan	grounding line fan, ice-contact glaciomarine fan, subaqueous esker delta, ice-proximal fan, esker-fan complex,	(Hirst, 2012; Hirst and Khatatneh, 2019; Koch and Isbell, 2013; Lajeunesse and Allard, 2002; Lønne, 1995; Powell, 1990; Thomas, 1984)
Subaqueous outwash fan: used when describing a large body of sand and gravel without a defined association with a grounding line and deposited from meltwater entering	turbiditic outwash fan, glacial submarine fan	(Rose et al., 2016; Rust and Romanelli, 1975; Thomas and Chiverrell, 2006; Visser et al., 2003)

	a water body	
Iceberg ploughmarks	iceberg keel marks, iceberg grooves, iceberg plough marks	(Berkson and Clay, 1973; J. A. A. Dowdeswell and Bamber, 2007; Graham et al., 2007; Haavik and Landrø, 2014; Klages et al., 2016; Ottesen et al., 2017)
Ice rafted debris	IRD, iceberg rafted debris, ice rafted detritus	(Dowdeswell and Dowdeswell, 1989; Lucchi and Rebesco, 2007; Powell and Cooper, 2002)
Glaciomarine diamicton	glaciomarine muds, glaciomarine sediments, rainout diamicton, glaciomarine claystones	(Benn and Evans, 2010; Bennett et al., 2000; Domack, 1982; Domack and Lawson, 1985; Ó Cofaigh et al., 2001; Powell and Cooper, 2002)
Cross-shelf trough	ice stream trough, palaeo-ice stream, paleo-ice stream pathway	(Batchelor and Dowdeswell, 2015; Canals et al., 2016; Clark and Spagnolo, 2016; Heron, 2018; Klages et al., 2015; Rütger et al., 2013; Swartz et al., 2015; Todd, 2016; Van Landeghem et al., 2009)

1893

1894

1895

1896

1897

Table 2: A summary of landforms and sediments deposited by land terminating ice sheet. Every sediment/landform is assigned to a depositional zone with an accompanying assessment of reservoir quality.

Element	Description	Depositional zone	Reservoir potential			References
			Presence/distribution	Quality	Overall	
Esker	Elongated, curvilinear or sinuous sediment ridges of glaci-fluvial origin. They can extend over several hundreds of kilometres in length delineating major subglacial drainage pathways. Esker ridges have been reported to be up to 50 m high and are formed when sediments fill an ice-walled meltwater channel. Eskers sediments can range from cobble and boulder gravels through sands to poorly sorted, massive diamictos. Erosional contacts and re-activation surfaces are likely to be present. When sediment laden meltwaters escape the ice sheet an ice-contact fan may develop as a continuation of an esker. Often, a glaciotectonic signature is present together with late stage normal faulting due to loss of lateral ice support.	Subglacial	Patchy distribution. Elongated, ice margin perpendicular, curvilinear ribbons 100s m to 10s km long and 10s-1000s m wide	Moderately to well sorted boulders to pea gravels with subordinate sand and fine fraction	Moderate/good	<i>Brennand, 2000; Storrar, Stokes and Evans, 2014; Burke, Brennand and Sjogren, 2015</i>
Ribbed (Rogen) moraine sediments	Subglacially formed ridges of sediment orientated transverse to the ice flow. They usually cover large, concave or flat surfaces in core areas of former ice sheets in proximity to inferred frozen bed areas. Dimensions range from 300-1200 in length, 150-300 m in width and 1-30 m in height with similar spacing and size distribution for every locality. Ribbed moraines are usually formed of poorly sorted subglacial debris.	Subglacial	Patchy distribution. Irregular. Ice flow perpendicular mounds	Poorly sorted, subglacially derived and transported material-	Poor	<i>Dunlop and Clark, 2006</i>
Drumlins/ drumlin fields	Oval or egg-shaped, elongated hill with its longer axis parallel to the ice-flow direction. Drumlins can be up to few km long and up to 50 m high. They could be composed of different type of sediments, usually poorly sorted and homogenized by basal ice coupling over the available substratum. Erosional vs. depositional origin is still debated but most likely represent a case of equifinality.	Subglacial depositional	Patchy distribution in ice stream corridors. 10s-100s m long and wide, and 1s-10s m high	Poor sorting, textural and mineralogical maturity dependent on source sediment, over-compacted,	Poor	<i>Benn and Evans, 2010; Ely et al., 2016</i>
Traction till (diamicton)	Homogenized, poorly sorted sediment deposited at the ice-bed interface directly from the ice. Grainsize ranges from fine clays and muds through to cobbles, boulders and bedrock rafts	Subglacial	Discontinuous distribution. Variable thickness, 1s-10s of meters with possible erosional windows. and interbedded, localized sand/gravel lenses	Polymodal grainsize distribution Fine sediments and outsized clasts. Very poor sorting. Over-compacted	Poor	<i>Evans et al., 2006; Benn and Evans, 2010</i>
Mega-Scale Glacial Lineations (MSGL)	Elongated, parallel to each other and to the ice flow direction, corrugations in subglacial sediment. 6-70 km long, 200-1300 m wide, typically 1-5 m high, associated mainly with fast flowing ice streams. Their original is still debated, with evidence supporting both erosional and depositional processes.	Subglacial	Patchy distribution in ice stream areas. Elongated, ice flow parallel. 100m to 10 km long, 100s m wide and 1-10	Polymodal grainsize distribution. Fine sediments and outsized clasts. Very poor sorting.	Poor	<i>(Ely et al., 2016; Spagnolo et al., 2014, 2016)</i>

Element	Description	Depositional zone	Reservoir potential			References
			Presence/distribution	Quality	Overall	
			m high.	Over compacted		
Kames	Sediment mounds associated with fluvial reworking of supraglacial, ice-marginal and subglacial sediments. Kames are composed mainly of sands and gravels with subordinate poorly sorted diamictons and fine deposits prone to postglacial reworking. Extremely hard to identify in the subsurface. Predictability of distribution of kame deposits can be challenging. If the ice flow is constrained by topography kame terraces may form along the valley edges where supraglacial meltwater streams are preferentially flowing. After ice melts out kame deposits can be found in contact with subglacial landforms and sediments.	Subglacial - ice marginal	Localized and unpredictable. Irregular mounds, 10s-1000s m, wide and long and 10s m high.	Glaciofluvially sorted sands and gravels (well sorted) glacial diamictons. (poorly sorted) and fines	Variable	(Brodzikowski and van Loon, 1987; Gruszka et al., 2012)
Ice-contact fans	Deposited subaerially by meltwater directly in front of the ice margin. Boulders, gravels and diamictites prevail in the ice-proximal part. Glaciotectonic deformation can be expected due to oscillations of the ice front during deposition. Middle and distal parts of an ice-contact fan appear to be less complex with gravel and sand (middle part) and sand and silt (distal part) deposition prevailing. The term fan- refers to the mode of deposition but not necessarily the shape of the sediment body as ice front shape and position together with the existing topography are the controlling factors. As a result, fans can be irregular in shape or can resemble a frontal moraine when several fans coalesce along the ice front.	Ice marginal/ proglacial zone	Discontinuous distribution proximally, along the ice margin. Deposition from a point source	Boulders, cobbles and gravels poorly /moderately sorted in the proximal part. Cobbles and gravels and sands in the distal part. Glaciotectonic deformation/ bulldozing often present	Variable - poor in proximal part moderate to good in medial to distal	(Zieliński and van Loon, 2000, 1999, 1998)
Ice marginal moraine	Thrust block moraine Glaciotectonic deformed sediments in the subglacial and ice marginal zone as a result of stress exerted by the ice sheet during advance. Thrust block moraines can be laterally extensive along the ice front and over 100 m in relief. Deformation of sediments resembles thin skinned thrusting. The depth of the deformation is limited by failure along a decollement surface most likely corresponding to a zone of contrast of mechanical properties of the substratum (sand /mud, unfrozen sediments/permafrost). Ductile deformation results in the formation of large open folds in the sediments in front of the ice mass. Thrust block moraines can be composed of proglacial outwash sediments, subglacial traction till, or glaciomarine sediments. Primary sedimentary structures are generally	Ice marginal zone	Ice margin parallel mounds, 100s-1000s m wide, 100s m to 10s km long and 10s-100s m high.	Good reservoir quality if well sorted glaciofluvial sands and gravels are thrust. Variable/poor if other e.g. lacustrine or subglacial sediments are thrust - substratum dependent. Glaciotectonic deformations decreasing reservoir quality	Variable	(Benn and Evans, 2010; Bennett, 2001; Vaughan-Hirsch and Phillips, 2017)

Element	Description	Depositional zone	Reservoir potential			References
			Presence/distribution	Quality	Overall	
	preserved for most of the sedimentary units.					
Push moraines	Oscillations of the ice front result in bulldozing of proglacial sediments and formation of push moraines. Small ice-front parallel ridges of unsorted sediment delineate annual re-advances of the ice front. Larger ridges most likely mark positions of longer stillstands. Primary sedimentary structures are unlikely to be preserved. Internal composition of a push moraine is dependent on ice marginal zone sediments and the mode of sediment supply. If meltwater deposition prevails push moraines can be sand and gravel-rich whereas where traction till deposition is dominant or the ice sheet is advancing over sand-poor areas the push moraine will be composed of glacial diamicton.	Ice marginal zone	10s-1000s m long, 10s-100m wide and 10s m high, ice-front parallel, elongated hills, often present in several parallel sets	Very poor sorting, Textural and mineralogical maturity dependent on the substratum. Outsized clasts and large boulders often present (up to several m)	Low	
Sandur	A large sediment body deposited by glacial, braided, meltwater streams in front of an ice terminus known also	Proximal: gravelly deposits of high energy braided channels may prevail in vertical succession. Distal: both gravel and sand channels deposits can be observed.	Proglacial Broad plains/belts of glaciofluvial sediments, 1-10s km wide, 1-100 km long. Thickness of sediments is highly variable and	Well sorted, rounded and sub-rounded sands and gravels. Multiple erosional internal contacts.	Good Good	(Magilligan et al., 2002; Maizels, 2007, 1997; Pisarska-Jamrozy and Zieliński, 2014; Zielinski and Van Loon, 2003)

Element	Description	Depositional zone	Reservoir potential			References
			Presence/distribution	Quality	Overall	
	as an outwash plain. Sandar associated with large ice sheets are described as braided river plains rather than alluvial fans with poor proximal-to-distal grainsize variation.					
	Pitted sandur: glaciofluvial rivers can bury dead ice blocks which subsequently melt out causing local depressions. Peat accumulations can often be observed in pitted sandar formed during interglacials.					
	Jökulhlaup deposits: sediments associated with high magnitude outburst floods. Due to the extremely high energy of a jökulhlaup and high sediment concentrations, mega-scale ripples, dunes or boulder bars may be formed. Some may form thick, hyper-concentrated sandur sequences. It may be difficult to distinguish jökulhlaup deposits from normal flood sediments (Maizels, 1997; Gomez et al., 2000; Björnsson, 2003).					
Ice marginal streamway	Large ice-front-parallel fluvial system develops when meltwaters escaping the ice sheet, after flowing over sandar, do not enter a water body directly. Such situations occur on uplifted areas where little or no sediment accommodation space is available.	Proglacial	100s km long and 10s km wide. Ice margin parallel and formed perpendicular to sandar.	Well sorted fluvial sands and gravels and over bank deposits. Hard to distinguish from a typical fluvial succession	Good	(Pisarska-Jamrozy, 2015; Van Loon and Pisarska-Jamrozy, 2017)
Aeolian Dunes	Wind reworking of sandur plains prior to the onset of vegetation may result in winnowing of finer fractions and re-mobilization of fine sands and local deposition of aeolian dunes or cover sands. Finer fractions are transported over longer distances and deposited as loess covers.	Proglacial	Localized distribution mainly on unvegetated sandur plains.	Fine to medium sands-well sorted	Good	(C.K. Ballantyne, 2002; Benn and Evans, 2010; Mountney and Russell, 2009)
Lacustrine glacier-fed delta	Glacier-fed deltas build up when a sandur enters a proglacial water body. Such deltas may be extensive with multiple braided feeder channels. Alternatively, lacustrine deltas may form when smaller lakes are present on a sandur. Such deltas may potentially infill all available accommodation space in a lake resulting in continuation of sandur deposition. Annual cyclicity of flow regime and occasional catastrophic flood events may result in preferential preservation of sediments associated with high magnitude events in the proximal parts of the delta and longer depositional distance of sand facies in comparison with the classic delta model. High sedimentation rates may cause rapid progradation of delta front and frequent slope failures (slumping).	Proglacial	Localized distribution. Deposits filling proglacial lakes on the sandur plane. Variable size and shape.	Well sorted, texturally mature sands and gravels in the foresets. Topsets could be coarser due to winnowing and sediment bypass, fines deposited distally as prodelta-lake fill	Topsets: Good Foresets: Good Prodelta: Poor	(Benn and Evans, 2010; Dietrich et al., 2016; Fyfe, 1990; Lønne, 1995; Lønne and Nemeč, 2004; Nemeč, 2009; Osterloff et al., 2004a; Patton and Hambrey, 2009; Phillips et al., 2002; Postma, 1990; Powell, 1990; Powell and Molnia, 1989; Wang et al., 2011)
Lacustrine ice - contact delta	Flat topped ice -contact deltas may develop in places where subaqueous outwash fans fill in accommodation space between a proglacial lake bed and water surface. Deltaic	Ice marginal	Localized deposition controlled by the ice margin	Mostly well-sorted sands and gravels. Bulldozed,	Ice-contact: Variable	

Element	Description	Depositional zone	Reservoir potential			References	
			Presence/distribution	Quality	Overall		
	topsets are deposited subaerially and act as a sediment by-pass zone with the majority of the deposition occurring on the delta slope (foresets). Ice-contact deltas may not exhibit the classic shape. Ice-contact deltas mimic the shape of the ice margin in their proximal part. Glaciotectonic deformation is most likely to be present in the ice-proximal part. Hyperpycnal, density current deposits can be frequent due to the high sediment load of glacial meltwater. Backstepping of the ice front and secondary delta formation can be observed.		position. Point sourced or amalgamated, ice front parallel deltas may build. 100s m to several km long 100s-1000s m wide. Thickness controlled by the water depth.	subglacially reworked poorly sorted material and diamicton in the ice-contact part. Coarse gravels, in the topsets. Sands and finer gravels in the foresets. Fine fractions and sands in the prodelta.	Topset Foreset Prodelta	Variable Good Variable / poor	
Proximal glacial lake fill	Proglacial lake sedimentation is characterised by deposition from meltwater streams (deltas and fans) or density currents in the proximal zone close to an ice margin or sediment input point. In the distal part of the lake sedimentation occurs mainly by settling from suspension from the meltwater plume in seasonal cycles. As a result, proglacial lakes are usually filled with sands interbedded with silts or silts and clays. Climbing ripple cross lamination of sandy beds is common proximal to the sediment input point. Glacial lakes may develop several levels of shorefaces recording changes in water level during deglaciation.	Proglacial	Present in the proglacial lake distally from the sediment input point, or as a fill of a small, proglacial lake (e.g. kettle hole lake). Size and thickness controlled by the size and shape of the lake.	Interbedded fine sands and silts. Subordinate coarse sands in lenses or pockets.	Variable		(Ashley, 2002; Colin K. Ballantyne, 2002; Bogen et al., 2015; Carrivick and Tweed, 2013; García et al., 2015)
Distal glacial lake fill	Distal glacial lake fill is usually characterised by fine grained deposits (silts) deposited from suspension with occasional dropstones/ ice rafted debris. Rhythmites (varvites) represent periodical, often bi-annual, variations in sediment supply and/or oxygen level in the lake.	Proglacial zone	Laterally extensive deposits. The distribution is controlled by the size of the lake.	Fine silts and clays bedded and laminated. Dropstones and varves could be present.	Poor		

1898

1899

1900

Table 3: A summary of landforms and sediments deposited by water terminating ice sheets is provided below. Every sediment/landform is assigned to a depositional zone with an assessment of reservoir quality.

Element	Description	Depositional zone	Reservoir potential			Reference
			Presence/distribution	Quality	Overall	
Esker	For description see Table 2.	Subglacial / ice marginal	For description see Table 2	For description see Table 2	Variable/good	(Brennand, 2000; Burke et al., 2015; Storrar et al., 2014)
Ribbed (Rogen) moraine sediments	For description see Table 2.	Subglacial	For description see Table 2	For description see Table 2	Poor	(Dunlop and Clark, 2006)
Drumlins/ drumlin fields	For description see Table 2.	Subglacial	For description see Table 2	For description see Table 2	Poor	(Benn and Evans, 2010; Bjarnadóttir and Andreassen, 2016; Ely et al., 2016)

Element	Description	Depositional zone	Reservoir potential			Reference	
			Presence/distribution	Quality	Overall		
Traction till (diamicton)	For description see Table 2.	Subglacial	For description see Table 2	For description see Table 2	Poor	(Boulton and Deynoux, 1981; Evans et al., 2006)	
Mega Scale Glacial Lineations (MSGGL)	For description see Table 2.	Subglacial	For description see Table 2	For description see Table 2	Poor	(Bingham et al., 2017; Bjarnadóttir and Andreassen, 2016; Ely et al., 2016; Jamieson et al., 2016; Ottesen et al., 2017; Spagnolo et al., 2016)	
Grounding zone wedge	Sedimentary depocenters formed at the grounding line of a marine terminating ice stream with steep distal and shallow dipping proximal slope. Grounding zone wedges are composed mainly of glaciogenic debris derived by melt out from basal ice and lodgement from subglacial traction till. They are found only in the locations of ice streams (cross shelf troughs) and fjords, punctuating stillstand positions of the grounding line, most likely, during ice retreat.	Subglacial	Localized, belts or bands of sediments 100s-1000s m long, 1000s m wide (constrained by the cross-shelf trough width) and 10s m high.	Mostly poorly sorted subglacial till interbedded with debris flow deposits and glaciomarine muds. Localized lenses, beds of better sorted material may be present.	Poor	(Batchelor and Dowdeswell, 2015; Dowdeswell et al., 2016b; Dowdeswell and Fugelli, 2012; Evans et al., 2012; Koch and Isbell, 2013; Powell and Alley, 1996; Powell and Domack, 1995)	
Ice marginal moraine	Thrust block moraine	Subaqueous thrust block moraines can be composed of subaqueous outwash sediments, traction till, glaciomarine muds or non-glacial marine sediments. For a detailed description see Table 1.	Ice marginal	For a description see Table 2	For a detailed description see Table 2.	Variable - dependent on substratum	(Benn and Evans, 2010; Bennett, 2001; Vaughan-Hirsch and Phillips, 2017)
	Push moraine	Subaqueous push moraines can be composed of subaqueous outwash sediments, traction till, glaciomarine muds or non-glacial marine sediments. For a detailed description see Table 1.	Ice marginal	For a description see Table 2	For a detailed description see Table 2.	Poor	
Grounding line fan	Small sediment depocenters at the grounding line of an ice sheet. Sediments are deposited by a mixture of grounding line processes (traction, debris flows) and fallout from meltwater. As a result glaciofluvial sands and gravels are mixed with cohesive debris flow sediments. Ice front oscillations are responsible for sediment re-deposition and mixing.	Ice marginal	Localized distribution associated with point-sourced meltwater discharge at the grounding line. 10s-100s m long and wide and 10s m thick.	Well sorted, glaciofluvial sands and gravels, interbedded with poorly sorted debris flow deposits and/or glaciomarine/subglacial till. Glacitectonic deformation often present.	Variable- dependent on the proportion of glaciofluvially sorted sediment is in the package.	(Evans et al., 2012; Powell, 1990; Powell and Alley, 1996; Rose et al., 2016)	

Element	Description	Depositional zone	Reservoir potential			Reference	
			Presence/distribution	Quality	Overall		
Subaqueous outwash fan (grounding line fan)	Large sedimentary body comprised of sands and gravels deposited by glacial meltwaters entering a water body at the grounding line of an ice sheet. The water at the time of the deposition is deep enough to prevent the fan from reaching the surface (if the surface is reached an ice-contact delta develops). Sediments may include proximal boulders and gravels sharply transitioning into distal sands and silts. Glaciotectonic deformation and dewatering structures are likely to be present. Characteristic features, distinguishing subaqueous outwash from sandur sediments, are: ripple cross laminations in sand units, large channels with massive fill, co-occurrence of cohesive and non-cohesive subaqueous debris flows deposits.	Ice marginal-proglacial	Large, localized sediment accumulation on the seabed associated with the ice margin position at the time. Deposited during the ice sheet retreat when meltwater discharge is high. 100s to 1000s m wide and long, 10s m thick	Well sorted sands are dominant. Silt and marine mud interbeds can be present in the distal part. Boulders and gravels could be present proximal to the grounding line.	Good		(Batchelor and Dowdeswell, 2015; Evans et al., 2012; Koch and Isbell, 2013; Lønne, 1995; Powell, 1990; Rose et al., 2016; Rust and Romanelli, 1975)
Lacustrine glacier-fed delta	For a detailed description see Table 2.	Proglacial	For a description see Table 2	For a detailed description see Table 2	Topsets	Good	(Benn and Evans, 2010; Dietrich et al., 2016; Lønne, 1995; Lønne and Nemeč, 2004; Nemeč, 2009; Osterloff et al., 2004a; Patton and Hambrey, 2009; Phillips et al., 2002; Postma, 1990; Powell, 1990; Powell and Molnia, 1989; Wang et al., 2011)
					Foresets	Good	
					Prodelta	Low	
Lacustrine ice - contact delta	For a detailed description see Table 2.	Ice marginal	For a description see Table 2	For a detailed description see Table 2	Ice-contact	Variable	
					Topsets	Variable	
					Foresets	Good	
					Prodelta	Low	
Marine glacier-fed delta	If a sandur enters the sea a glacier-fed delta is likely to build up. Such deltas may be extensive with multiple braided feeder channels. Annual cyclicity of flow regime and occasional catastrophic flood events may result in preferential preservation of sediments associated with high magnitude events in the proximal parts of the delta and longer depositional distance of sand facies in comparison with classic delta model. High sedimentation rates may cause rapid progradation of delta front and frequent slope failures (slumping).	Proglacial	Large sediment body deposited as an extension of a sandur entering a marine basin. 1000s m long and wide. Depth controlled by changes in water depth.	Well sorted sands with subordinate gravels in the foresets unconformably overlain by topsets that can be coarser and resemble sandur successions. Silts and muds present in the distal part.	Topsets	Good	
					Foresets	Good	
					Prodelta	Low	
Marine ice-contactdelta	Flat topped, marine ice-contact deltas may develop in places where subaqueous outwash fans fill-in accommodation space between the sea bed and water surface. Deltaic top sets are deposited subaerially and act as a sediment by-pass	Ice marginal	Localized distribution in front of and parallel to the ice margin. Deltas form from	Quality and facies distribution is similar to lacustrine ice-contact	Ice-contact	Variable	

Element	Description	Depositional zone	Reservoir potential			Reference
			Presence/distribution	Quality	Overall	
	zone with the majority of the deposition occurring on the delta foresets. Ice-contact deltas may not exhibit the classic D-shape of a delta as it may be controlled by the ice margin geometry in its proximal part. Glacitectonic deformation is most likely to be present in the ice-proximal part of the lobe. Due to the higher density of seawater rainout from suspension can be expected distally from the delta front. Backstepping of the ice front and secondary delta formation can be observed.		one or multiple point sources. Lobate in shape if not topographically constrained. 100s - 1000s m wide, 100s m to 10s km long and 10s m thick.	deltas. Larger proportion of deposition from buoyant sediment plume due to the increased density of sea water. (For details see Table 2)	Topsets Good Foresets Good Prodelta Poor	
Proximal glacial lake fill	For a detailed description see Table 2	Proglacial	For description see Table 2	For description see Table 2.	Variable - substratum dependent	(Ashley, 2002; Colin K. Ballantyne, 2002; Bogen et al., 2015; Carrivick and Tweed, 2013; García et al., 2015)
Distal glacial lake fill	For a detailed description see Table 2	Proglacial	For description see Table 2	For description see Table 2.	Poor	García et al., 2015)
Trough mouth fan	Fan-like sedimentary depocenters originating at the shelf break and extending for up to several hundreds of kilometres into the abyssal plain. Thickness of sediments can reach 5 km. The sediment forming a TMF is delivered to the shelf break by ice streams from ice sheets and deposited by gravity flows down the continental slope causing progradation. It is inferred that gravity flow sediments are interbedded with glaciogenic muds and interglacial marine muds. The exact sedimentary composition of a TMF is poorly constrained. Poorly sorted and mud rich mass wasting deposits are inferred from remote sensing surveys (sonar). Long runout distances of some lobes may indicate that deposition from density currents takes place in the distal part of the fan.	Proglacial	Deposited on the shelf slope and extending into the abyss. Located at the distal end of cross-shelf troughs. 10s km to 100 km wide and long, 100s to 1000s m thick.	Poorly constrained. Glaciogenic gravity flow deposits are usually poorly sorted and mud/clay rich. Localized meltwater supply and long runout distance of gravity flows may indicate the presence of better sorted packages.	Variable - poorly known and substratum dependent	(Dowdeswell et al., 2008; Ó Cofaigh et al., 2003; Taylor et al., 2002; Vorren and Laberg, 1997)
Gravity flows deposits	Sediment gravity flow sediments are frequently redeposited from sediments of glacial marine or lacustrine origin. Slope instability is a common characteristic of ice marginal landforms due to high sedimentation rates, ice margin oscillations, isostatic rebound-related earthquakes and localised deposition of ice derived sediments. Sediment type in an individual flow depends on the type of material available. High meltwater discharge from the ice sheet during the summer months can lead to deposition of turbidites in the proglacial zone of a marine/lacustrine terminating ice sheet.	Proglacial	Common in all glaciogenic successions. Remobilized from over steepened slopes of previously deposited landforms. Variable in size and thickness	Most of the glaciogenic gravity flow deposits will have decreased sorting with respect to the source lithology. Gravity flows associated with TMFs may be an exception.	Variable- dependent on substratum	(Dowdeswell et al., 2004; Koch and Isbell, 2013; Lønne, 1995; Pisarska-Jamroz and Weckwerth, 2013; Powell and Molnia, 1989)

Element	Description	Depositional zone	Reservoir potential			Reference
			Presence/distribution	Quality	Overall	
Contourites	Sediments delivered to the ocean floor are often reworked by slow, semi-permanent bottom currents – contourites, which reflect the thermohaline circulation in global ocean when cold and dense water flows along the base of the continental slope. Two types of contourites are reported: muddy- with up to 15% sand content and sandy- with laminate, rippled or structureless layers of sand up to 25 cm thick. They are extremely hard to identify in the rock record and can be easily mistaken for distal turbidites.	Proglacial	In the abyssal plain at the base of a continental slope. Forming belts or mounds of sediment parallel to the slope base.	Usually fine (silts and v. fine sands) but well sorted sediments. Grainsize controlling reservoir properties. Could have good reservoir properties if coarser sediment were supplied to the abyss - (e.g. by trough mouth fans).	Low / moderate	(Camerlenghi et al., 2001; Jones et al., 1993; Lucchi and Rebesco, 2007; Reading, 2002)
Marine diamicton (glaciomarine muds)	Fine grained, laminated or massive muds deposited by settling from suspension with occasional floating clasts (dropstones). Higher degree of lamination, lower clast content and normal compaction allowing differentiation of glaciomarine muds from subglacial traction till. Glaciomarine muds may be altered by iceberg ploughing in which case lamination will not be preserved.	Proglacial	Regional, large scale distribution within the basin. Dropstone and iceberg rafted debris increases in density proximal to the outlet. Thickness depends on the longevity of glaciation. Often interbedded with typical marine muds.	Poor reservoir quality due to low grainsize. Good seal. Local scouring by iceberg keels (iceberg ploughmarks) can reduce sealing properties.	Low	(Eyles et al., 1985; Lønne, 1995; Powell and Molnia, 1989; Rust, 1965)

1901

1902

1903

1904

Table 4: Sediments and landforms diagnostic of glacial erosion, deposition and presence in the basin enabling unequivocal interpretation of glaciogenic sediments. Mode of identification has been provided for every entry in the table.

Diagnostic element	Description	Depositional zone	Mode of identification	Reference
Striations/ Striated pavement	Grooves in bedrock or underlying sediments. The grooves are formed by debris encased in ice in traction of over the bedrock/sediments. Striations are good indicators of ice movement direction.	Subglacial erosional zone	Outcrops	(Clerc et al., 2013; Le Heron, 2007; Leveill et al., 1988; Martin et al., 2012; Stroeven et al., 2016)
Traction till (glacial diamictite / diamicton)	For a detailed description see Table 2.	Subglacial depositional zone	Core/outcrop/well log data/drilling data	(Boulton and Deynoux, 1981; Evans et al., 2006)
Mega Scale Glacial Lineations	For a detailed description see Table 2.	Subglacial zone	3D seismic data	(Bingham et al., 2017; Bjarnadóttir and Andreassen, 2016; Ely et al., 2016; Jamieson et al., 2016; Ottesen et

(MSGL)				al., 2017; Spagnolo et al., 2016, Benjamin Bellwald et al., 2019; Piasecka et al., 2016)
Boulder pavements	A layer of boulders with striated surfaces in traction till. Sediments are deposited subglacially as traction till. Subsequently, after ice retreat, fine grained sediments are winnowed by water and wind leaving a layer of boulders and cobbles.	Subglacial zone-reworked	Outcrops, drilling data, well logs/micro imaging logs	(C.K. Ballantyne, 2002; Boulton, 1996)
Sediment/rock rafts	Blocks of rock/sediment excavated, transported and deposited by ice without disaggregation of its primary structure. Rafts are known to reach sizes of up to several km long and wide.	Subglacial zone	2D/3D seismic/core (very rare)	(Rüther et al., 2013; Winsborrow et al., 2016)
Shear margin moraine	Ridge of sediments formed subglacially at the boundary between slow-moving is and fast-moving ice (ice stream). 10s m high, 100-1000s m wide and 10s km long. They are composed of available subglacial material (diamicton).	Subglacial zone	3D seismic data	(Batchelor and Dowdeswell, 2016; Benjamin Bellwald et al., 2019; Bellwald and Planke, 2019; Stokes and Clark, 2002)
Tunnel valleys	Elongated, deep incisions up to 100 km long, 5 km wide and 400 m deep. Tunnel valleys are oriented perpendicular to former ice margins. Their formation is linked to meltwater erosion in proximity to the ice margin during ice retreat or deglaciation. They are usually filled with deglaciation - to - postglacial sediments.	Ice marginal zone (subglacial to proglacial)	Seismic (2D and 3D)	(L. R. Bjarnadóttir et al., 2017; Ghienne and Deynoux, 1998; Kristensen et al., 2007; Praeg, 2003; Stumm, 2012; van der Vegt et al., 2016)
Glaciotectonic deformations	Deformation and remobilization of sediments due to ice front oscillations. Types of deformation include pushing, folding and thrusting of sediments. Shallow decollement and thrusting is known from Pleistocene and older sediments of the North Sea, Denmark and Germany (Cretaceous chalk cliffs of Rhugen).	Ice marginal zone (ice-contact to proglacial)	Seismic (2D and 3D)	(Pedersen, 2014; Vaughan-Hirsch and Phillips, 2017)
Iceberg scours/ keel marks	Curvilinear, irregular corrugation in the lake/sea bed. Corrugations are usually V or W shaped in cross-section and can me several km long, and up to 10-20 meters deep. The plough marks are formed by grounded icebergs.	Proglacial zone - water terminating ice sheet (grounded)	3D seismic data,	(J. A. Dowdeswell and Bamber, 2007; Graham et al., 2007; Haavik and Landrø, 2014)
Dropstones	Outsized clasts of cobble/ gravel size encased in laminated or massive marine/lacustrine muds. Glacial dropstones are melted out from floating icebergs and dropped onto the seabed/lake bottom. Other mechanisms including plant root rafting and rock projectiles have been suggested as other possible transport mechanisms, but they are likely to be of minor importance in the rock record.	Proglacial zone - water terminating ice sheet	Core/micro imaging logs	(Bennett et al., 1996)
Heinrich Layers (Ice rafted debris layers)	Terrigenous material deposited in marine/lacustrine conditions by melt out of sediments from icebergs. Coarse - grained clastic layers encased in marine muds are interpreted as evidence of marine terminating ice sheet dynamics – massive calving and iceberg release.	Proglacial zone -water terminating ice sheet	Core/micro imaging logs	(Bond et al., 1992; Hodell et al., 2017)
Varves (varvites)	Alternating layers of light and dark coloured clays or silts deposited in quiescent conditions in a proglacial lake/sea. Dark laminae are seasonal, associated with periods of low oxygen levels when ice covers the lake/sea. Lighter colour laminae are linked to oxygenated meltwater water influx during spring and summer months. Can develop in non-glacial conditions too.	Proglacial zone	Core/micro imaging logs	(Evans and Thomson, 2010; Gold, 2009; Powell and Cooper, 2002)

1905

1906

1907

- A novel conceptual model for the distribution of glaciogenic reservoirs
- First-pass interpretation tool for complex glaciogenic sequences
- Ice margin position controlling reservoir quality
- Identification of landforms and sediments crucial to reservoir predictability

Journal Pre-proof

Declaration of interests

The authors declare that they have no known competing financial interests or personal relationships that could have appeared to influence the work reported in this paper.

The authors declare the following financial interests/personal relationships which may be considered as potential competing interests:

Journal Pre-proof